

SAFETY AND STRUCTURAL IMPLICATIONS OF SEAT BELTS ON TRANSIT BUSES

FINAL REPORT

(Phase II)

By

Ralph Alan Dusseau

Associate Professor

Department of Civil Engineering

Snehamay Khasnabis

Professor

Department of Civil Engineering

Sami Zaher

Graduate Research Assistant

Department of Civil Engineering

Wayne State University

Detroit, MI 48202

September 1991

This study was sponsored jointly by the Michigan Department of Transportation and the U.S. Department of Transportation through the Great Lakes Center for Truck Transportation Research program at the University of Michigan, Ann Arbor.

TABLE OF CONTENTS

	PAGE
Table of Contents.....	i
List of Tables.....	ii
List of Figures.....	iii
Chapter 1: Introduction.....	1
Chapter 2: Bus Models With and Without Seat Belts.....	2
Chapter 3: Bus Models With and Without Wheelchairs.....	65
Chapter 4: Status of Laboratory Testing.....	80
Chapter 5: Summary and Conclusions.....	92
Acknowledgements.....	97
References.....	98

LIST OF TABLES

TABLE	PAGE
1. Bus Load Cases.....	13
2. Maximum Element Stresses and Corresponding Bus Floor Angles Versus Bus Load Cases.....	14
3. Longitudinal and Lateral Locations Corresponding to Maximum Element Stresses.....	15

LIST OF FIGURES

FIGURE	PAGE
1. Plywood Floor Elements for 21-Foot Bus.....	16
2. Steel Plate Elements for 21-Foot Bus.....	17
3. Bus Frame Elements, Chassis Elements, and Boundary Conditions for 21-Foot Bus.....	18
4. Bus Body Elements for 21-Foot Bus.....	19
5. Bus Body Elements for 25-Foot Bus.....	20
6. Passenger Seats and Load Application for 21-Foot Bus with Wall-Mounted Seats and Full Seat Belt Usage.....	21
7. Passenger Seats and Load Application for 25-Foot Bus with Wall-Mounted Seats and Front Seat Belt Usage Only.....	22
8. Passenger Seats and Load Application for 21-Foot Bus with Floor-Mounted Seats and Staggered Seat Belt Usage.....	23
9. Passenger Seats and Load Application for 25-Foot Bus with Floor-Mounted Seats and Staggered Seat Belt Usage.....	24
10. 21-Foot Bus with Floor-Mounted Seats - Maximum Stresses in Plywood Floor Elements.....	25
11. 21-Foot Bus with Wall-Mounted Seats - Maximum Stresses in Plywood Floor Elements.....	26
12. 25-Foot Bus with Floor-Mounted Seats - Maximum Stresses in Plywood Floor Elements.....	27
13. 25-Foot Bus with Wall-Mounted Seats - Maximum Stresses in Plywood Floor Elements.....	28
14. 21-Foot Bus with Floor-Mounted Seats - Maximum Stresses in Lateral Frame Elements.....	29

LIST OF FIGURES (CONTINUED)

FIGURE	PAGE
15. 21-Foot Bus with Wall-Mounted Seats - Maximum Stresses in Lateral Frame Elements.....	30
16. 25-Foot Bus with Floor-Mounted Seats - Maximum Stresses in Lateral Frame Elements.....	31
17. 25-Foot Bus with Wall-Mounted Seats - Maximum Stresses in Lateral Frame Elements.....	32
18. 21-Foot Bus with Floor-Mounted Seats - Maximum Stresses in Longitudinal Chassis Elements.....	33
19. 21-Foot Bus with Wall-Mounted Seats - Maximum Stresses in Longitudinal Chassis Elements.....	34
20. 25-Foot Bus with Floor-Mounted Seats - Maximum Stresses in Longitudinal Chassis Elements.....	35
21. 25-Foot Bus with Wall-Mounted Seats - Maximum Stresses in Longitudinal Chassis Elements.....	36
22. 21-Foot Bus with Floor-Mounted Seats - Maximum Stresses in Body Elements.....	37
23. 21-Foot Bus with Wall-Mounted Seats - Maximum Stresses in Body Elements.....	38
24. 25-Foot Bus with Floor-Mounted Seats - Maximum Stresses in Body Elements.....	39
25. 25-Foot Bus with Wall-Mounted Seats - Maximum Stresses in Body Elements.....	40
26. 21-Foot Bus with Floor-Mounted Seats - Maximum Stresses in Steel Plate Elements.....	41

LIST OF FIGURES (CONTINUED)

FIGURE	PAGE
27. 21-Foot Bus with Wall-Mounted Seats - Maximum Stresses in Steel Plate Elements.....	42
28. 25-Foot Bus with Floor-Mounted Seats - Maximum Stresses in Steel Plate Elements.....	43
29. 25-Foot Bus with Wall-Mounted Seats - Maximum Stresses in Steel Plate Elements.....	44
30. 21-Foot Bus with Floor-Mounted Seats - Maximum Stresses in Perimeter Floor Elements.....	45
31. 21-Foot Bus with Wall-Mounted Seats - Maximum Stresses in Perimeter Floor Elements.....	46
32. 25-Foot Bus with Floor-Mounted Seats - Maximum Stresses in Perimeter Floor Elements.....	47
33. 25-Foot Bus with Wall-Mounted Seats - Maximum Stresses in Perimeter Floor Elements.....	48
34. 21-Foot Bus with Floor-Mounted Seats - Maximum Stresses in Skirting Elements.....	49
35. 21-Foot Bus with Wall-Mounted Seats - Maximum Stresses in Skirting Elements.....	50
36. 25-Foot Bus with Floor-Mounted Seats - Maximum Stresses in Skirting Elements.....	51
37. 25-Foot Bus with Wall-Mounted Seats - Maximum Stresses in Skirting Elements.....	52
38. 21-Foot Bus with Floor-Mounted Seats - Maximum Stresses in Wheel Well Elements.....	53

LIST OF FIGURES (CONTINUED)

FIGURE	PAGE
39. 21-Foot Bus with Wall-Mounted Seats - Maximum Stresses in Wheel Well Elements.....	54
40. 25-Foot Bus with Floor-Mounted Seats - Maximum Stresses in Wheel Well Elements.....	55
41. 25-Foot Bus with Wall-Mounted Seats - Maximum Stresses in Wheel Well Elements.....	56
42. 21-Foot Bus with Floor-Mounted Seats - Maximum Stresses in Longitudinal Chassis Cap Elements.....	57
43. 21-Foot Bus with Wall-Mounted Seats - Maximum Stresses in Longitudinal Chassis Cap Elements.....	58
44. 25-Foot Bus with Floor-Mounted Seats - Maximum Stresses in Longitudinal Chassis Cap Elements.....	59
45. 25-Foot Bus with Wall-Mounted Seats - Maximum Stresses in Longitudinal Chassis Cap Elements.....	60
46. 21-Foot Bus with Floor-Mounted Seats - Maximum Stresses in Lateral Chassis Elements.....	61
47. 21-Foot Bus with Wall-Mounted Seats - Maximum Stresses in Lateral Chassis Elements.....	62
48. 25-Foot Bus with Floor-Mounted Seats - Maximum Stresses in Lateral Chassis Elements.....	63
49. 25-Foot Bus with Wall-Mounted Seats - Maximum Stresses in Lateral Chassis Elements.....	64
50. 25-Foot Bus - Wheelchair Lift and Right Sidewall Model.....	68
51. 25-Foot Bus - Wheelchair and Wheelchair Restraints Model.....	69
52. 25-Foot Bus - Maximum Stresses in Plywood Floor Elements.....	70

LIST OF FIGURES (CONTINUED)

FIGURE	PAGE
53. 25-Foot Bus - Maximum Stresses in Lateral Frame Elements.....	71
54. 25-Foot Bus - Maximum Stresses in Longitudinal Chassis Elements.....	72
55. 25-Foot Bus - Maximum Stresses in Body Elements.....	73
56. 25-Foot Bus - Maximum Stresses in Steel Plate Elements.....	74
57. 25-Foot Bus - Maximum Stresses in Perimeter Floor Elements.....	75
58. 25-Foot Bus - Maximum Stresses in Skirting Elements.....	76
59. 25-Foot Bus - Maximum Stresses in Wheel Well Elements.....	77
60. 25-Foot Bus - Maximum Stresses in Longitudinal Chassis Cap Elements.	78
61. 25-Foot Bus - Maximum Stresses in Lateral Chassis Elements.....	79
62. Front View of Load Platform.....	83
63. Side View of Load Platform.....	84
64. Top View of Load Platform.....	85
65. Section A-A of Load Platform.....	86
66. Section B-B of Load Platform.....	87
67. Section C-C of Load Platform.....	88
68. Perspective View of Load Platform Base.....	89
69. Perspective View of Test Specimen.....	90
70. Perspective View of MTS Connection Detail.....	91

CHAPTER 1

INTRODUCTION

This report is the result of a study conducted at the Department of Civil Engineering, Wayne State University to assess the safety and structural implication of seat belts on transit buses. Phase II of this investigation, jointly funded by the U.S. Department of Transportation and the Michigan Department of Transportation, had three primary objectives:

1. Development and analysis of finite element computer models of two medium-duty transit buses utilizing floor-mounted seats and seats that are wall- and floor-mounted, and utilizing three loading conditions: full seat belt usage, staggered seat belt usage, and front seat belt usage only.
2. Development and analysis of finite element computer models of a medium-duty transit bus with a wheelchair lift and two wheelchairs with restraints utilizing floor-mounted seats and seats that are wall- and floor-mounted.
3. Preliminary laboratory testing of the bus chassis-to-body connections.

The remaining portion of this report is presented in four additional chapters. The results of the finite element modeling and analyses listed under Objectives 1 and 2 above are presented in Chapters 2 and 3. The status of the laboratory testing (Objective 3) is discussed in Chapter 4, while final conclusions for Phase II are presented in Chapter 5.

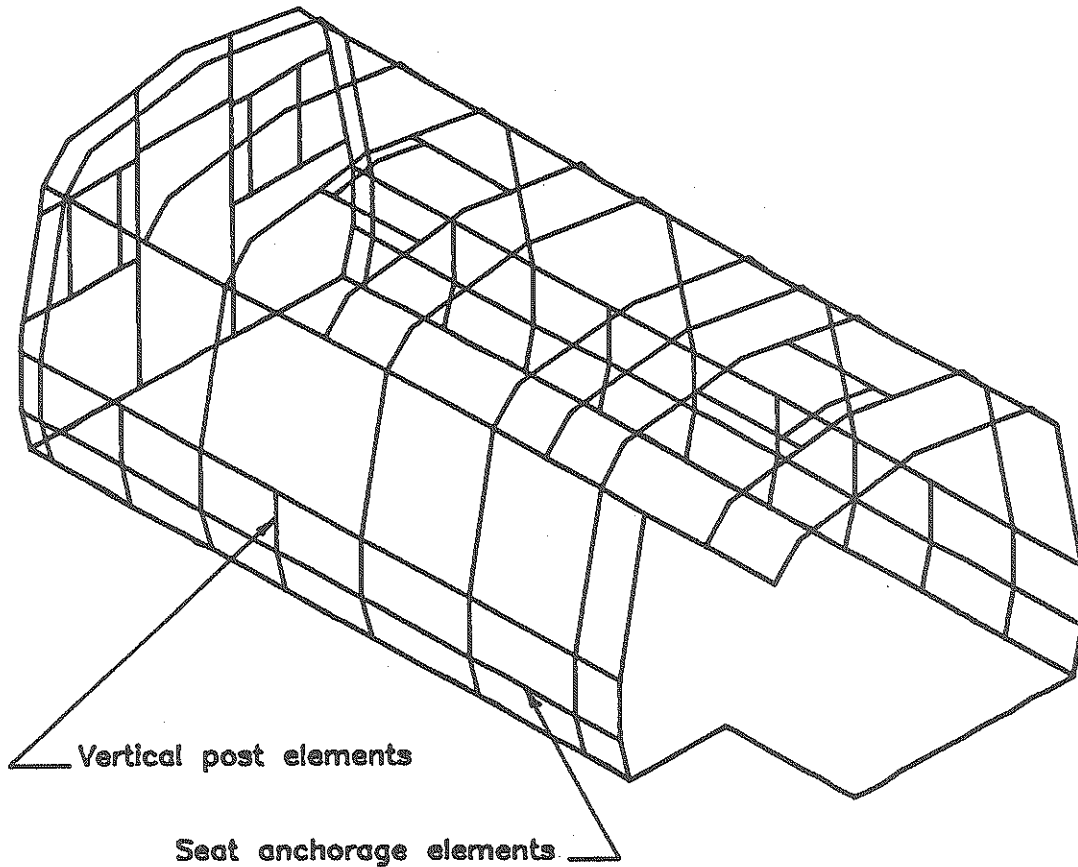


Fig. 4. Bus Body Elements for 21-Foot Bus.

CHAPTER 2

BUS MODELS WITH AND WITHOUT SEAT BELTS

INTRODUCTION

A study to assess the structural responses of medium-duty transit buses under large dynamic loads is currently underway at the Department of Civil Engineering, Wayne State University. The principal objective of this investigation is to analyze the structural members of the bus frame to insure that the frame will withstand the instantaneous stress build-up resulting from sudden bus decelerations (front-end impacts).

A comprehensive literature review conducted as a part of the project showed very little research to assess the behavior of the structural components of a bus frame following a rapid deceleration. Reports dealing with front-end crash tests of school and transit buses have concentrated on "visible" damage including: passenger seat detachment from the floors (1)(2)(3)(4), slippage of the frame-to-chassis connections (1)(5)(6), and buckling of the floor (1)(2)(4). The crash responses of the remaining structural components of the buses tested were not reported, however.

One previously-reported use of finite-element computer modeling in the analysis of transit buses was a series of models developed by DAF Trucks, Eindhoven, The Netherlands (7). The goal was to measure the effects of bending stiffness and torsional stiffness on the dynamic responses and hence the ride comfort of passengers. No analyses under rapid deceleration were performed, however.

The work presented here is a continuation of the research conducted by Dusseau, Khasnabis, and Dombrowski (8)(9). That effort involved finite-element analysis of the basis structure of a 25-foot transit bus which included the frame, floor, and chassis. Assumptions were made regarding the

loading conditions in the event of a rapid deceleration. Parametric results for floor angles from 0 to 30 degrees at maximum deceleration were derived for floor-mounted seats using two loading patterns: with seat belts installed and used on all passenger seats and with seat belts installed and used on the front seats only. It was found that the structural members in the frame could experience moderate to substantial decreases in maximum stress if seat belts are installed and used on all seats, while the maximum stresses in the chassis members could be slightly higher to moderately higher if seat belts are installed and used on all seats.

In the present study, finite-element computer models were developed for two medium-duty transit buses: a 21-foot bus with 11 seats for a capacity of 22 passengers and a 25-foot bus with 13 seats for a capacity of 26 passengers. Two finite-element models were derived for each transit bus studied: one with passenger seats fastened to the floor only ("the model with floor-mounted seats") and one with seats attached to both the sidewalls and the floor ("the model with wall-mounted seats"). The four bus models were each analyzed under three cases of rapid deceleration: with seat belts installed and used on all seats ("full seat belt usage"), with seat belts installed on all seats and used by about half of the passengers ("staggered seat belt usage"), and with seat belts installed and used on the front seats only ("front seat belt usage only"). Results using seven angles of tilt from 0 to 30 degrees for the floor at maximum deceleration were derived for each load case.

The major additions in the present study compared with the previous investigation are: the analysis of the 21-foot bus; the inclusion of the sidewalls, backwall, and roof for each model; the analysis of models with wall-mounted seats; and the load case with staggered seat belt usage.

MODELS AND ASSUMPTIONS

The 21-foot bus is a shorter version of the 25-foot bus with two less seats and about four feet less chassis, frame, floor, and body. The same basic chassis and axle spacing is used for both buses, however. All of the steel members in the frame, chassis, body, and seats are cold-formed steel sections with minimum yield stresses of 30,000 psi. The floor is composed of exterior grade plywood with steel plate reinforcing along the lines where the interior legs of the seats are bolted to the floor and along the plywood seam which follows the centerline of the floor. Steel plate is also used in the tops of the rear wheel wells.

The floor is supported by lateral frame members which are fabricated from channel sections, which run between the sidewalls, and which support the body, floor, and frame. Angle sections are used for the skirting and other frame members around the perimeter of the floor. The lateral frame members are welded to longitudinal chassis caps that are fabricated from channel sections and are attached to the chassis with U-bolt connections. The chassis is composed of two longitudinal members that are fabricated from channel sections and are connected at intervals by lateral chassis members which are also fabricated from channel sections. The body is fabricated from square tubes and channel sections, while the seats are fabricated from square tubes and steel plates. The floor-mounted seats have two inverted "T" legs with the interior legs fastened to the floor and the exterior legs fastened to the perimeter of the frame. The wall-mounted seats are similar to the floor-mounted seats but with the exterior legs deleted and the exterior edges of the seats fastened to seat anchorage members which run the length of the body.

The simplifications and assumptions that were made in developing the bus

models were as follows:

1. Because the goal of the research was to assess the relative effects of seat mounting and seat belt usage on the dynamic responses of the transit buses modeled, two key simplifications were made in modeling the buses: 1) only the inertial forces due to the passengers were considered in the analyses, and 2) the front portion of the body, the stairs, the battery tray, and other minor structural members that contribute little to the stiffness and strength of the bus structure were excluded from the models.
2. The plywood floor was modeled using plate finite elements as depicted in Fig. 1 for the 21-foot bus. Because the plywood floor was modeled without seams, the steel plate reinforcing along the centerline of the floor was not included in the model. The steel plate reinforcing along the bolt line of the interior seats and in the rear wheel wells was modeled using plate elements as shown in Fig. 2 for the 21-foot bus.
3. The lateral frame members, perimeter frame members, and longitudinal chassis caps were all modeled using beam finite elements as illustrated in Fig. 3 for the 21-foot bus. For simplicity, the centroids of these beam elements were all placed in the same horizontal plane as the plywood floor. The longitudinal chassis members, lateral chassis members, and skirting members were also modeled using beam elements as depicted in Fig. 3. Also shown in Fig. 3 are semi-rigid (high-stiffness) elements which were used to connect the centroids of the longitudinal chassis members with the lateral frame members at the points where the lateral frame members are welded to the longitudinal chassis caps. The sidewalls, backwall, and roof members were modeled using beam elements as depicted in Figs. 4 and 5 for the 21-foot and 25-foot bus models, respectively.
4. The front axle is assumed to "bottom out" under rapid deceleration.

Therefore, as shown in Fig. 3, the buses were modeled with vertical and lateral restraints at the points where rubber stops are attached to the longitudinal chassis members to prevent damage due to bottoming out of the front axle. Longitudinal and lateral restraints were used at the front of the longitudinal chassis members where the front bumper is attached, while vertical restraints were used at the points where the rear leaf springs are attached to the longitudinal chassis members.

5. Each floor-mounted and wall-mounted seat was represented by five semi-rigid members which were arranged like a swingset with one horizontal element connecting the nodal points representing the centers-of-gravity (CG's) of the two passengers in the seat and two diagonal elements connecting each of these CG points to the floor or sidewalls at or near the points where the actual seats are attached. Figs. 6 and 7 show the 21-foot and 25-foot buses, respectively, with wall-mounted seats; while Figs. 8 and 9 depict the 21-foot and 25-foot buses, respectively, with floor-mounted seats.
6. The finite-element computer code used for the present investigation was the ANSYS finite-element program developed by Swanson Analysis Systems, Inc., Houston, Pennsylvania.

LOAD CASES

To simulate the loads generated by passenger inertia under rapid deceleration, a force of 2500 pounds was assumed for each passenger. This is the same force required by the Federal Motor Vehicle Safety Standards (10) for testing bus seats. These forces were applied using seven angles of tilt from 0 to 30 degrees for the bus floor at maximum deceleration. These angles of tilt were simulated by "tilting" the forces as opposed to tilting the models.

The loading pattern used to represent rapid deceleration with full seat belt usage consisted of two 2500-pound forces applied to each passenger seat

(as shown in Fig. 6 for the 21-foot bus with wall-mounted seats). For load cases with unbelted passengers, a 2500-pound force was applied to the seat in front of each unbelted passenger. For rapid deceleration with front seat belt usage only (as depicted in Fig. 7 for the 25-foot bus with wall-mounted seats) no forces were applied to the rear seats, two 2500-pound forces were applied to each intermediate seat, and two 5000-pound forces were applied to each front seat. For rapid deceleration with staggered seat belt usage, the checkerboard loading patterns depicted in Figs. 8 and 9 were used for the 21-foot and 25-foot buses, respectively, with floor-mounted seats.

ANALYSIS RESULTS

Table 1 lists the 12 load cases analyzed, Table 2 contains the maximum element stresses and the corresponding floor angles, and Table 3 lists the lateral and longitudinal locations of the maximum element stresses. The longitudinal locations listed in Table 3 are measured along the centerline of the bus beginning at the back and are normalized with respect to the bus length. Thus the longitudinal location 0.00 refers to the point where the rear bumper is attached, while the location 1.00 refers to the point where the front bumper is attached. The lateral locations listed in Table 3 are measured from the centerline of the bus and are normalized with respect to the half-width of the floor. Thus the lateral location -1.00 refers to the left edge of the floor, while the lateral location +1.00 refers to the right edge.

Primary Structural Members

The floor-frame-chassis system is the primary structural system which provides strength and stiffness for the transit buses modeled. Thus the plywood floor members, lateral frame members, and longitudinal chassis members were classified as primary structural members based on their relative size, location, and importance as members of the floor-frame-chassis system.

Plywood Floor Elements

For the plywood floor elements, the most severe case was the 25-foot bus with wall-mounted seats and staggered seat belt usage (25W2) at a floor angle of 0 degrees. The maximum stress of 2.79 ksi for this case was 96% higher than full seat belt usage (25W1), 23% higher than front seat belt usage only (25W3), 86% higher than floor-mounted seats (25F2), and 22% higher than the 21-foot bus (21W2). The maximum stresses for case 25W2 and two other cases occurred near the rear wheel wells. The skirting members and other perimeter frame members are discontinuous at the rear wheel wells. The maximum stresses for six cases were near the left front passenger seat. The loads acting on the front seats are doubled for cases with staggered seat belt usage and with front seat belt usage only. The maximum stresses for the remaining three cases occurred between the left rear wheel well and the left front seat.

Plots of maximum plywood element stress versus bus floor angle are presented in Figs. 10 and 11 for the 21-foot bus with floor-mounted and wall-mounted seats, respectively. Similar plots are presented in Figs. 12 and 13 for the 25-foot bus.

Lateral Frame Elements

The most severe case for the lateral frame elements was the 21-foot bus with floor-mounted seats and staggered seat belt usage (21F2) at a floor angle of 0 degrees. For this case, the maximum stress of 46.9 ksi was 64% larger than full seat belt usage (21F1), 4% larger than front seat belt usage only (21F3), 3% larger than wall-mounted seats (21W2), and 11% larger than the 25-foot bus (25F2). The maximum stresses occurred near the left front seat for case 21F2 and eight other cases, and between the left rear wheel well and the left front seat for three cases.

Figs. 14 and 15 contain plots of maximum lateral frame element stress

versus bus floor angle for the 21-foot bus with floor-mounted and wall-mounted seats, respectively. Similar plots are presented in Figs. 16 and 17 for the 25-foot bus.

Longitudinal Chassis Elements

For the longitudinal chassis elements, the worst case was the 21-foot bus with wall-mounted seats and front seat belt usage only (21W3) at a floor angle of 30 degrees. The maximum stress of 38.2 ksi for this case was 33% higher than full seat belt usage (21W1), 21% higher than staggered seat belt usage (21W2), 41% higher than floor-mounted seats (21F3), and 15% higher than the 25-foot bus (25W3). The maximum stresses occurred between the left rear wheel well and the left front seat for case 21W3 and three other cases, near the right rear wheel well for four cases, and near the front seats for four cases.

Plots of maximum longitudinal chassis element stress versus bus floor angle are presented in Figs. 18 and 19 for the 21-foot bus with floor-mounted and wall-mounted seats, respectively. Similar plots are presented in Figs. 20 and 21 for the 25-foot bus.

Secondary Structural Members

Because they contribute less to the strength and stiffness of the buses that were modeled and hence are of less overall importance to structure of these buses, the following were classified as secondary structural members: the body members, steel plate members, perimeter frame members, longitudinal chassis caps, and lateral chassis members.

Body Elements

The worst case for the body elements was the 21-foot bus with wall-mounted seats and staggered seat belt usage (21W2) at a floor angle of 30 degrees. For this case, the maximum stress of 193.0 ksi was 83% larger than full seat belt usage (21W1), 50% larger than front seat belt usage only

(21W3), 278% larger than floor-mounted seats (21F2), and 40% larger than the 25-foot bus (25W2). For all six cases with wall-mounted seats, the maximum stresses occurred in the seat anchorage members. For the cases with floor-mounted seats, five cases had maximum stresses in the vertical posts below the windows and one case had maximum stress along the left edge of the frame.

Figs. 22 and 23 contain plots of maximum body element stress versus bus floor angle for the 21-foot bus with floor-mounted and wall-mounted seats, respectively. Similar plots are presented in Figs. 24 and 25 for the 25-foot bus.

Steel Plate Elements

For the steel plate elements, the most severe case was the 25-foot bus with wall-mounted seats and staggered seat belt usage (25W2) at a floor angle of 0 degrees. The maximum stress of 31.5 ksi for this case was 84% higher than full seat belt usage (25W1), 2% higher than front seat belt usage only (25W3), 99% higher than floor-mounted seats (25F2), and 5% higher than the 21-foot bus (21W2). The maximum stresses occurred near the rear wheel wells for case 25W2 and one other case, near the left front seat for six cases, and between the left rear wheel well and the left front seat for four cases.

Plots of maximum steel plate element stress versus bus floor angle are presented in Figs. 26 and 27 for the 21-foot bus with floor-mounted and wall-mounted seats, respectively. Similar plots are presented in Figs. 28 and 29 for the 25-foot bus.

Perimeter Frame Elements

The most severe case for the perimeter frame elements was the 21-foot bus with floor-mounted seats and staggered seat belt usage (21F2) at a floor angle of 0 degrees. For this case, the maximum stress of 99.8 ksi was 77% larger than full seat belt usage (21F1), 10% larger than front seat belt usage only

angle are presented in Figs. 42 and 43 for the 21-foot bus with floor-mounted and wall-mounted seats, respectively. Similar plots are presented in Figs. 44 and 45 for the 25-foot bus.

Lateral Chassis Elements

The most severe case for the lateral chassis elements was the 21-foot bus with floor-mounted seats and staggered seat belt usage (21F2) at a floor angle of 30 degrees. For this case, the maximum stress of 17.4 ksi was 32% larger than full seat belt usage (21F1), 14% larger than front seat belt usage only (21F3), 118% larger than wall-mounted seats (21W2), and 51% larger than the 25-foot bus (25F2). The maximum stresses occurred between the rear wheel wells and the front seats for case 21F2 and seven other cases, at the rear wheel wells for three cases, and at the front of the bus for one case.

Figs. 46 and 47 contain plots of maximum lateral chassis element stress versus bus floor angle for the 21-foot bus with floor-mounted and wall-mounted seats, respectively. Similar plots are presented in Figs. 48 and 49 for the 25-foot bus.

(21F3), 214% larger than wall-mounted seats (21W2), and 4% larger than the 25-foot bus (25F2). The maximum stress occurred between the left rear wheel well and the left front seat for case 21F2 and six other cases, near the rear wheel wells for four cases, and near the left rear seat for one case.

In plotting the stress results, the perimeter frame elements were divided into three groups: the elements around the perimeter of the bus floor only, the elements in the side skirting, and the elements in the rear wheel wells. Figs. 30 and 31 contain plots of maximum perimeter floor element stress versus bus floor angle for the 21-foot bus with floor-mounted and wall-mounted seats, respectively. Similar plots are presented in Figs. 32 and 33 for the 25-foot bus. Plots of maximum skirting element stress versus bus floor angle are presented in Figs. 34 and 35 for the 21-foot bus with floor-mounted and wall-mounted seats, respectively. Similar plots are presented in Figs. 36 and 37 for the 25-foot bus. Figs. 38 and 39 contain plots of maximum wheel well element stress versus bus floor angle for the 21-foot bus with floor-mounted and wall-mounted seats, respectively. Similar plots are presented in Figs. 40 and 41 for the 25-foot bus.

Longitudinal Chassis Cap Elements

For the longitudinal chassis cap elements, the worst case was the 21-foot bus with wall-mounted seats and staggered seat belt usage (21W2) at a floor angle of 0 degrees. The maximum stress of 32.1 ksi for this case was 40% higher than full seat belt usage (21W1), 64% higher than front seat belt usage only (21W3), 42% higher than floor-mounted seats (21F2), and 34% higher than the 25-foot bus (25W2). The maximum stresses occurred between the rear wheel wells and the front seats for case 25W2 and six other cases, near the rear wheel wells for four cases, and near the left rear seat for one case.

Plots of maximum longitudinal chassis cap element stress versus bus floor

TABLE 2. MAXIMUM ELEMENT STRESSES AND CORRESPONDING BUS FLOOR ANGLES VERSUS BUS LOAD CASES

ELEMENT DESCRIPTIONS	MAXIMUM ELEMENT STRESSES (ksi) / CORRESPONDING BUS FLOOR ANGLES (degrees)											
	LOAD CASE 21F1	LOAD CASE 21F2	LOAD CASE 21F3	LOAD CASE 21W1	LOAD CASE 21W2	LOAD CASE 21W3	LOAD CASE 25F1	LOAD CASE 25F2	LOAD CASE 25F3	LOAD CASE 25W1	LOAD CASE 25W2	LOAD CASE 25W3
Primary Structural Members												
Plywood Floor Elements	1.37 0	1.52 0	1.61 0	1.38 0	2.29 0	2.33 0	1.38 0	1.50 0	1.65 0	1.42 0	2.79 0	2.26 0
Lateral Frame Elements	28.6 0	46.9 0	45.1 0	27.2 10	45.6 0	32.0 0	29.4 0	42.3 0	43.1 0	28.1 0	29.5 0	32.1 0
Longitudinal Chassis Elements	21.7 0	25.9 0	27.0 0	28.8 30	31.7 30	38.2 30	34.1 25	33.1 20	25.2 0	31.2 25	25.7 15	33.2 30
Secondary Structural Members												
Body Elements	39.1 10	51.0 0	54.4 0	105.7 30	193.0 30	128.7 0	47.0 30	74.1 15	39.8 15	70.3 30	137.8 5	137.4 30
Steel Plate Elements	14.3 0	15.9 0	16.9 0	17.1 0	29.9 0	30.4 0	14.5 30	15.8 0	17.4 0	17.1 0	31.5 0	31.0 0
Perimeter Frame Elements	56.3 0	99.8 0	90.9 15	23.2 0	31.8 0	24.8 30	46.1 0	95.9 0	91.9 15	29.9 30	30.4 30	20.7 30
Longitudinal Chassis Cap Elements	22.1 30	22.6 0	15.3 0	23.0 0	32.1 0	19.6 30	22.5 30	17.4 30	17.0 30	24.5 30	23.9 30	21.6 30
Lateral Chassis Elements	13.2 30	17.4 30	15.3 30	8.5 30	8.0 30	9.8 30	7.5 30	11.5 30	10.2 30	6.8 30	10.4 30	6.7 30

TABLE 1. BUS LOAD CASES

LOAD CASE	BUS VERSION AND SEAT TYPE	SEAT BELT USAGE
21F1	21-Foot Bus with Floor-Mounted Seats	Full Seat Belt Usage
21F2	21-Foot Bus with Floor-Mounted Seats	Staggered Seat Belt Usage
21F3	21-Foot Bus with Floor-Mounted Seats	Front Seat Belt Usage Only
21W1	21-Foot Bus with Wall-Mounted Seats	Full Seat Belt Usage
21W2	21-Foot Bus with Wall-Mounted Seats	Staggered Seat Belt Usage
21W3	21-Foot Bus with Wall-Mounted Seats	Front Seat Belt Usage Only
25F1	25-Foot Bus with Floor-Mounted Seats	Full Seat Belt Usage
25F2	25-Foot Bus with Floor-Mounted Seats	Staggered Seat Belt Usage
25F3	25-Foot Bus with Floor-Mounted Seats	Front Seat Belt Usage Only
25W1	25-Foot Bus with Wall-Mounted Seats	Full Seat Belt Usage
25W2	25-Foot Bus with Wall-Mounted Seats	Staggered Seat Belt Usage
25W3	25-Foot Bus with Wall-Mounted Seats	Front Seat Belt Usage Only

TABLE 3. LONGITUDINAL AND LATERAL LOCATIONS CORRESPONDING TO MAXIMUM ELEMENT STRESSES

ELEMENT DESCRIPTIONS	LONGITUDINAL LOCATIONS / LATERAL LOCATIONS											
	LOAD CASE 21F1	LOAD CASE 21F2	LOAD CASE 21F3	LOAD CASE 21W1	LOAD CASE 21W2	LOAD CASE 21W3	LOAD CASE 25F1	LOAD CASE 25F2	LOAD CASE 25F3	LOAD CASE 25W1	LOAD CASE 25W2	LOAD CASE 25W3
Primary Structural Members												
Plywood Floor Elements	0.82 -0.40	0.82 -0.40	0.82 -0.40	0.29 -0.46	0.69 -0.50	0.69 -0.50	0.84 -0.40	0.84 -0.40	0.84 -0.40	0.18 0.50	0.18 0.50	0.69 -0.31
Lateral Frame Elements	0.82 -0.45	0.82 -0.45	0.82 -0.45	0.33 -0.43	0.45 -0.45	0.55 -0.45	0.84 -0.35	0.84 -0.45	0.84 -0.45	0.84 -0.35	0.84 -0.35	0.84 -0.35
Longitudinal Chassis Elements	0.84 -0.35	0.84 -0.35	0.84 -0.35	0.53 -0.35	0.53 -0.35	0.53 -0.35	0.29 0.35	0.23 0.35	0.96 0.33	0.29 0.35	0.29 0.35	0.58 -0.35
Secondary Structural Members												
Body Elements	0.00 1.03	0.65 -1.03	0.65 -1.03	0.40 -1.06	0.40 -1.06	0.72 -1.06	0.18 -1.03	0.18 1.03	0.68 -1.00	0.68 -1.06	0.12 1.06	0.68 -1.06
Steel Plate Elements	0.82 -0.40	0.82 -0.40	0.82 -0.40	0.59 -0.40	0.59 -0.40	0.65 -0.40	0.84 -0.40	0.84 -0.40	0.84 -0.40	0.15 -0.40	0.15 0.40	0.69 -0.40
Perimeter Frame Elements	0.10 -1.00	0.47 -1.00	0.64 -1.00	0.20 -1.00	0.49 -1.00	0.64 -1.00	0.68 -1.00	0.19 1.00	0.68 -1.00	0.28 -1.00	0.28 1.00	0.66 -1.00
Longitudinal Chassis Cap Elements	0.03 -0.40	0.50 -0.40	0.18 0.40	0.18 -0.40	0.50 -0.40	0.34 -0.40	0.26 0.40	0.26 -0.40	0.40 -0.40	0.40 -0.40	0.40 0.40	0.40 -0.40
Lateral Chassis Elements	0.34 0.00	0.34 0.00	0.34 0.00	0.34 0.00	0.51 0.00	0.34 0.00	0.42 0.00	0.24 0.00	0.57 0.00	0.24 0.00	0.24 0.00	1.00 0.00

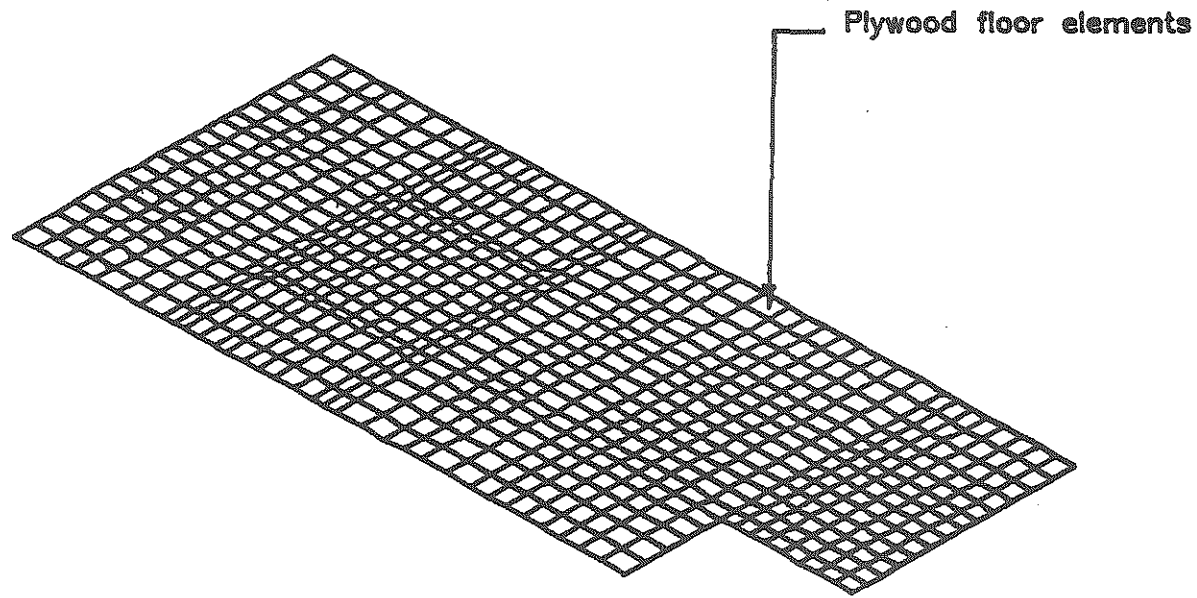


Fig. 1. Plywood Floor Elements for 21-Foot Bus.

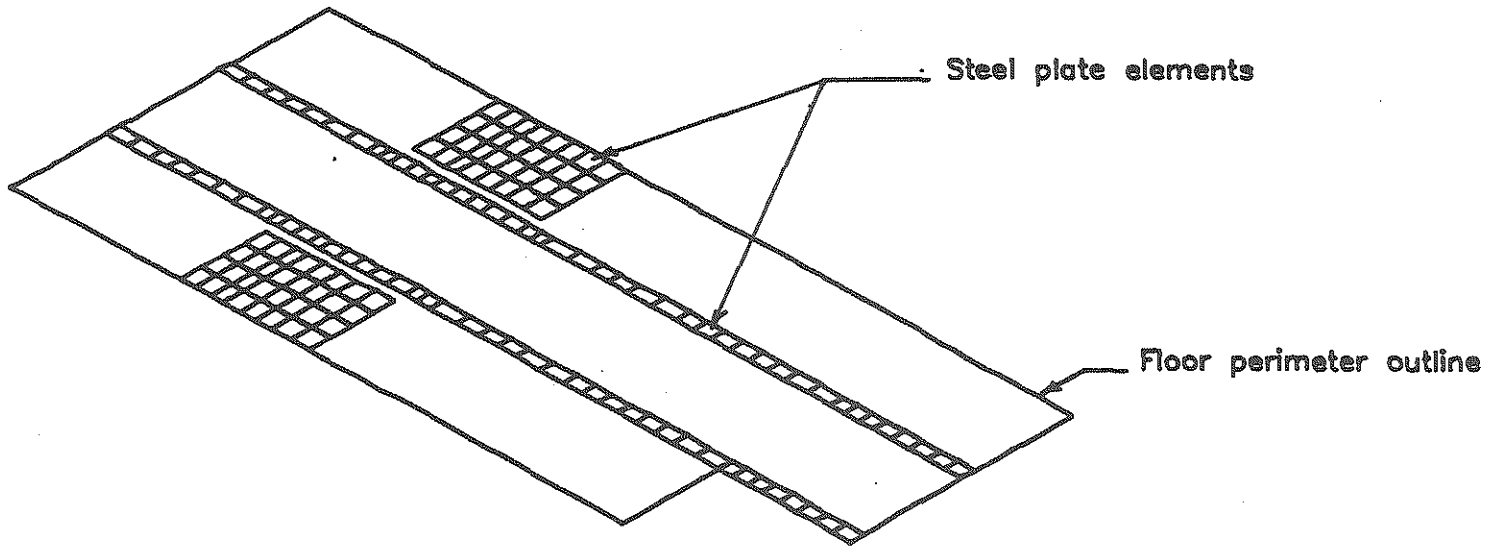


Fig. 2. Steel-Plate Elements for 21-Foot Bus.

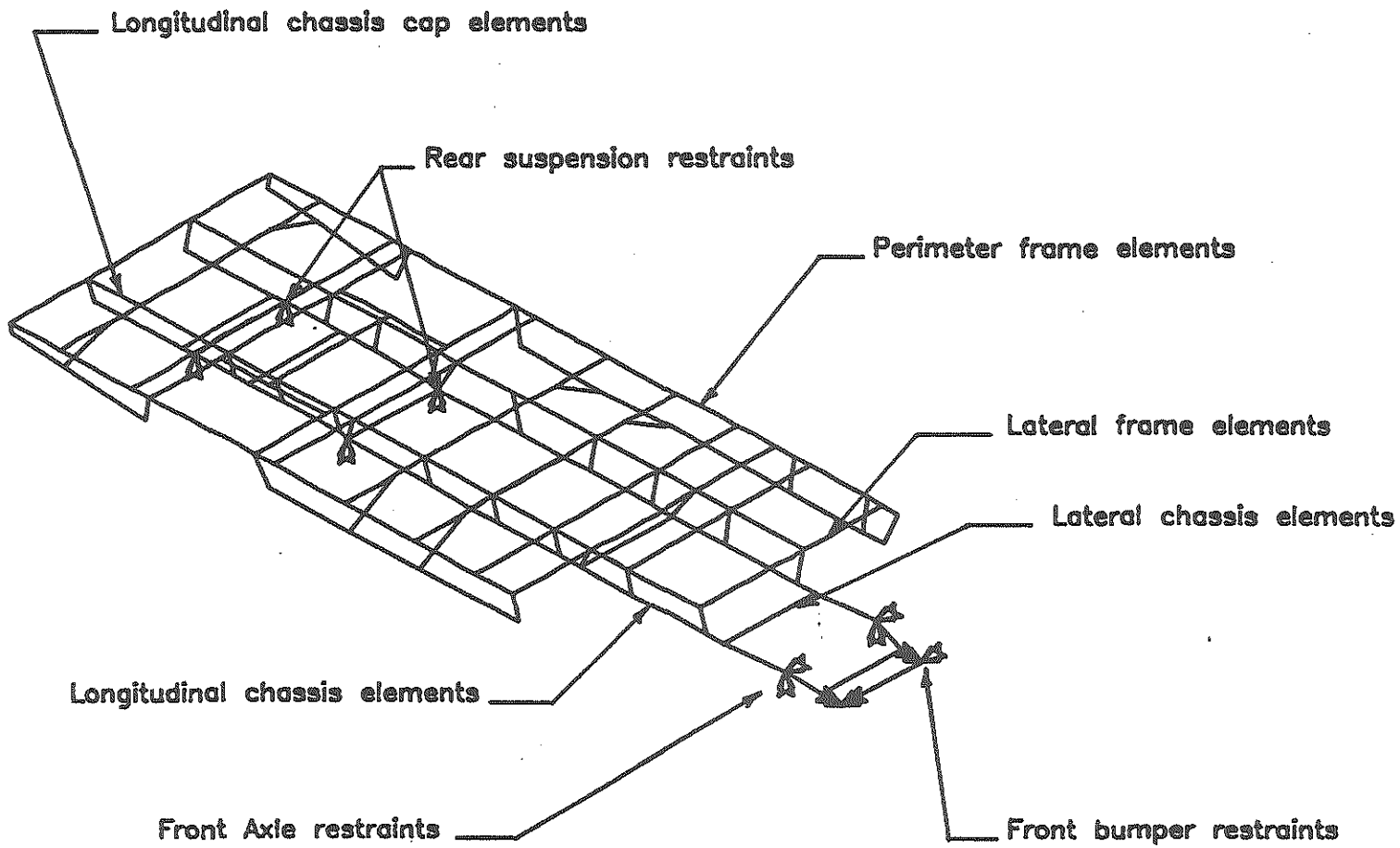


Fig. 3. Bus Frame Elements, Chassis Elements, and Boundary Conditions for 21-Foot Bus.

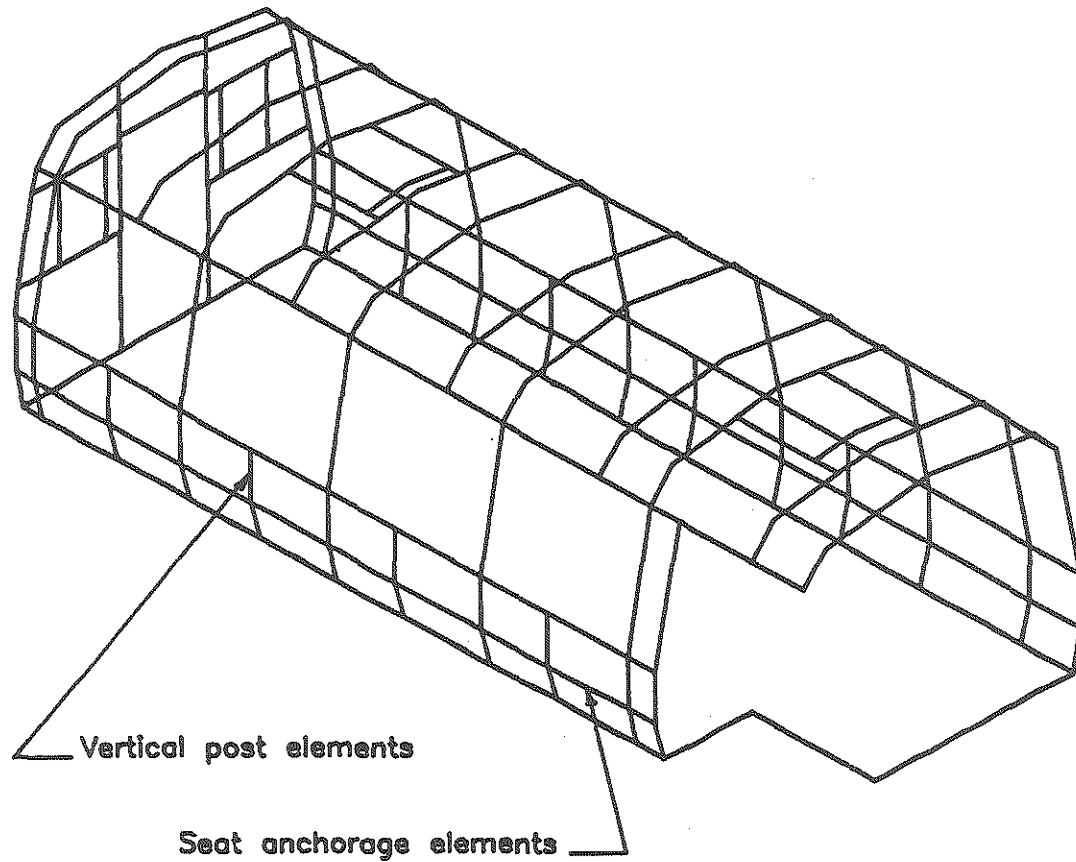


Fig. 5. Bus Body Elements for 25-Foot Bus.

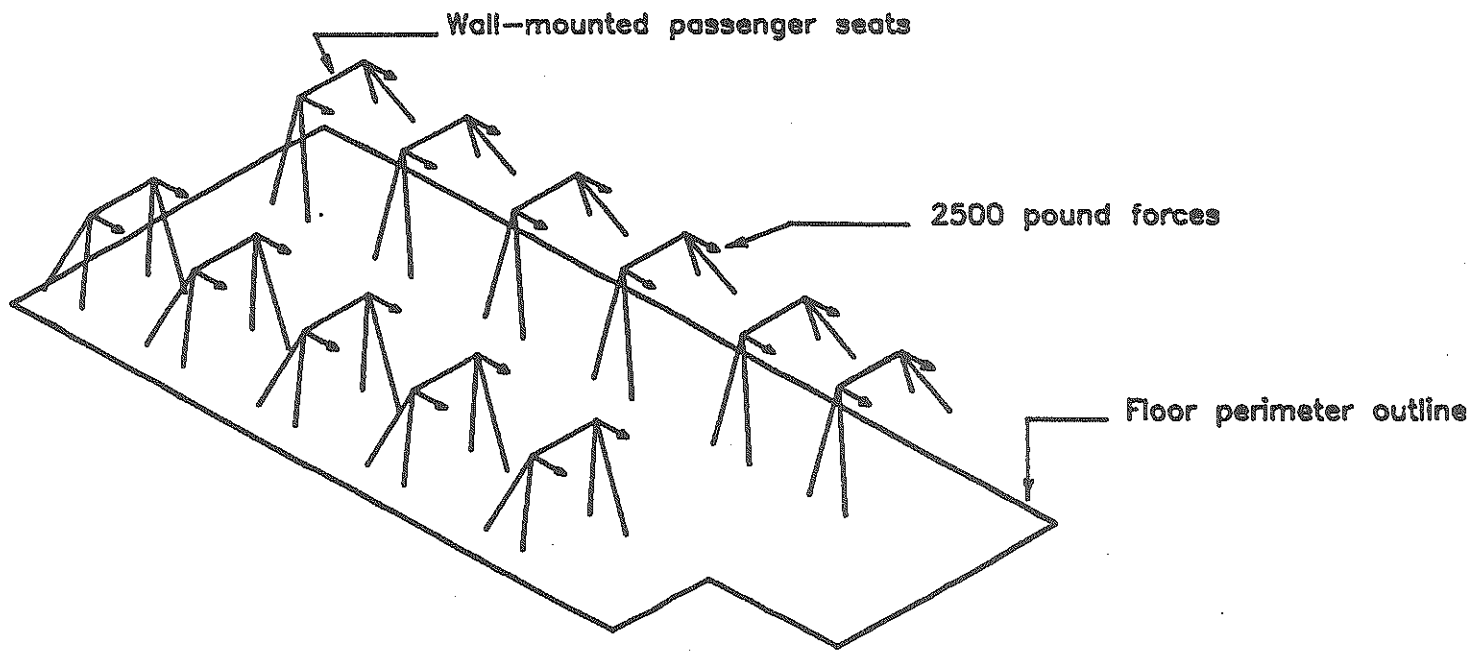


Fig. 6. Passenger Seats and Load Application for 21-Foot Bus with Wall-Mounted Seats and Full Seat Belt Usage.

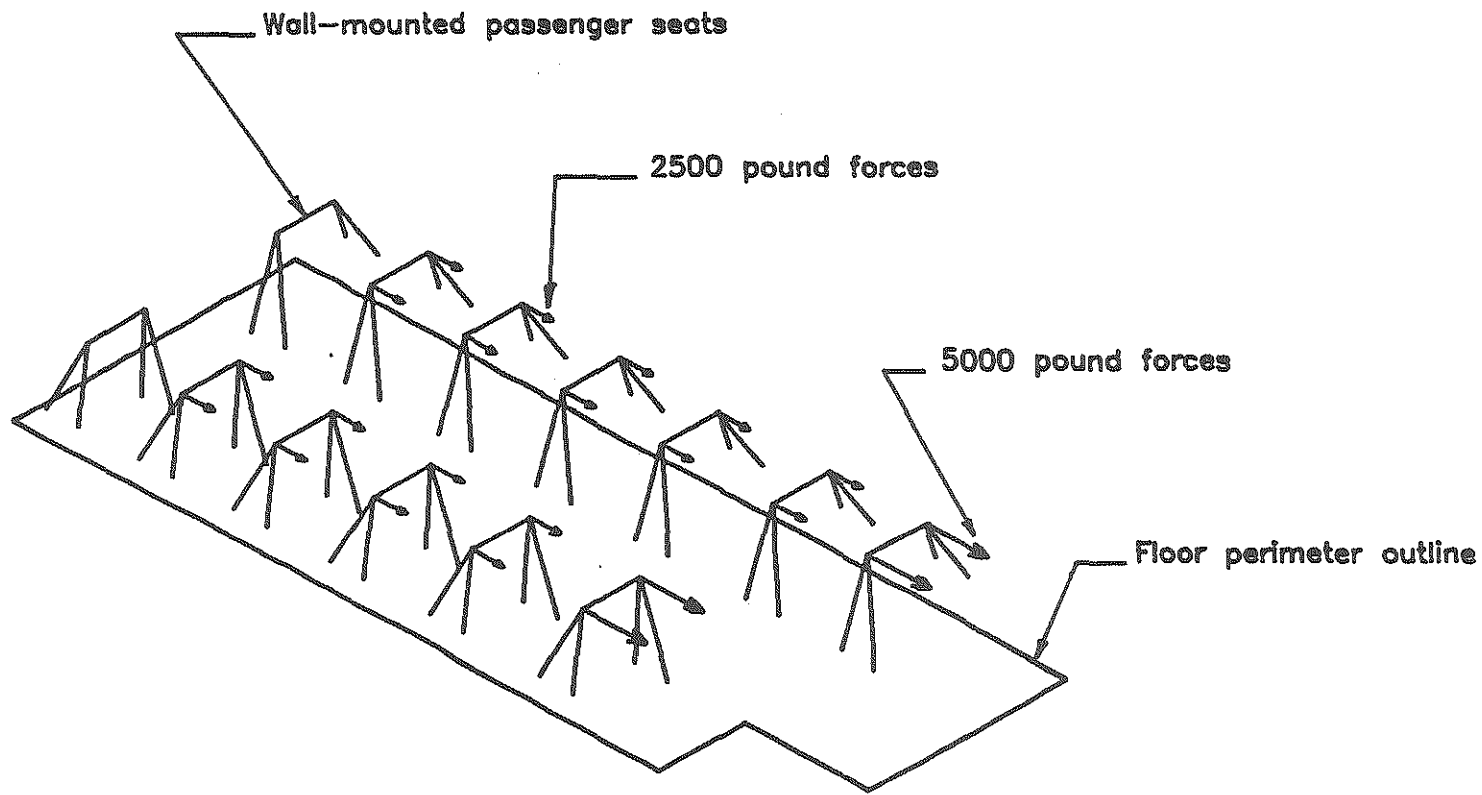


Fig. 7. Passenger Seats and Load Application for 25-Foot Bus with Wall-Mounted Seats and Front Seat Belt Usage Only.

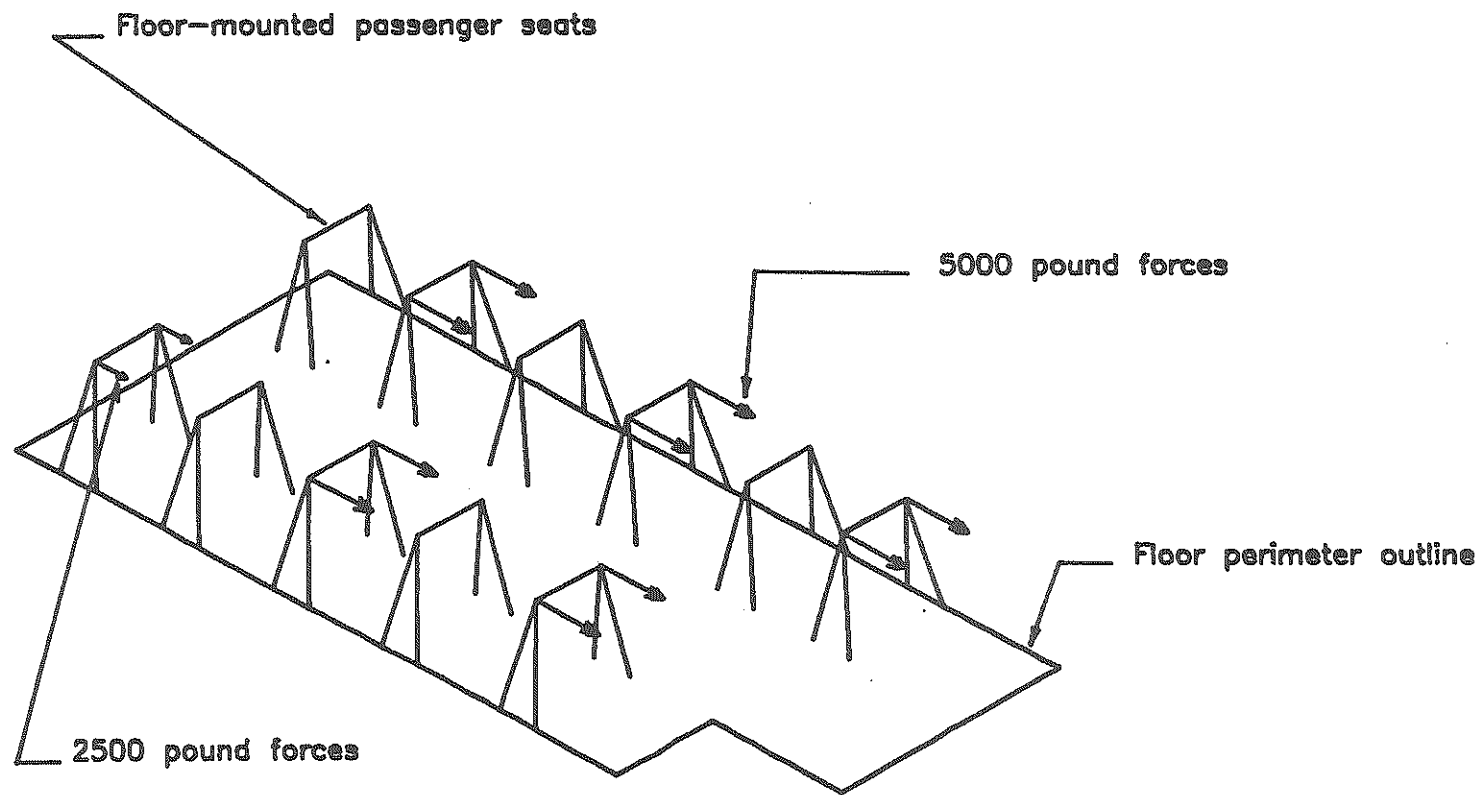


Fig. 8. Passenger Seats and Load Application for 21-Foot Bus with Floor-Mounted Seats and Staggered Seat Belt Usage.

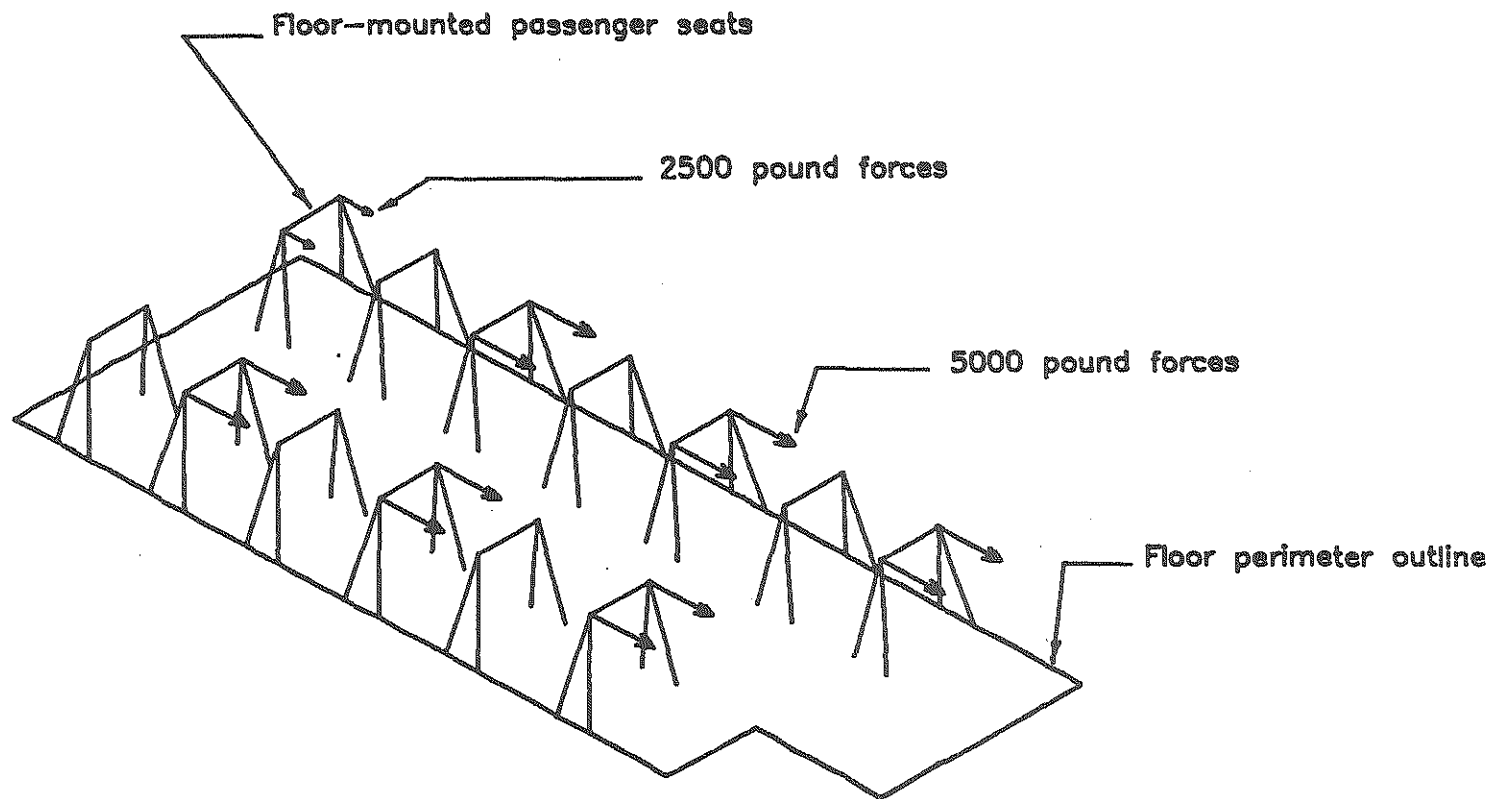


Fig. 9. Passenger Seats and Load Application for 25-Foot Bus with Floor-Mounted Seats and Staggered Seat Belt Usage.

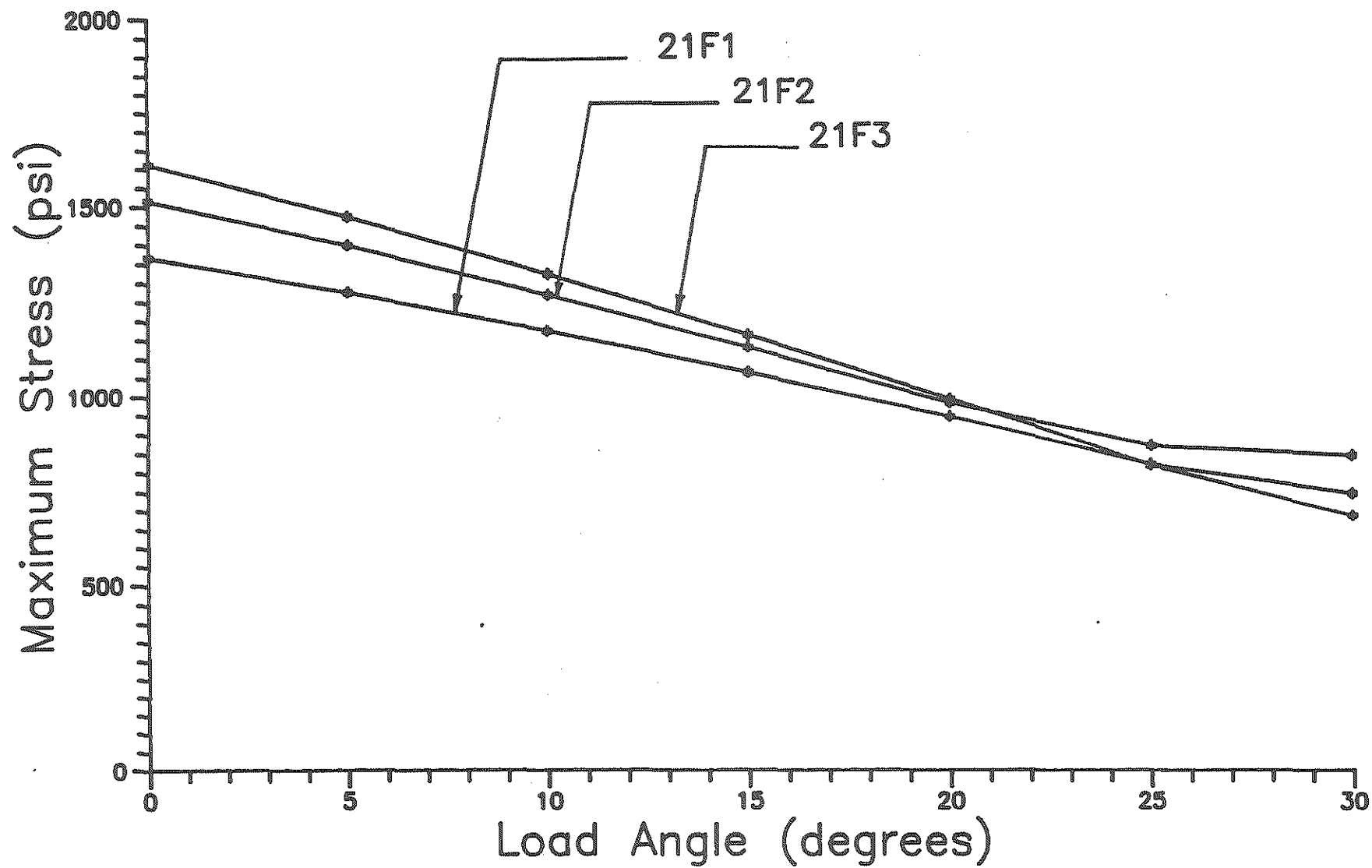


Fig. 10. 21-Foot Bus with Floor-Mounted Seats — Maximum Stresses in Plywood Floor Elements.

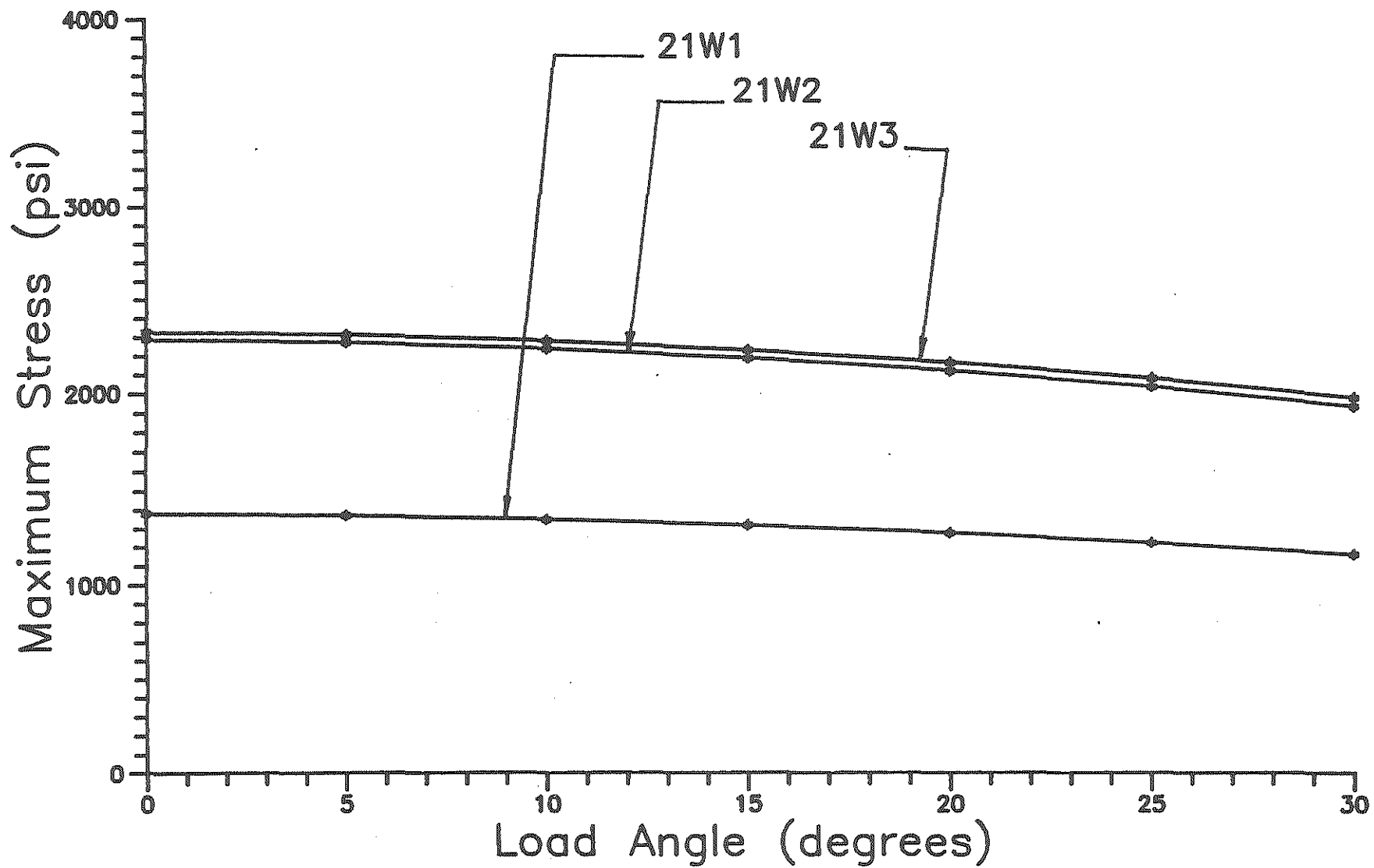


Fig. 11. 21-Foot Bus with Wall-Mounted Seats - Maximum Stresses in Plywood Floor Elements.

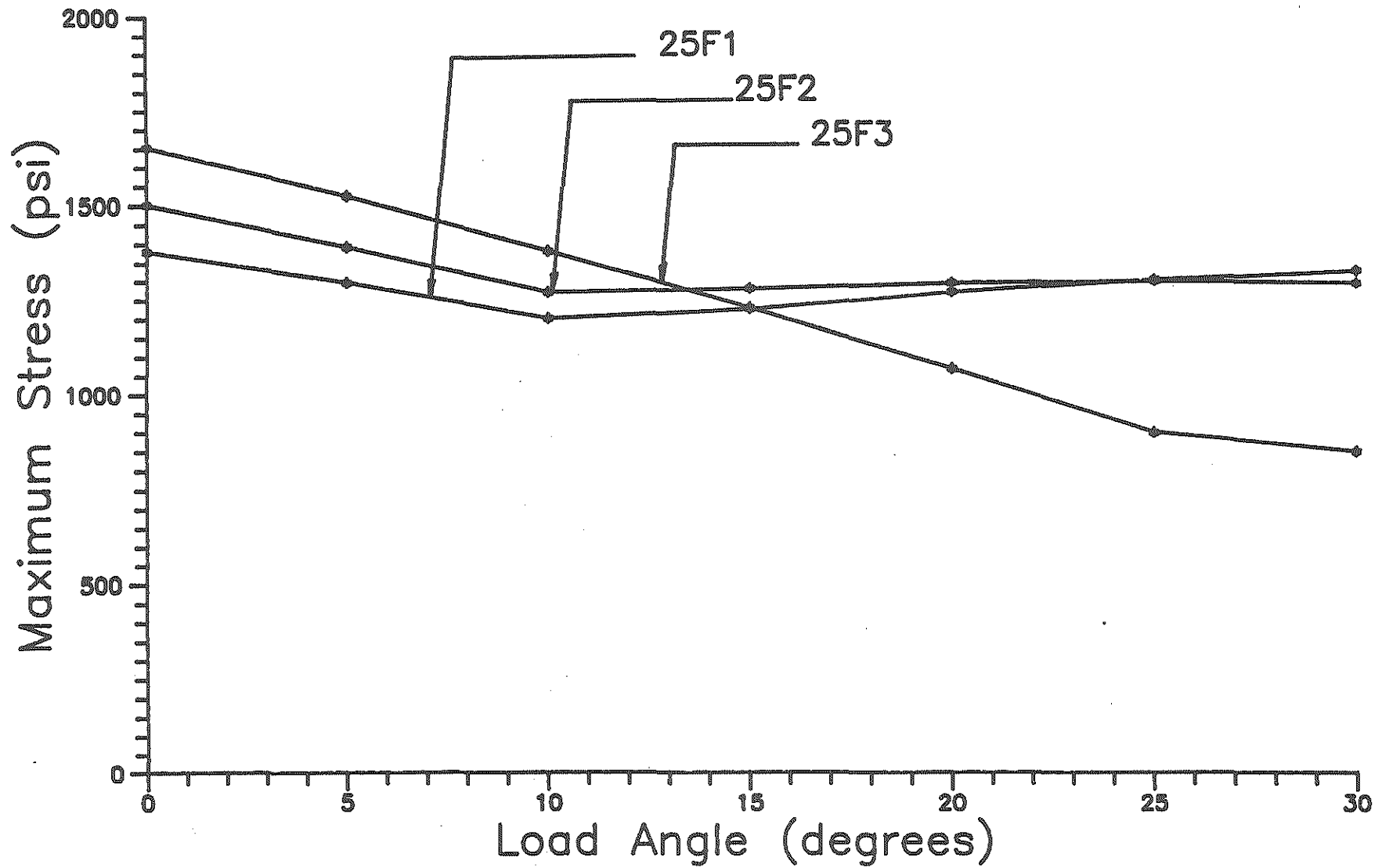


Fig. 12. 25-Foot Bus with Floor-Mounted Seats - Maximum Stresses in Plywood Floor Elements.

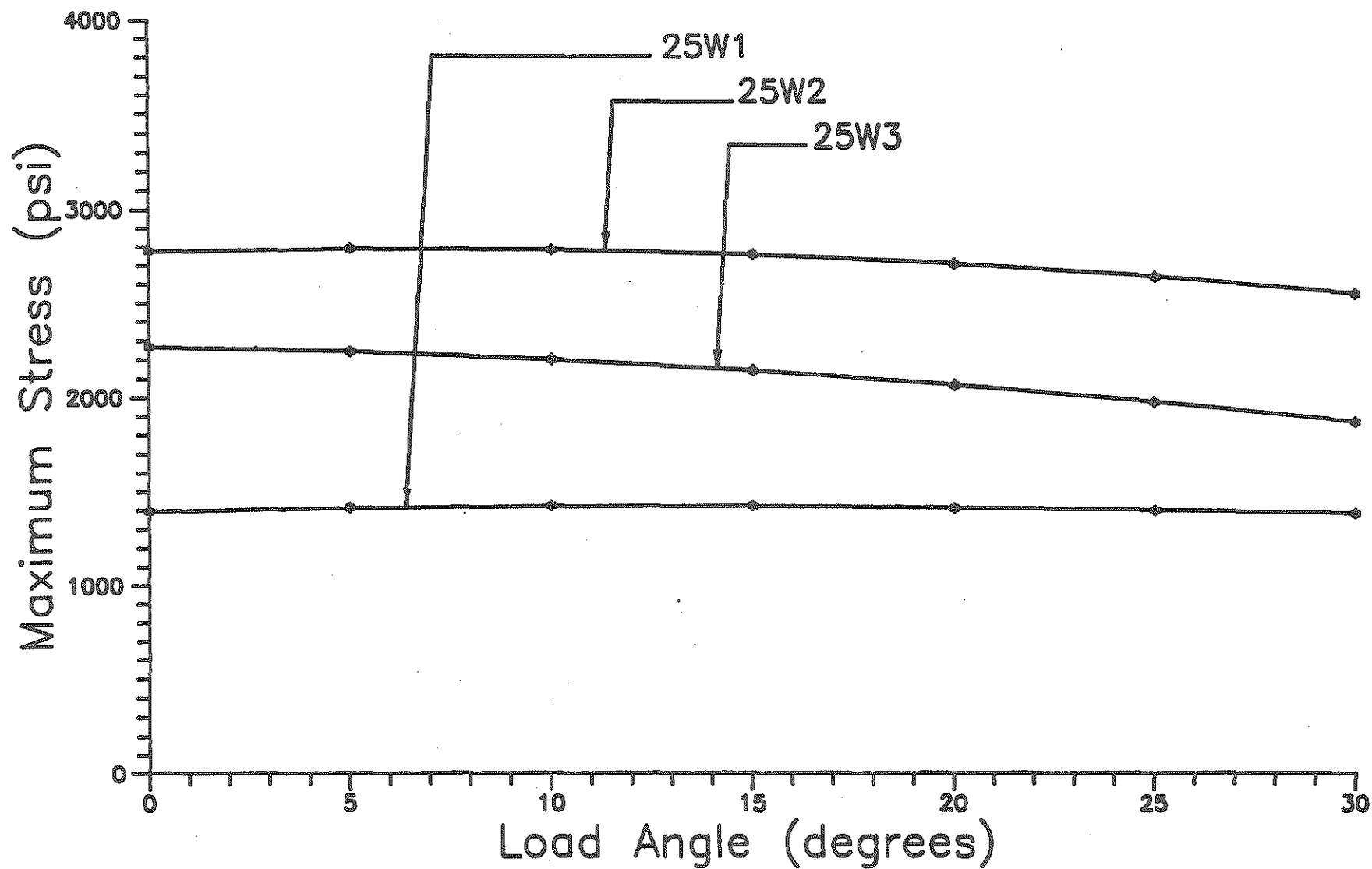


Fig. 13. 25-Foot Bus with Wall-Mounted Seats - Maximum Stresses in Plywood Floor Elements.

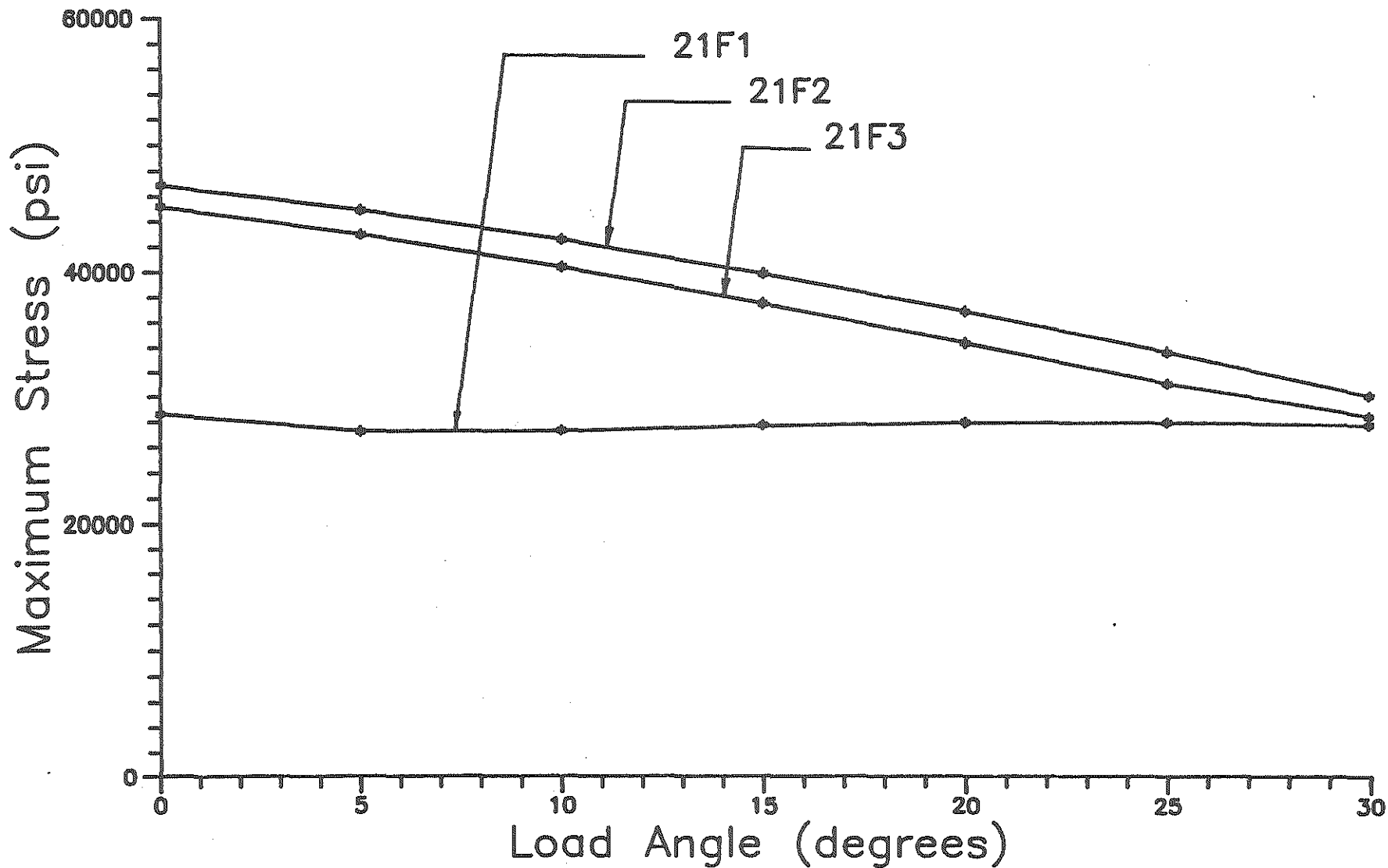


Fig. 14. 21-Foot Bus with Floor-Mounted Seats - Maximum Stresses in Lateral Frame Elements.

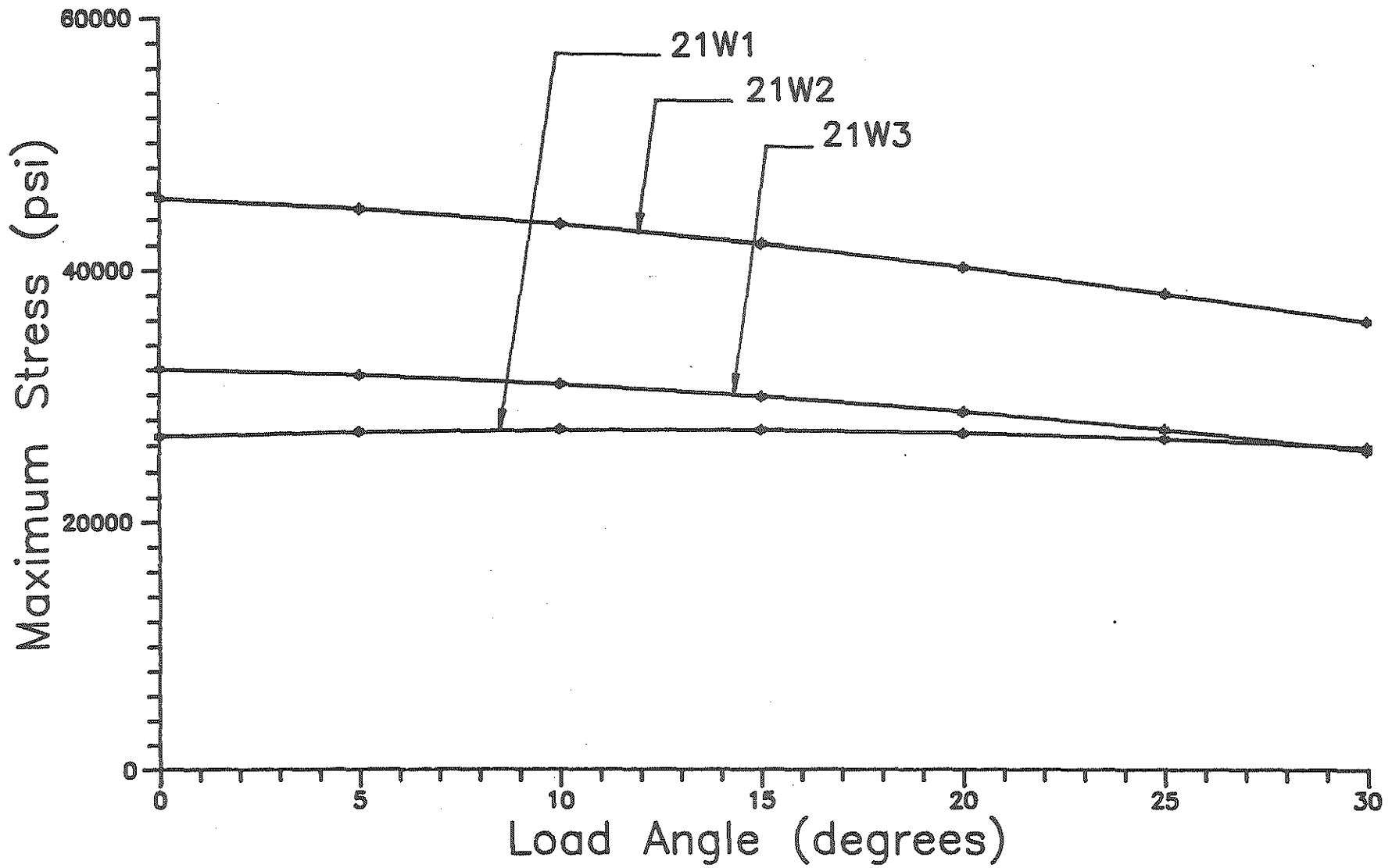


Fig. 15. 21-Foot Bus with Wall-Mounted Seats - Maximum Stresses in Lateral Frame Elements.

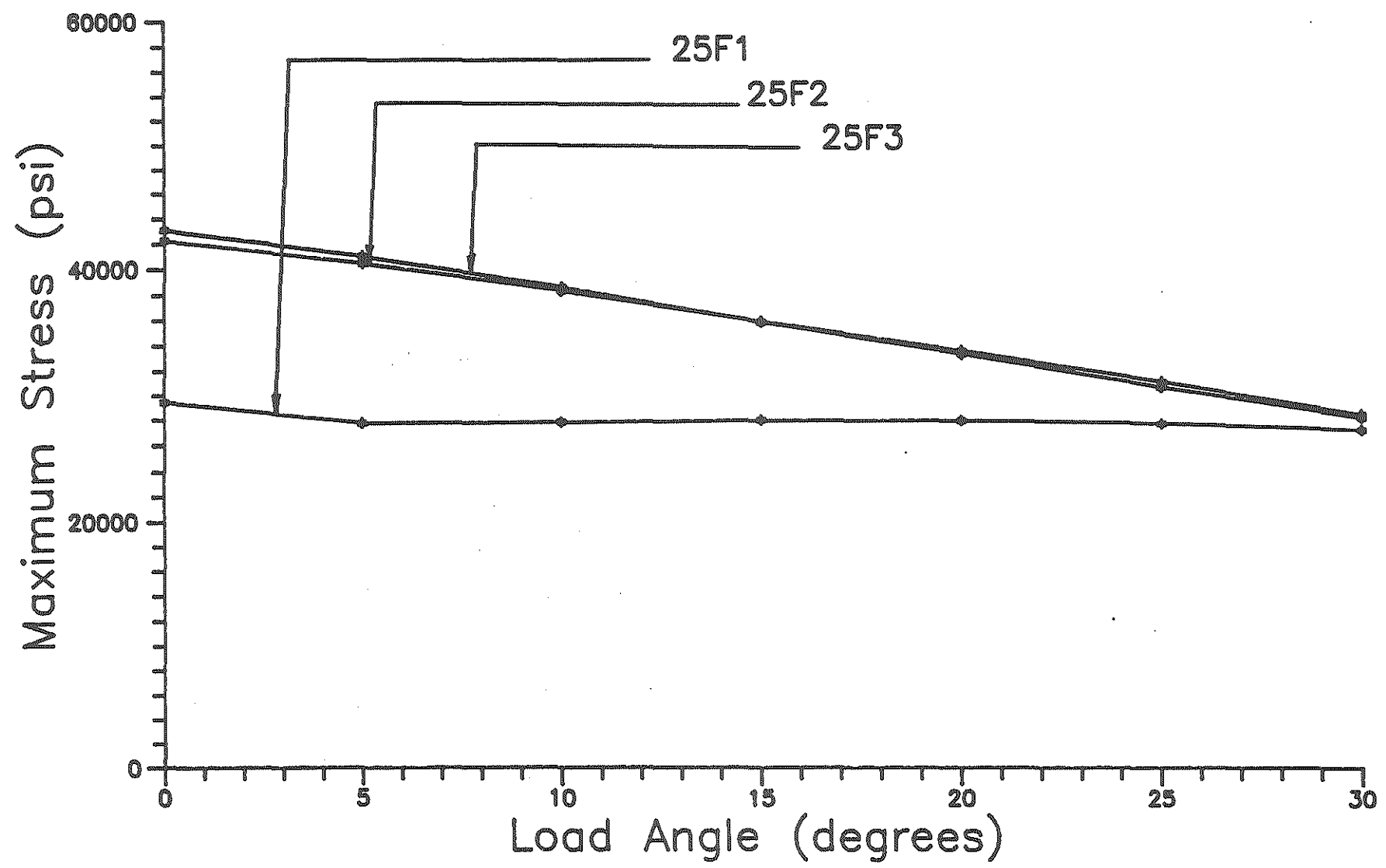


Fig. 16. 25-Foot Bus with Floor-Mounted Seats - Maximum Stresses in Lateral Frame Elements.

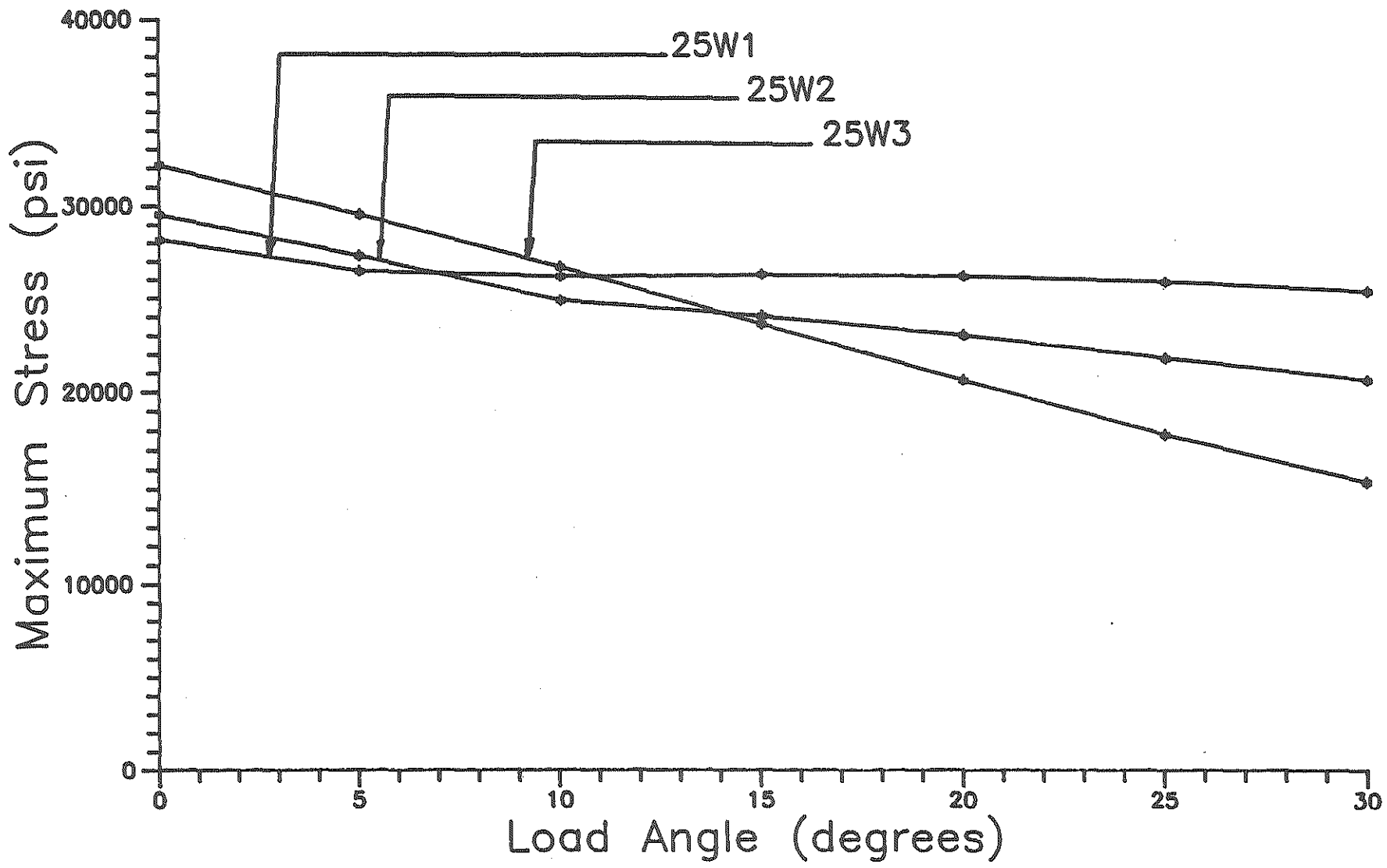


Fig. 17. 25-Foot Bus with Wall-Mounted Seats - Maximum Stresses in Lateral Frame Elements.

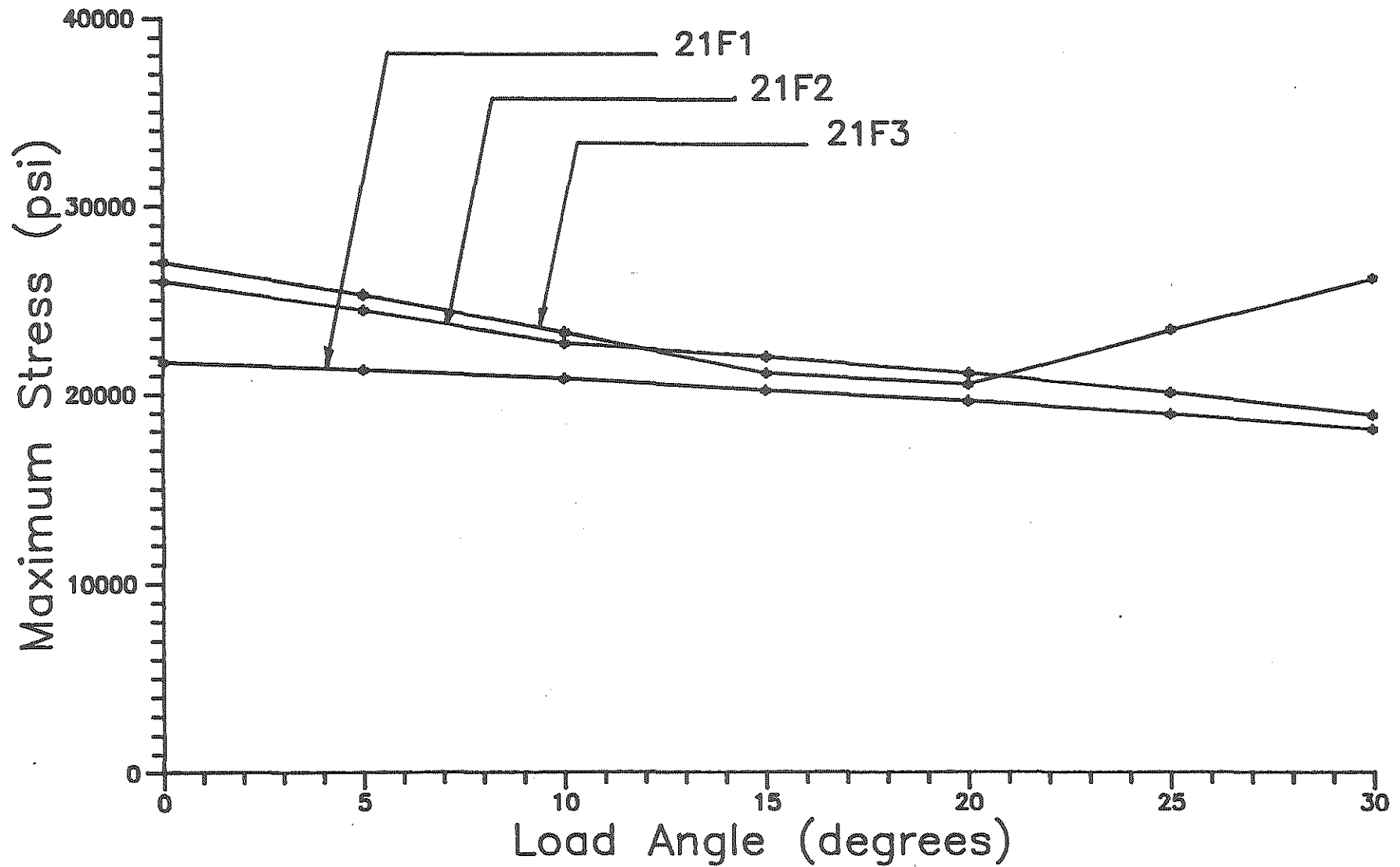


Fig. 18. 21-Foot Bus with Floor-Mounted Seats - Maximum Stresses in Longitudinal Chassis Elements.

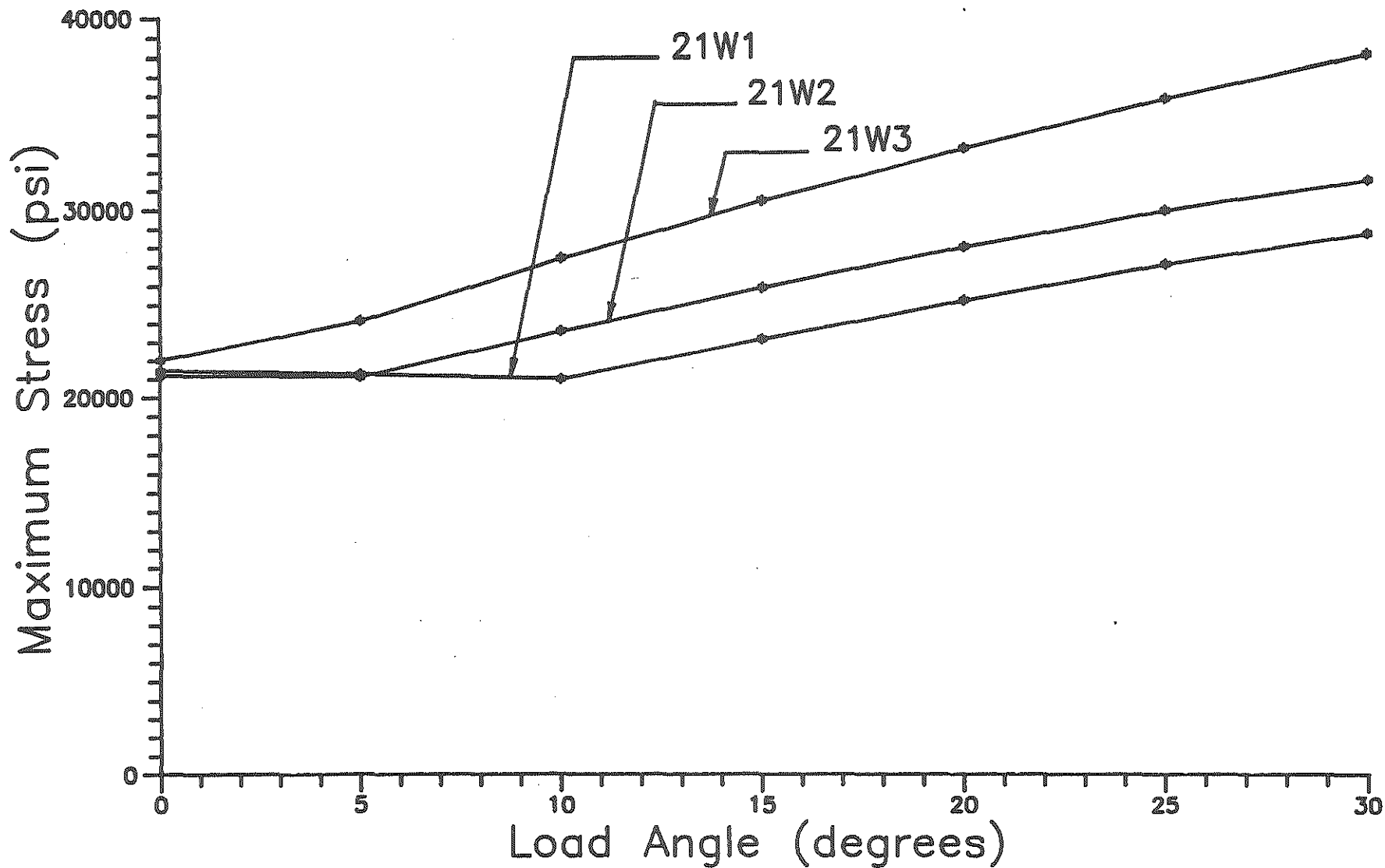


Fig. 19. 21-Foot Bus with Wall-Mounted Seats - Maximum Stresses in Longitudinal Chassis Elements.

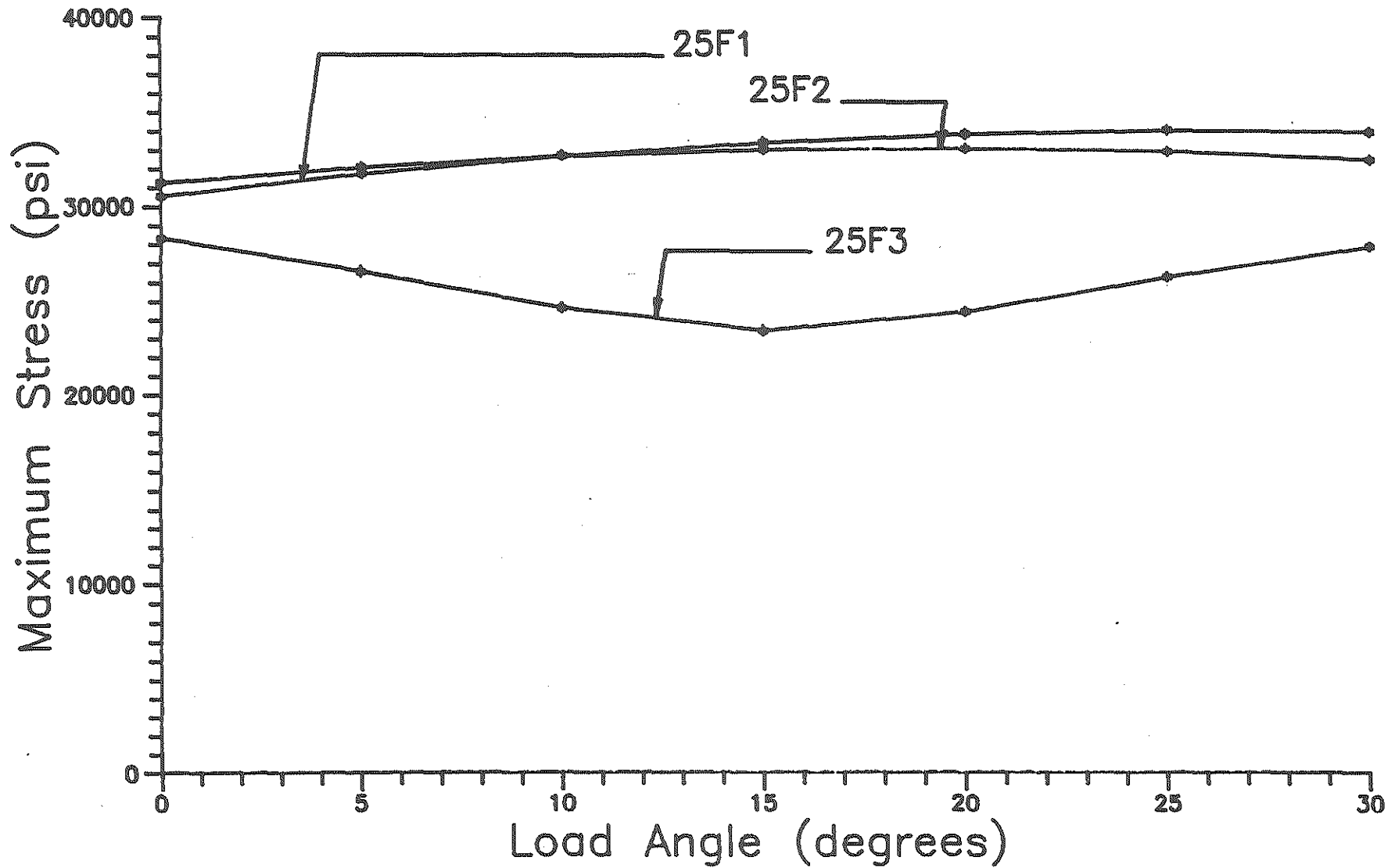


Fig. 20. 25-Foot Bus with Floor-Mounted Seats - Maximum Stresses in Longitudinal Chassis Elements.

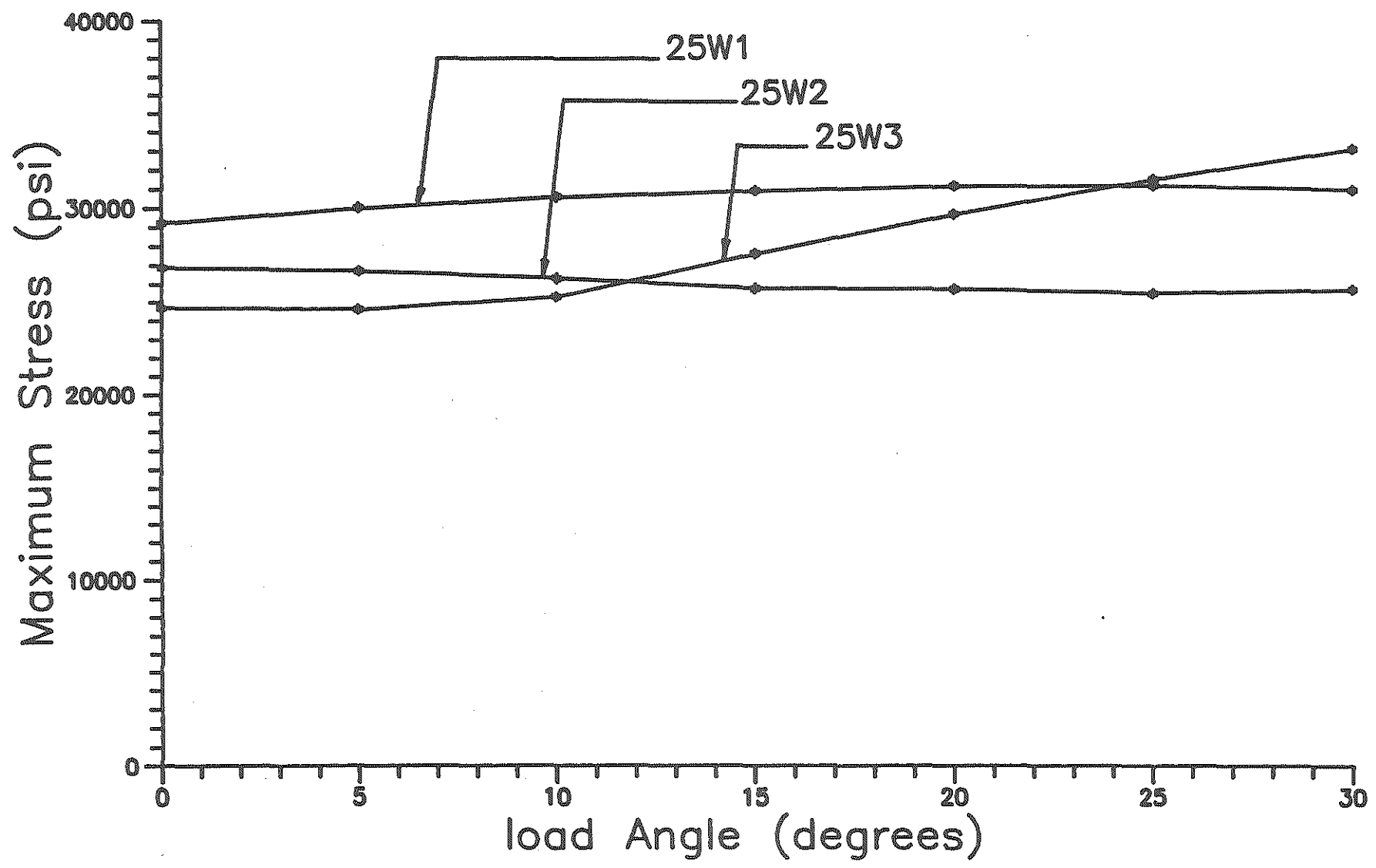


Fig. 21. 25-Foot Bus with Wall-Mounted Seats - Maximum Stresses in Longitudinal Chassis Elements.

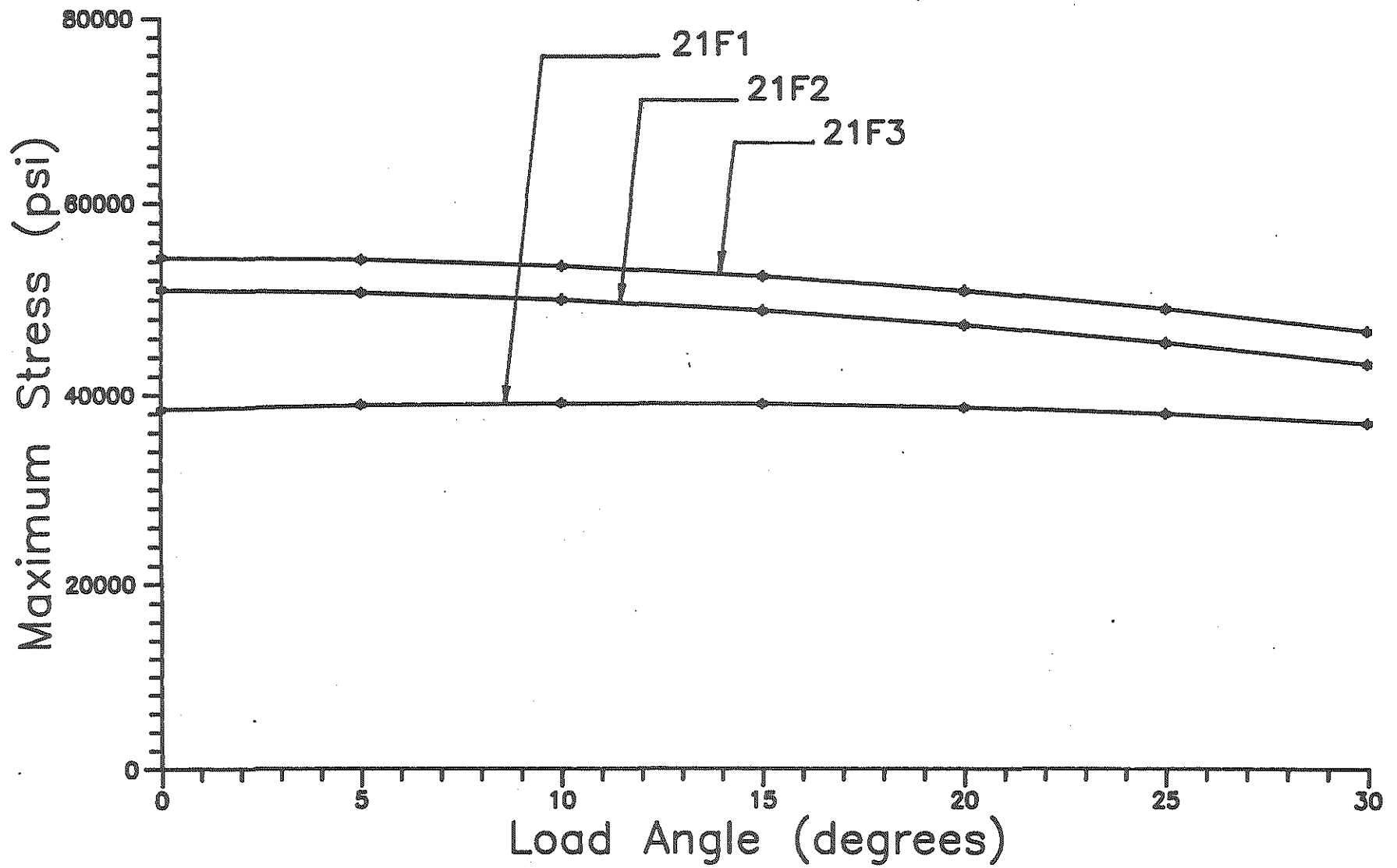


Fig. 22. 21-Foot Bus with Floor-Mounted Seats - Maximum Stresses in Body Elements.

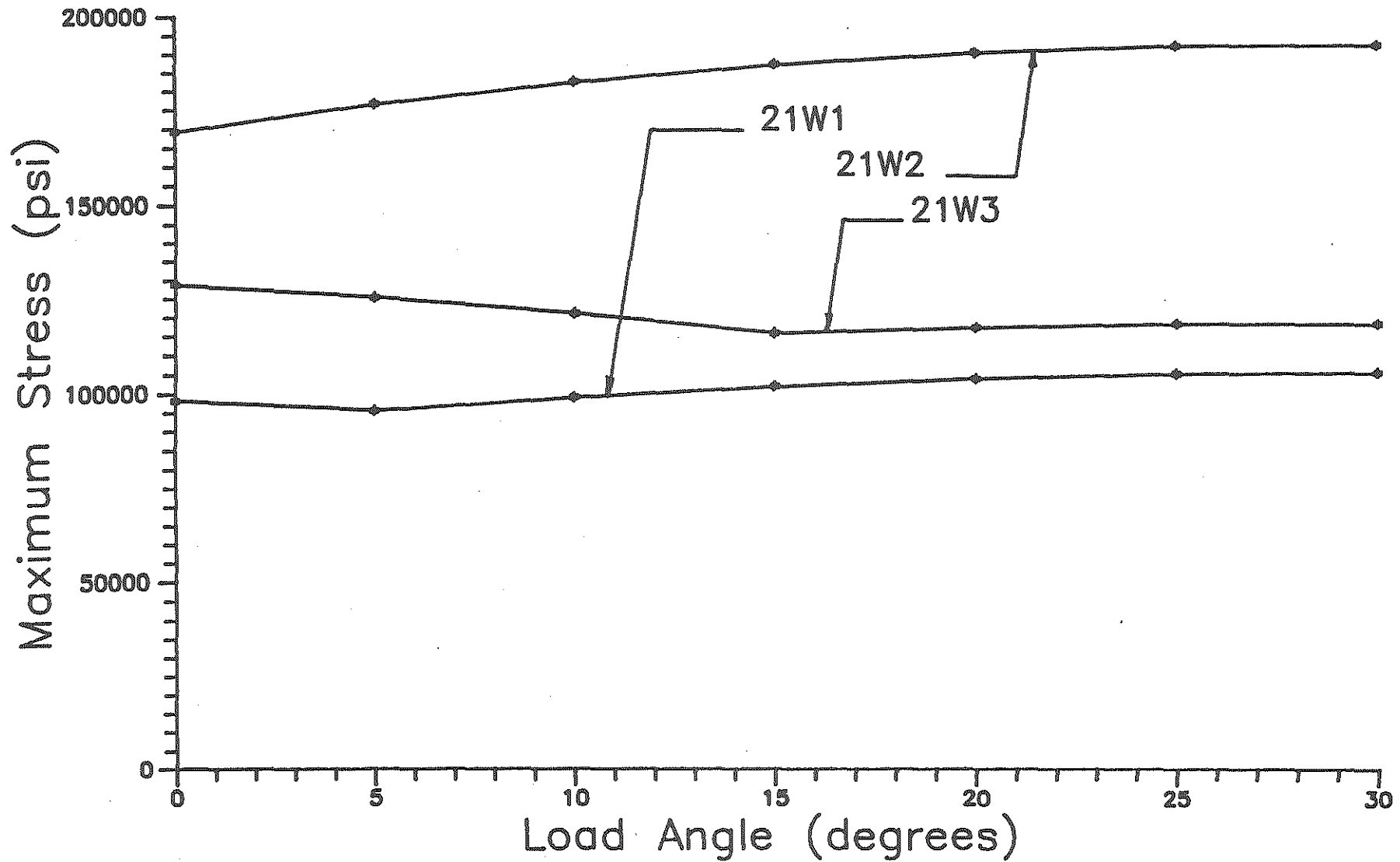


Fig. 23. 21-Foot Bus with Wall-Mounted Seats - Maximum Stresses in Body Elements.

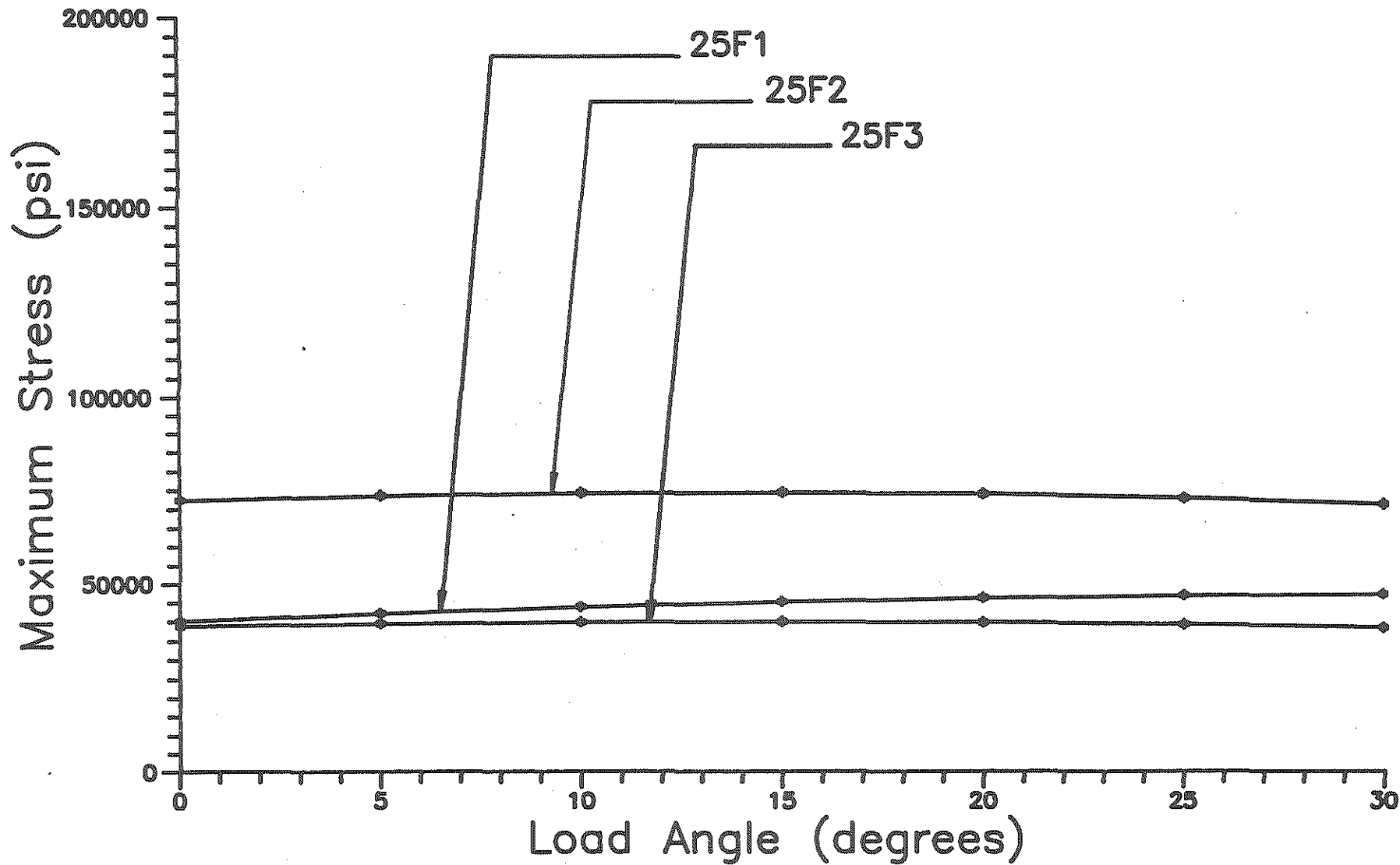


Fig. 24. 25-Foot Bus with Floor-Mounted Seats - Maximum Stresses in Body Elements.

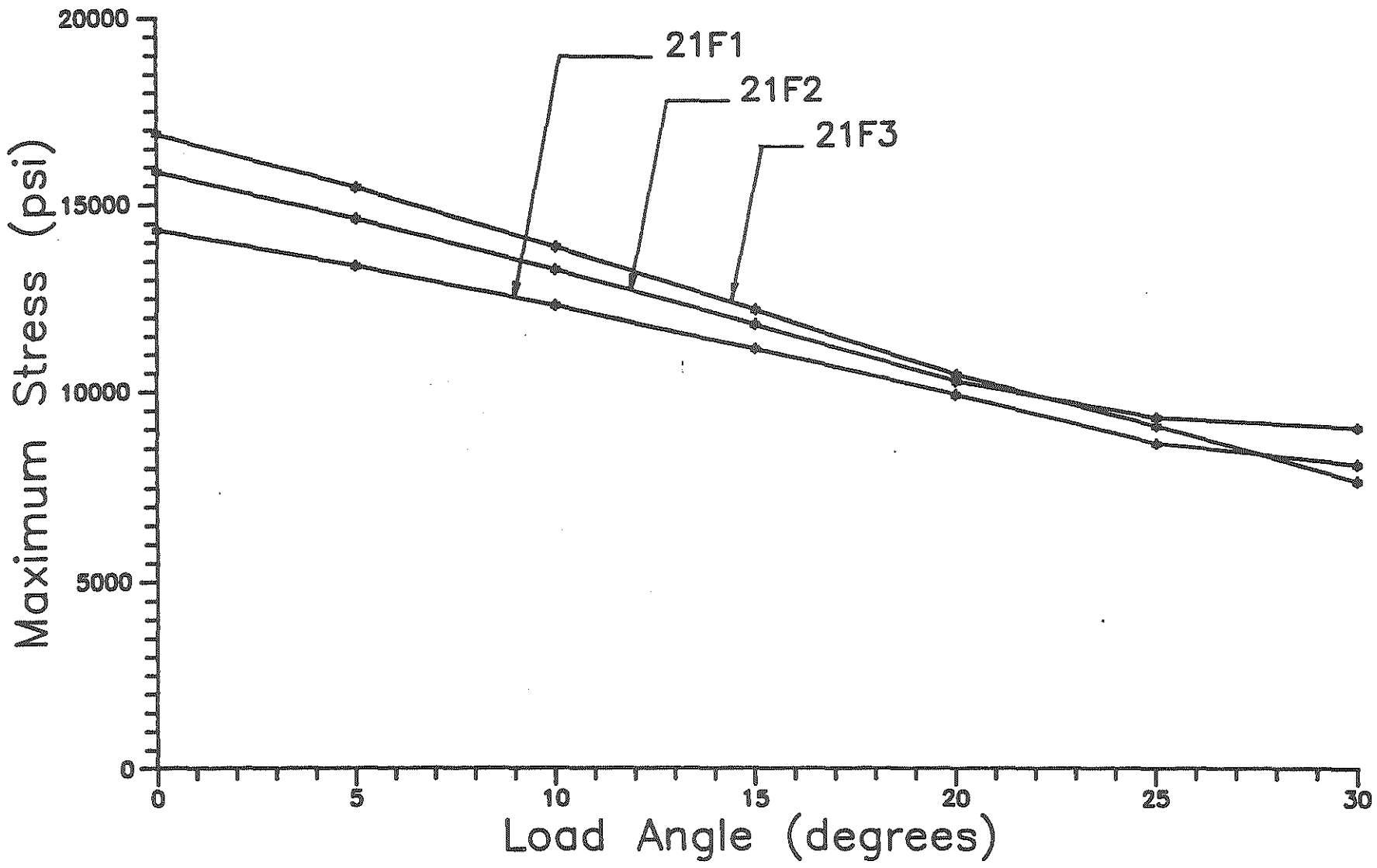


Fig. 26. 21-Foot Bus with Floor-Mounted Seats - Maximum Stresses in Steel Plate Elements.

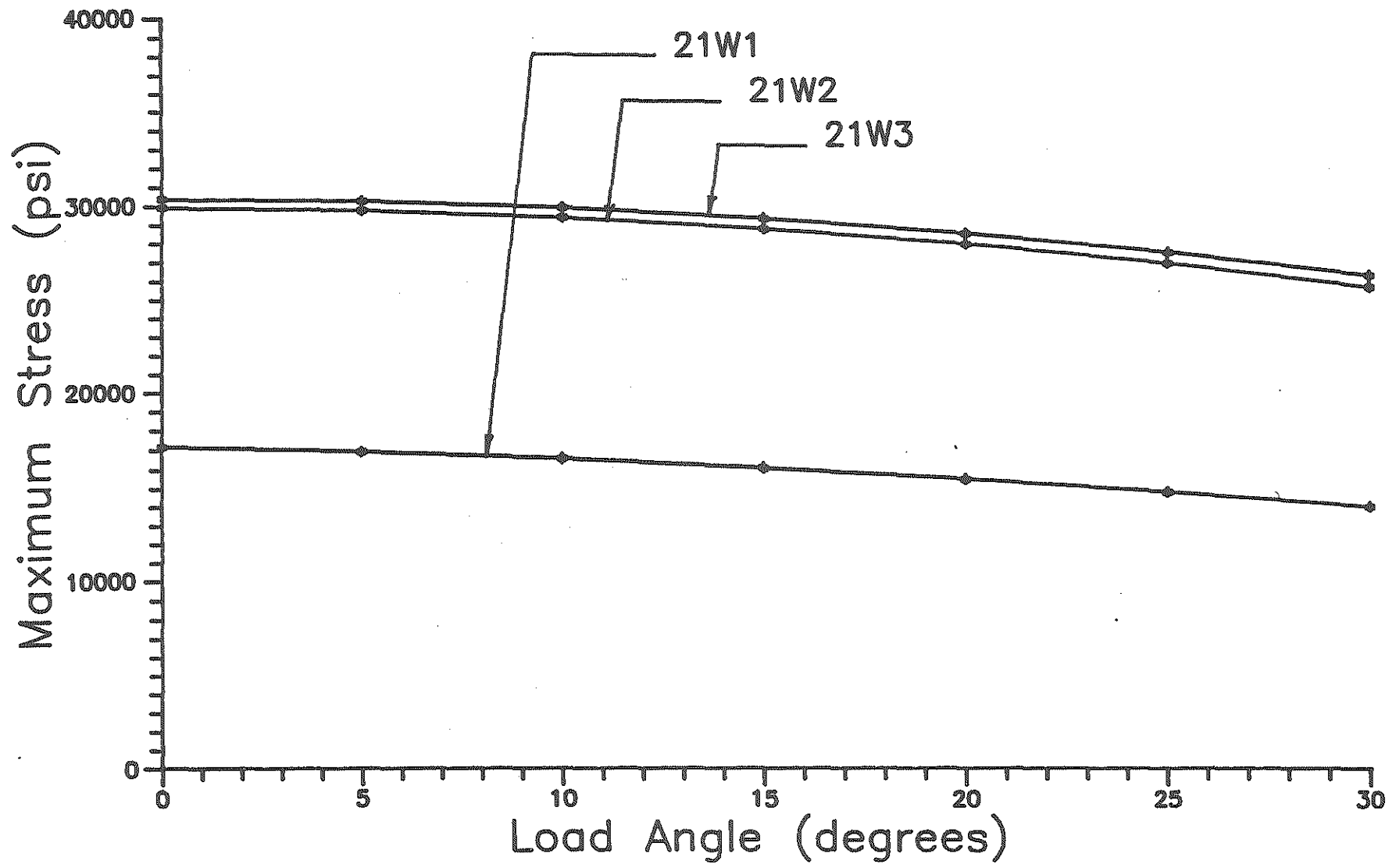


Fig. 27. 21-Foot Bus with Wall-Mounted Seats - Maximum Stresses in Steel Plate Elements.

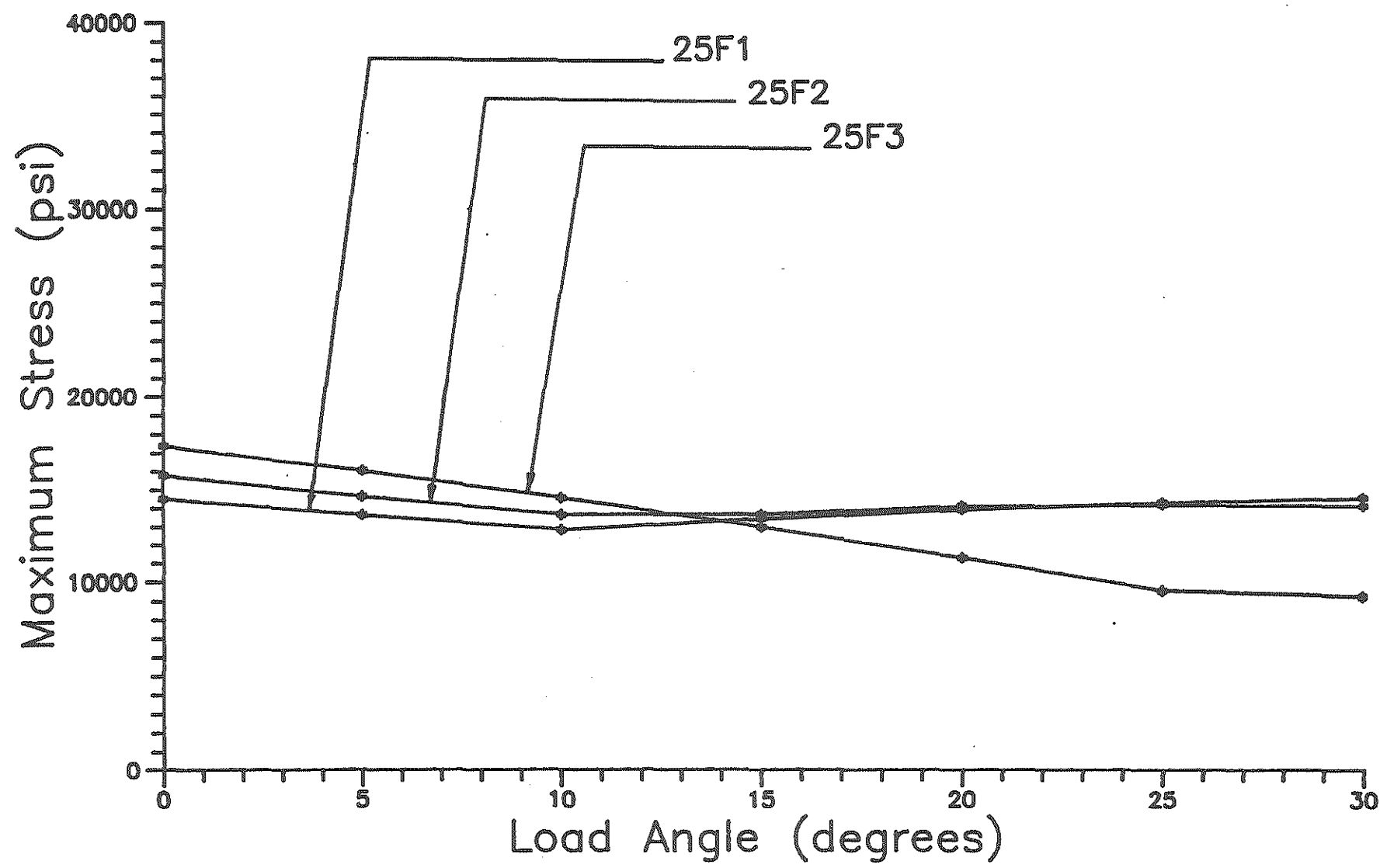


Fig. 28. 25-Foot Bus with Floor-Mounted Seats - Maximum Stresses in Steel Plate Elements.

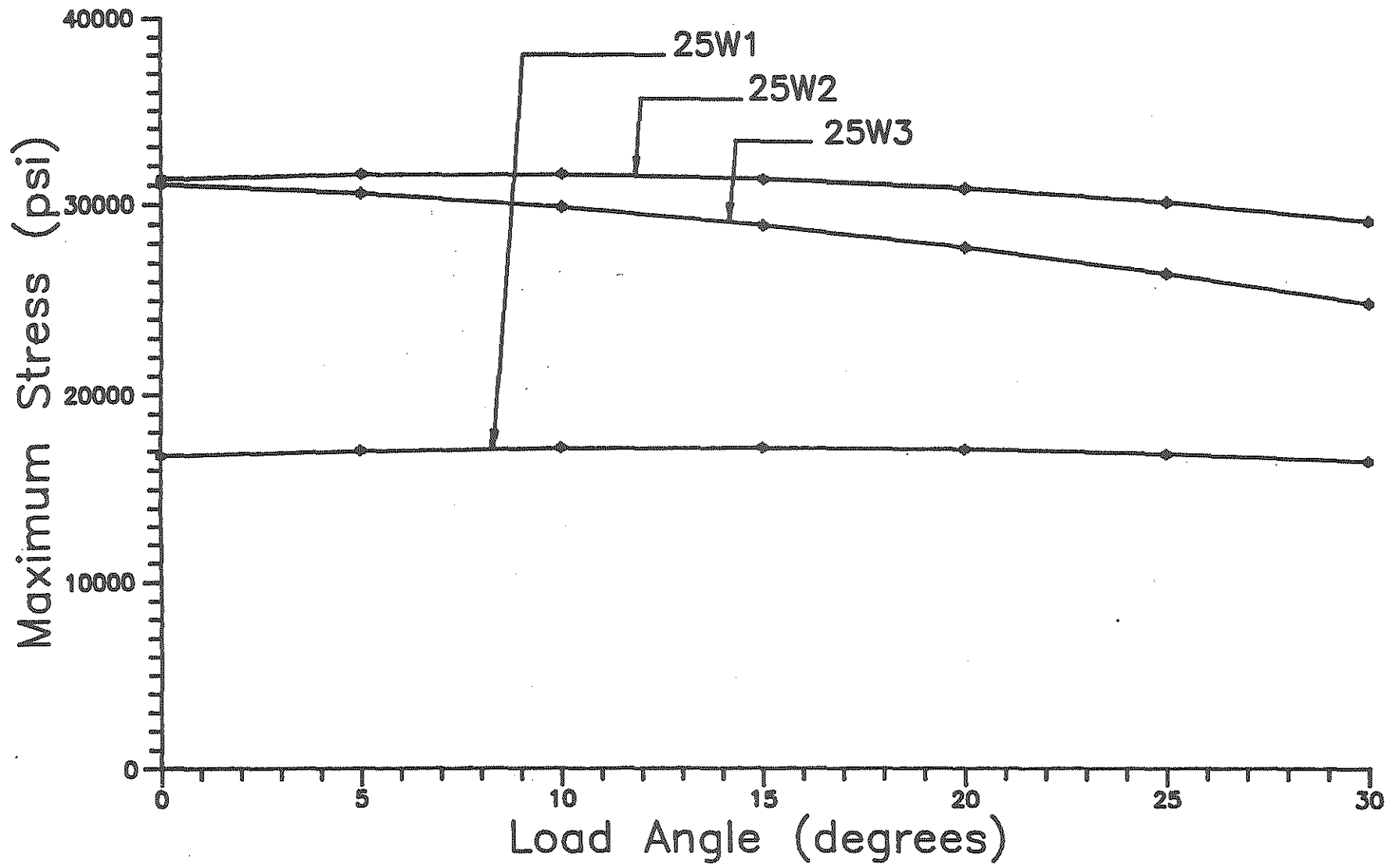


Fig. 29. 25-Foot Bus with Wall-Mounted Seats - Maximum Stresses in Steel Plate Elements.

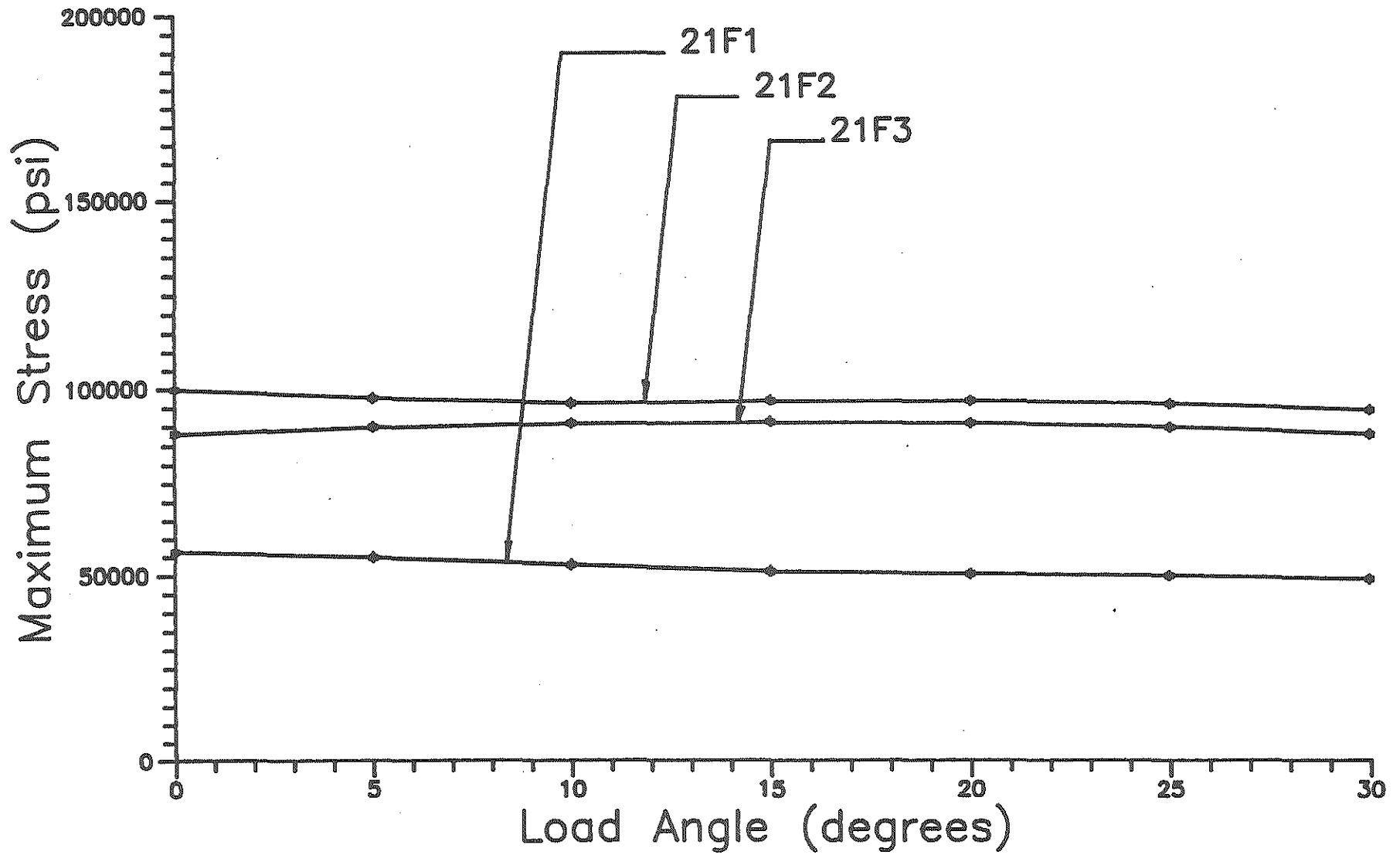


Fig. 30. 21-Foot Bus with Floor-Mounted Seats - Maximum Stresses in Perimeter Floor Elements.

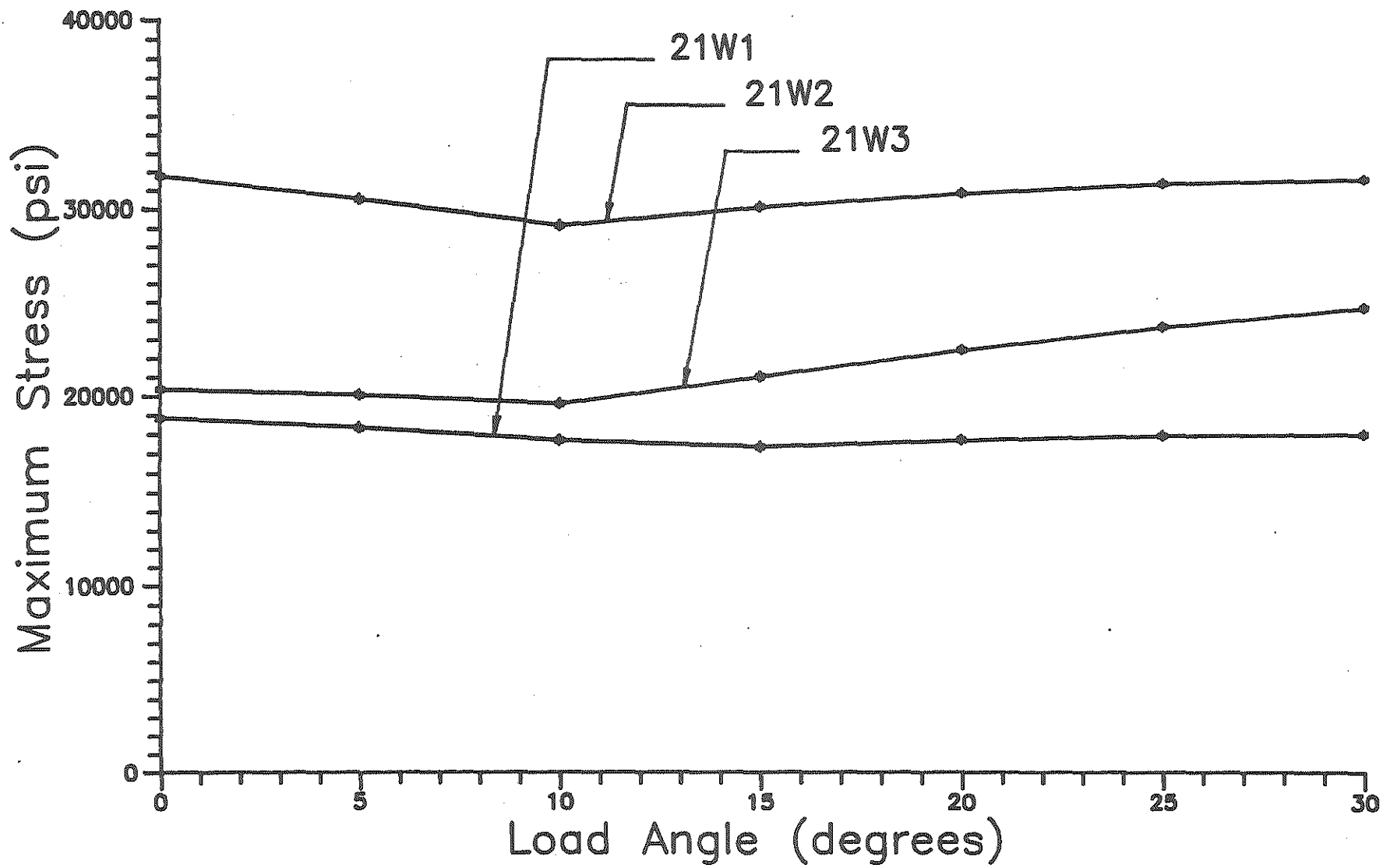


Fig. 31. 21-Foot Bus with Wall-Mounted Seats - Maximum Stresses in Perimeter Floor Elements.

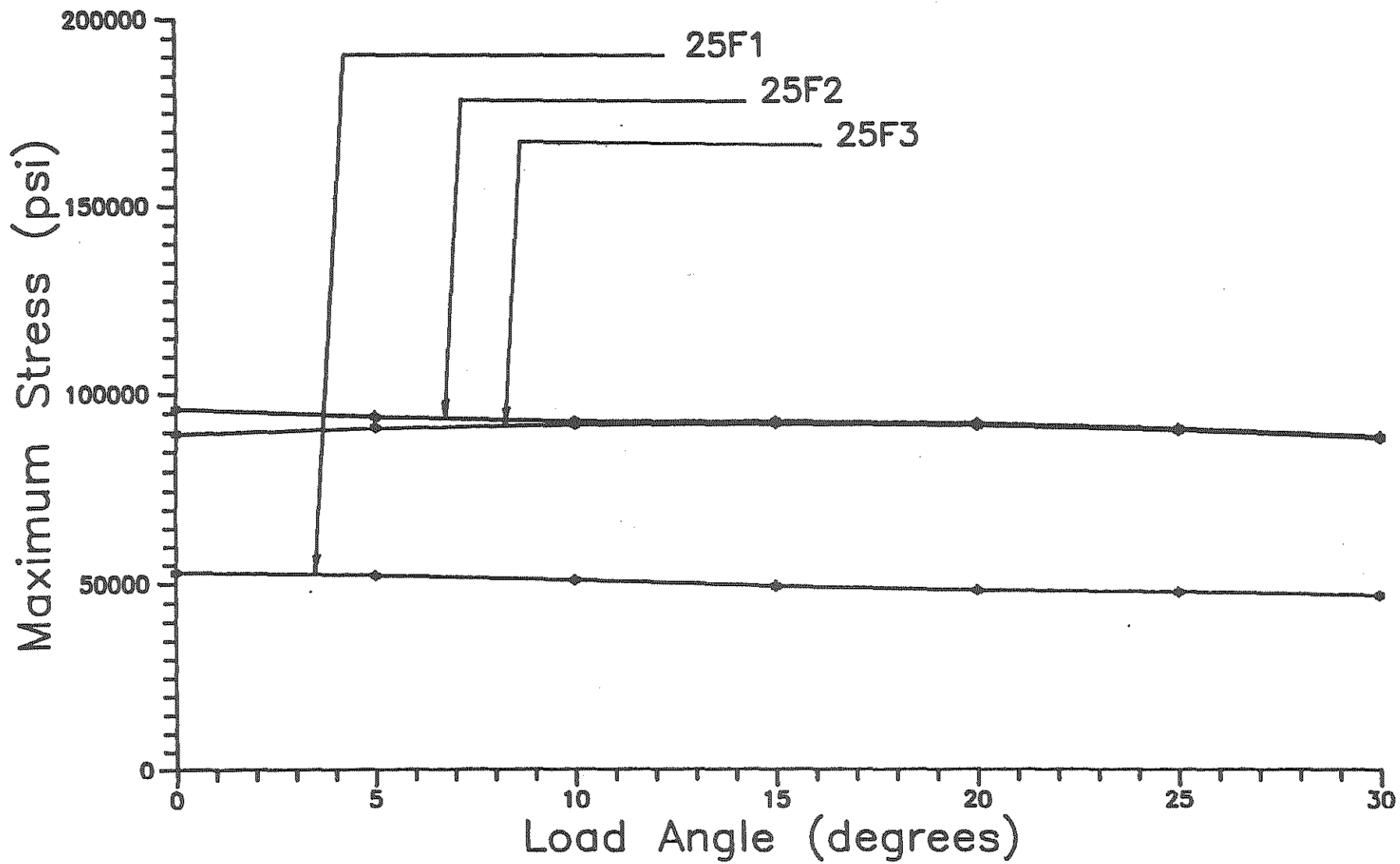


Fig. 32. 25-Foot Bus with Floor-Mounted Seats - Maximum Stresses in Perimeter Floor Elements.

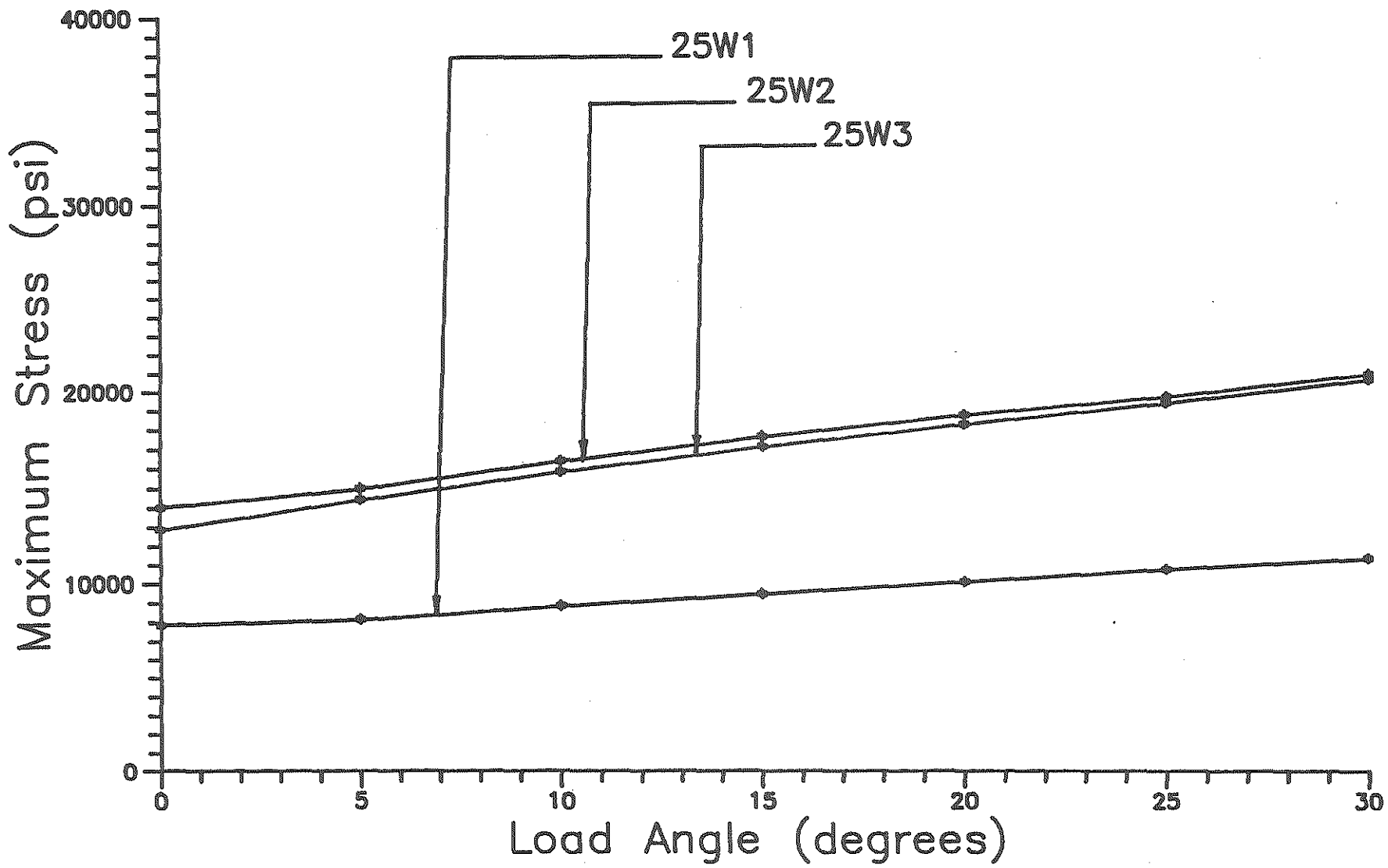


Fig. 33. 25-Foot Bus with Wall-Mounted Seats - Maximum Stresses in Perimeter Floor Elements.

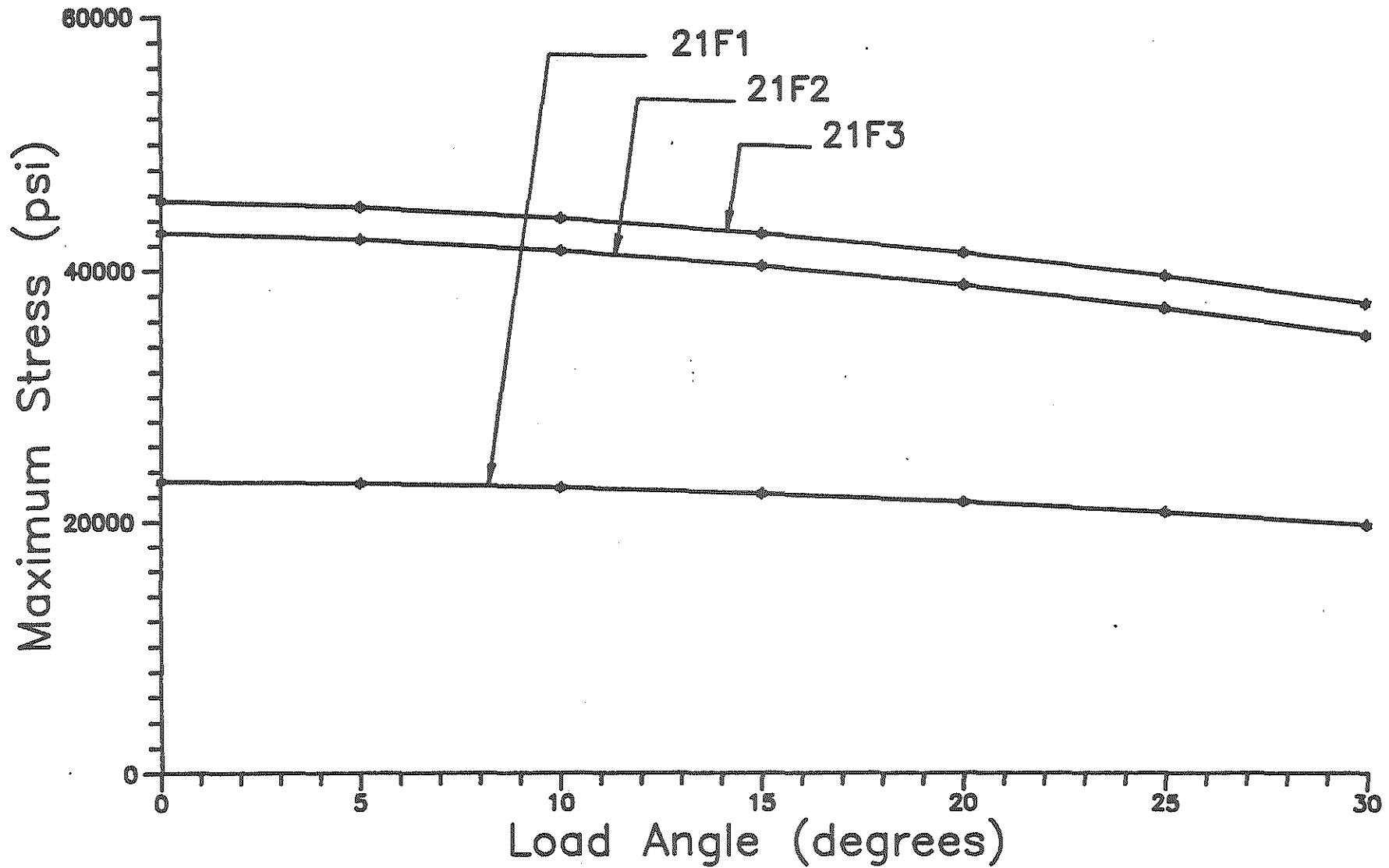


Fig. 34. 21-Foot Bus with Floor-Mounted Seats - Maximum Stresses in Skirting Elements.

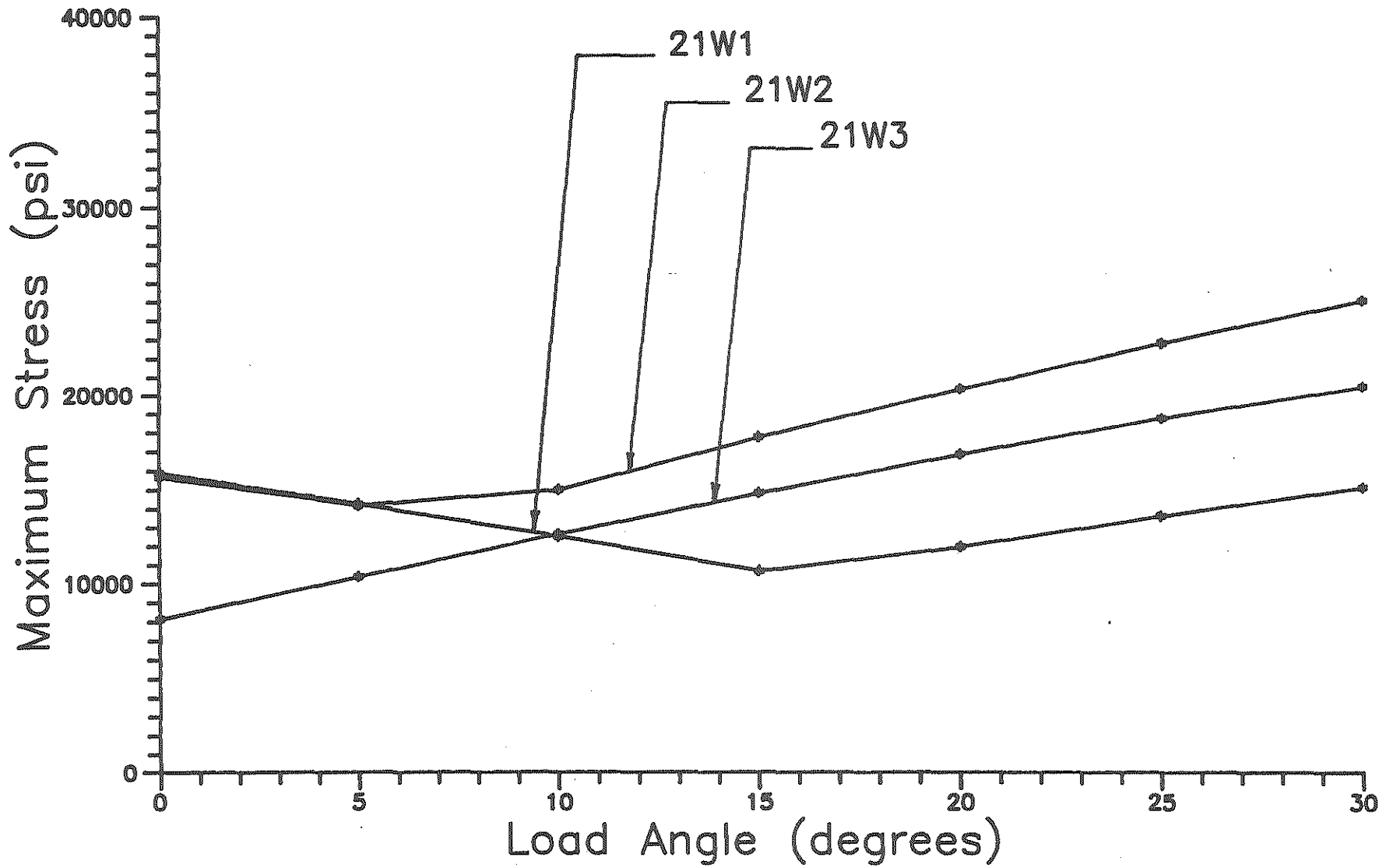


Fig. 35. 21-Foot Bus with Wall-Mounted Seats - Maximum Stresses in Skirting Elements.

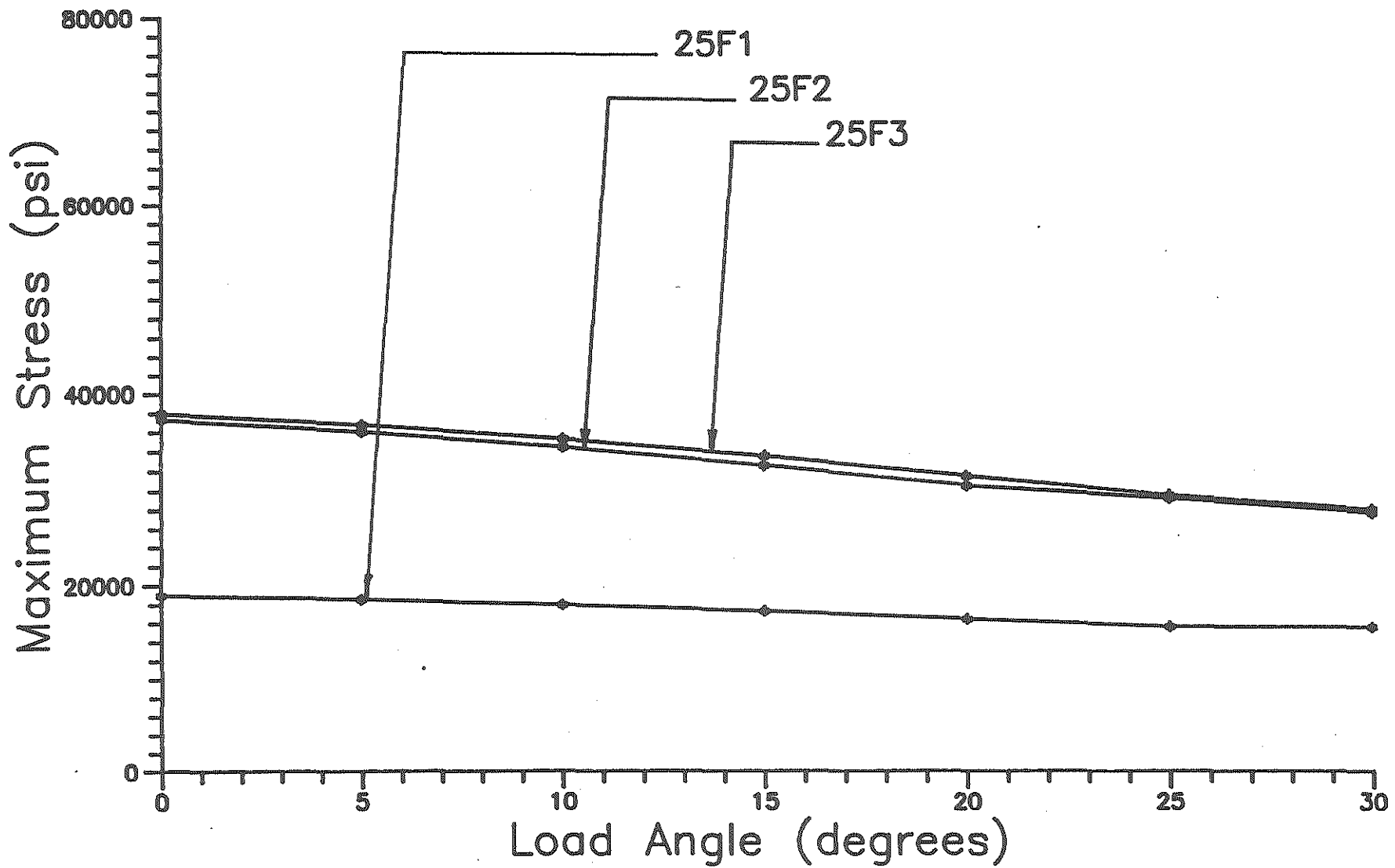


Fig. 36. 25-Foot Bus with Floor-Mounted Seats - Maximum Stresses in Skirting Elements.

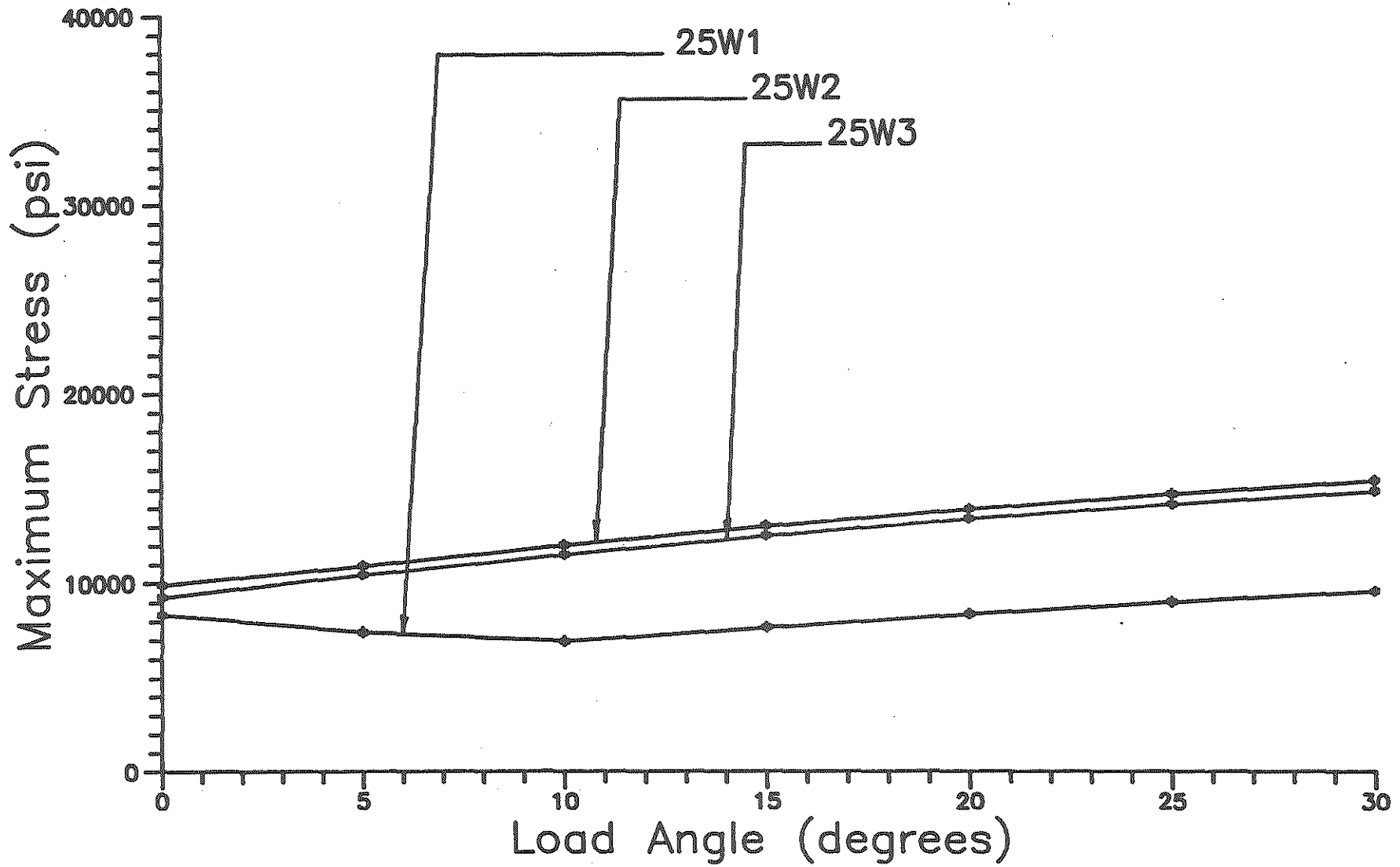


Fig. 37. 25-Foot Bus with Wall-Mounted Seats - Maximum Stresses in Skirting Elements.

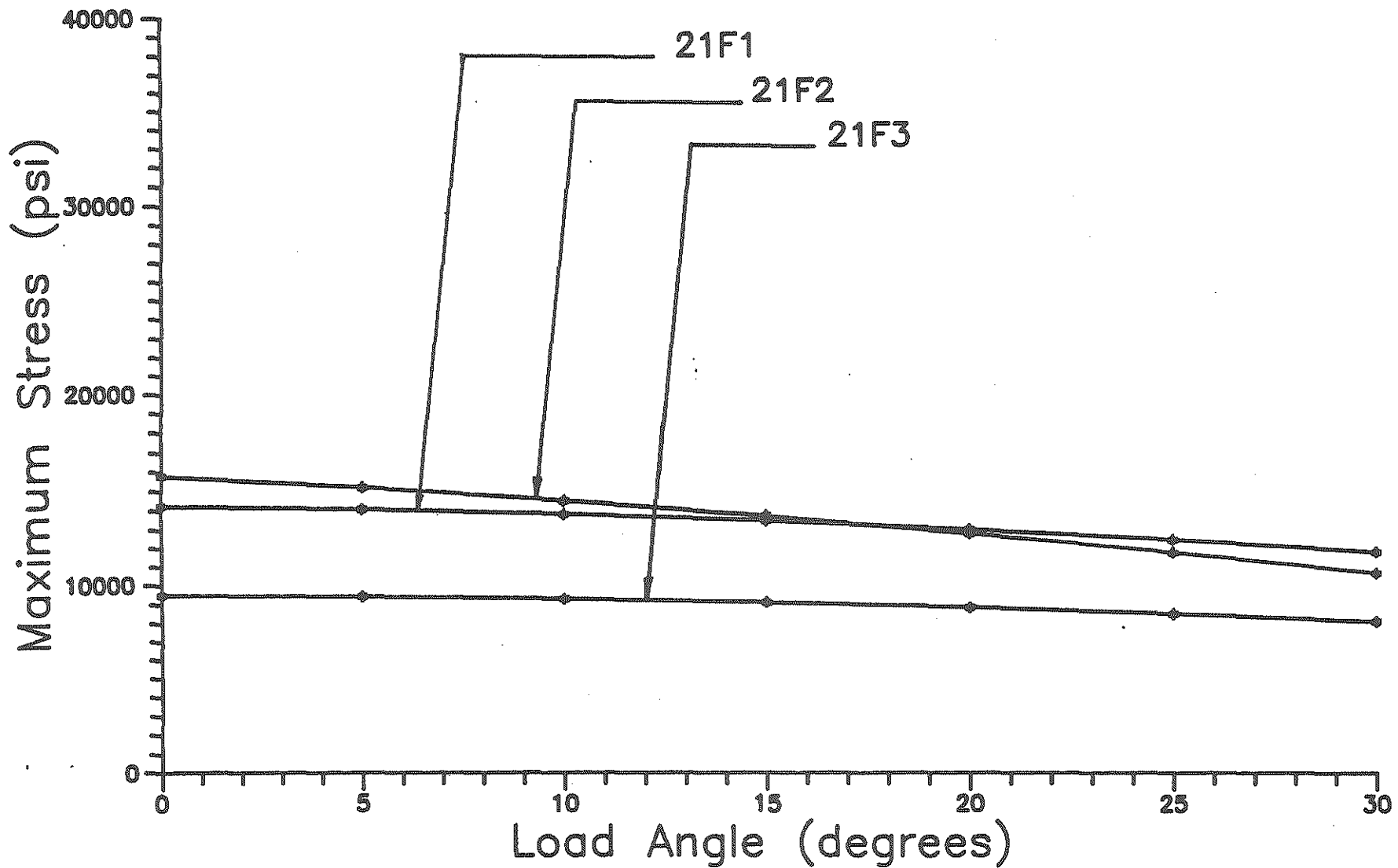


Fig. 38. 21-Foot Bus with Floor-Mounted Seats - Maximum Stresses in Wheel Well Elements.

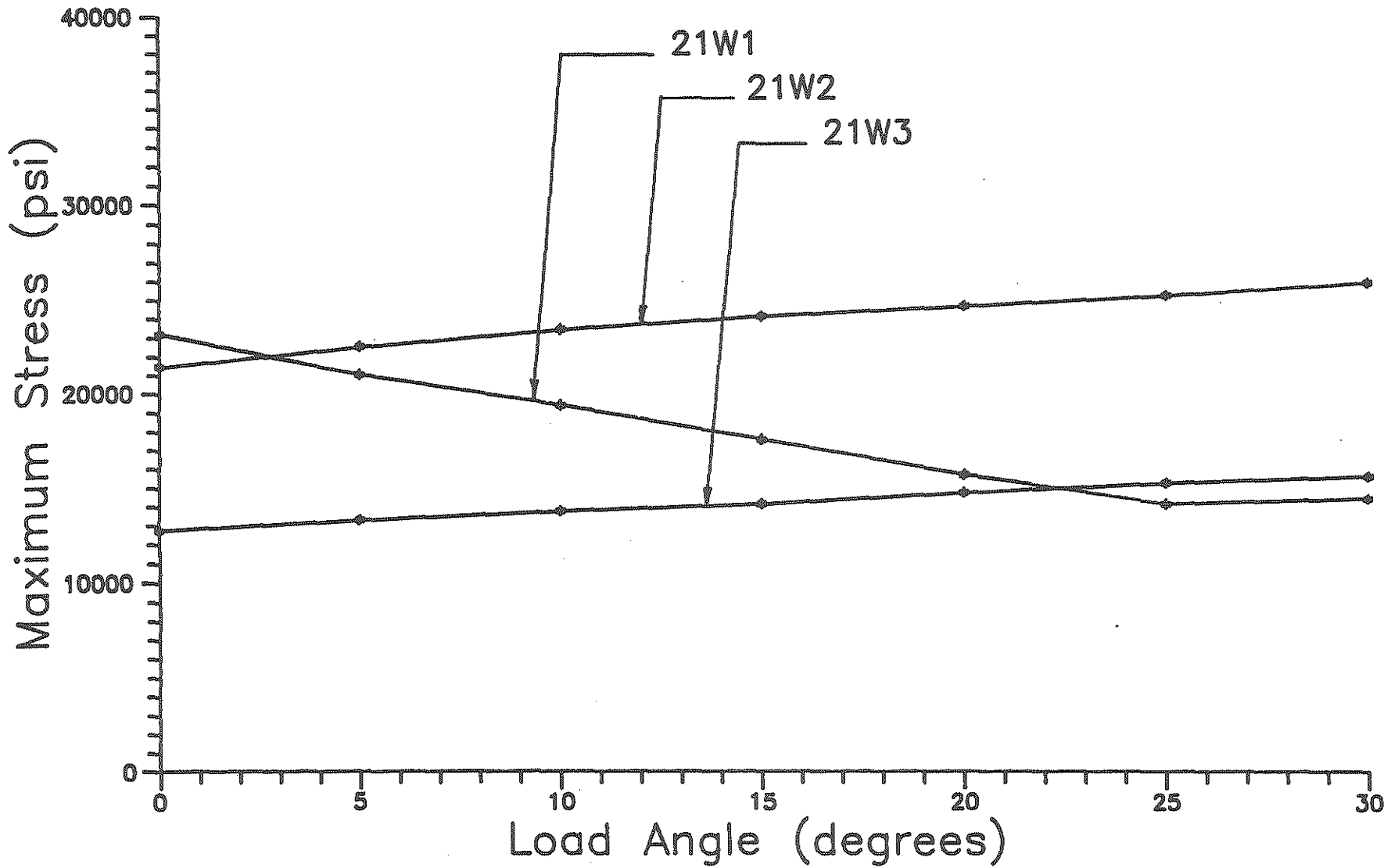


Fig. 39. 21-Foot Bus with Wall-Mounted Seats - Maximum Stresses in Wheel Well Element.

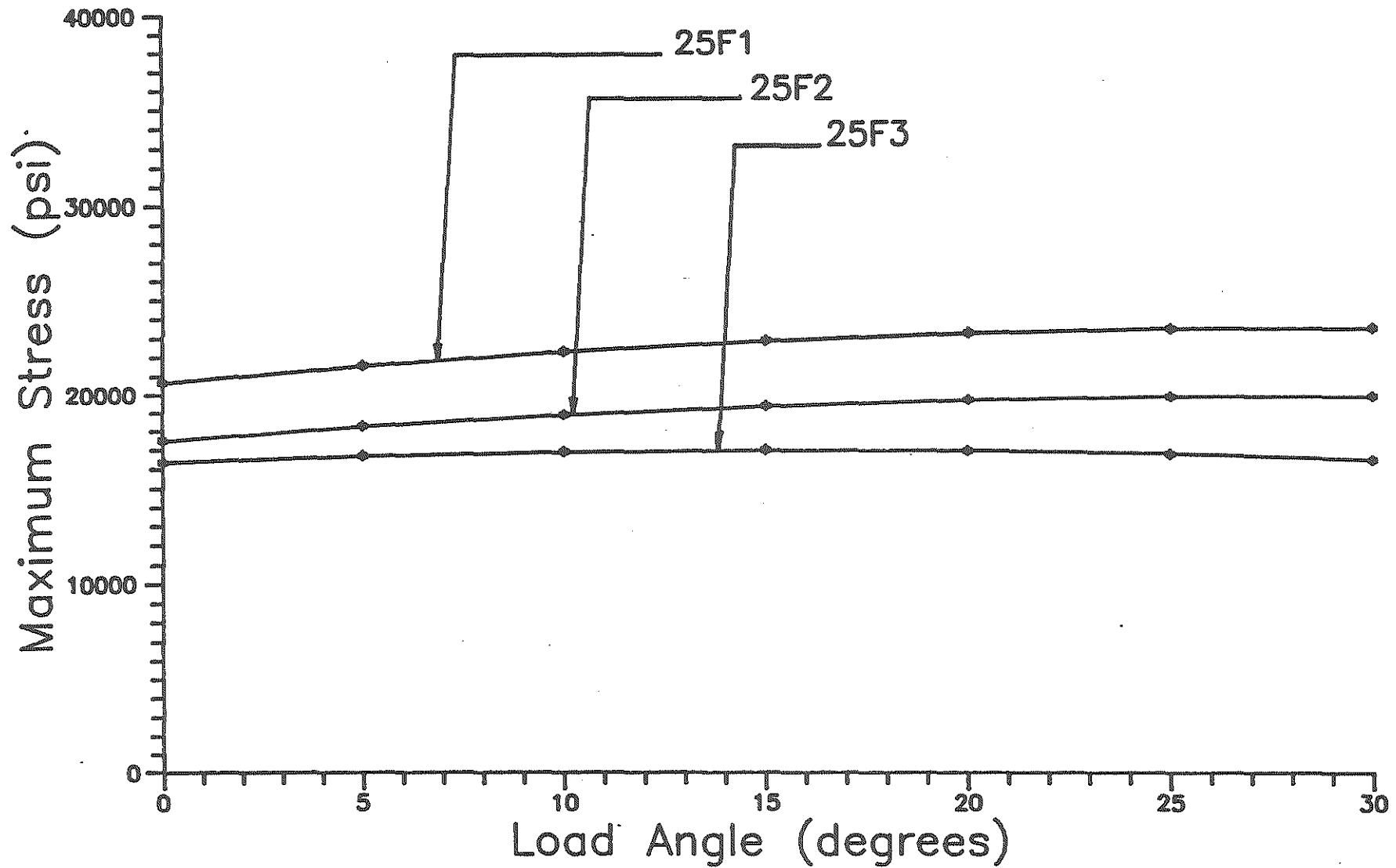


Fig. 40. 25-Foot Bus with Floor-Mounted Seats - Maximum Stresses in Wheel Well Elements.

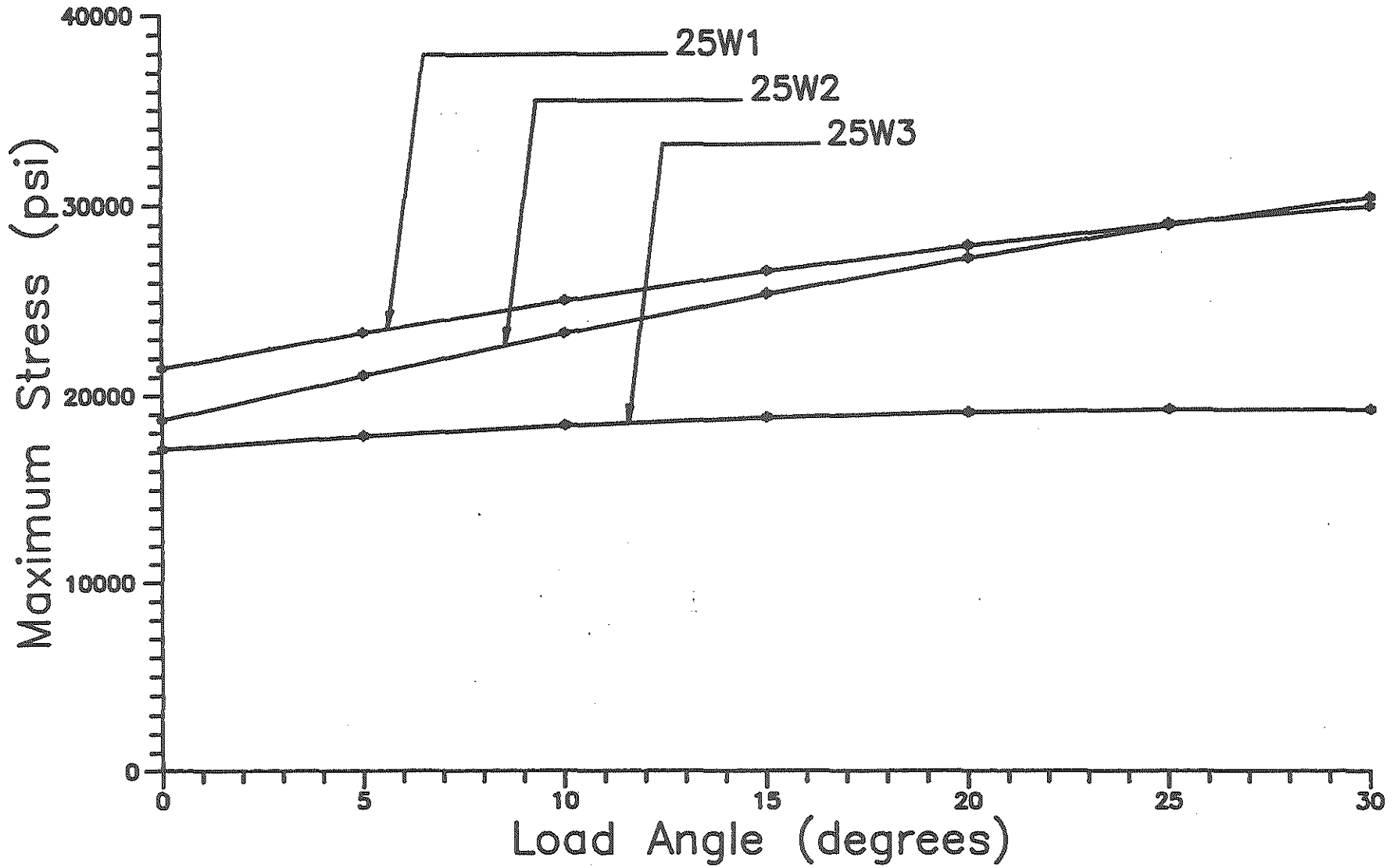


Fig. 41. 25-Foot Bus with Wall-Mounted Seats - Maximum Stresses in Wheel Well-Elements.

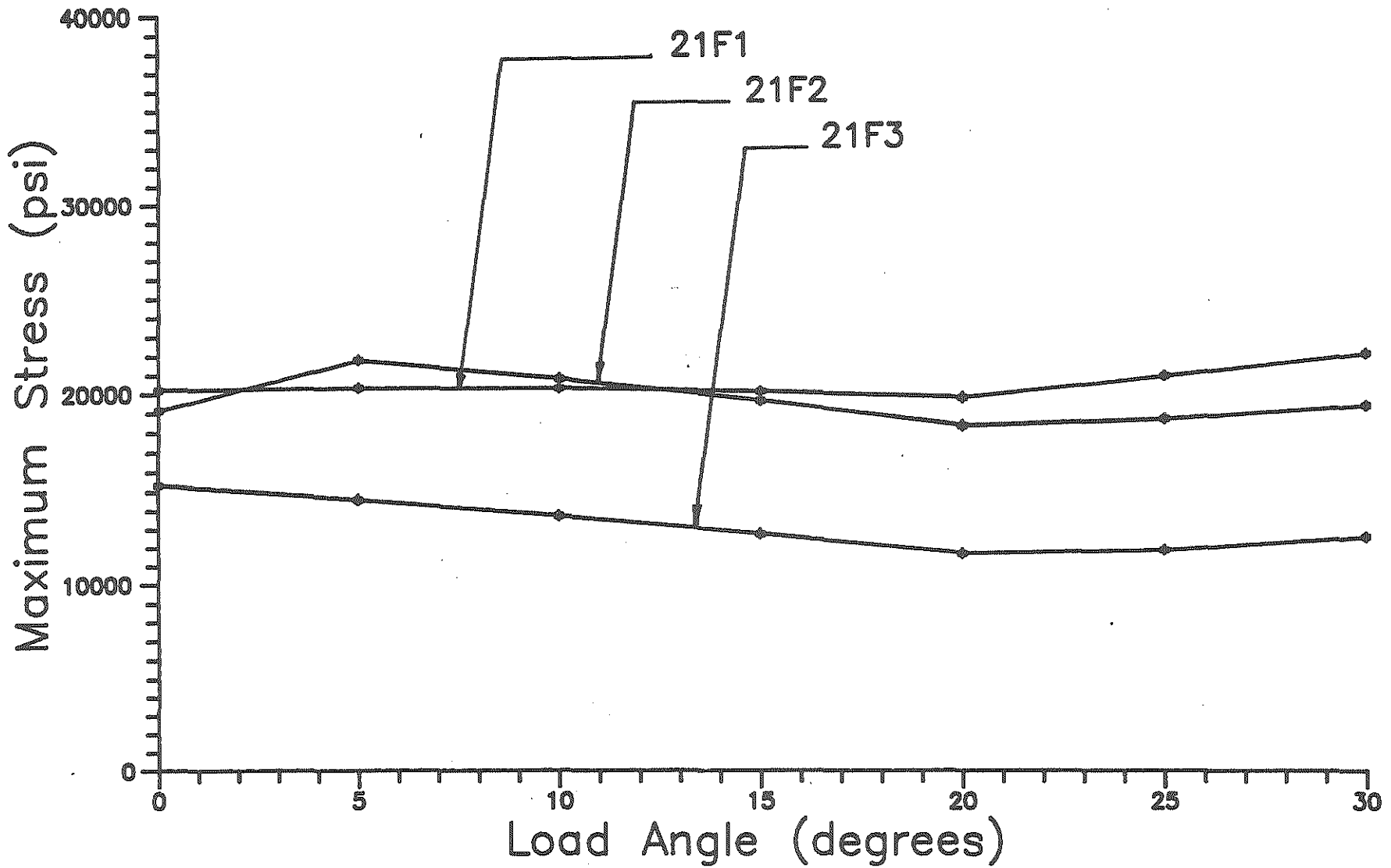


Fig. 42. 21-Foot Bus with Floor-Mounted Seats - Maximum Stresses in Longitudinal Chassis Cap Elements.

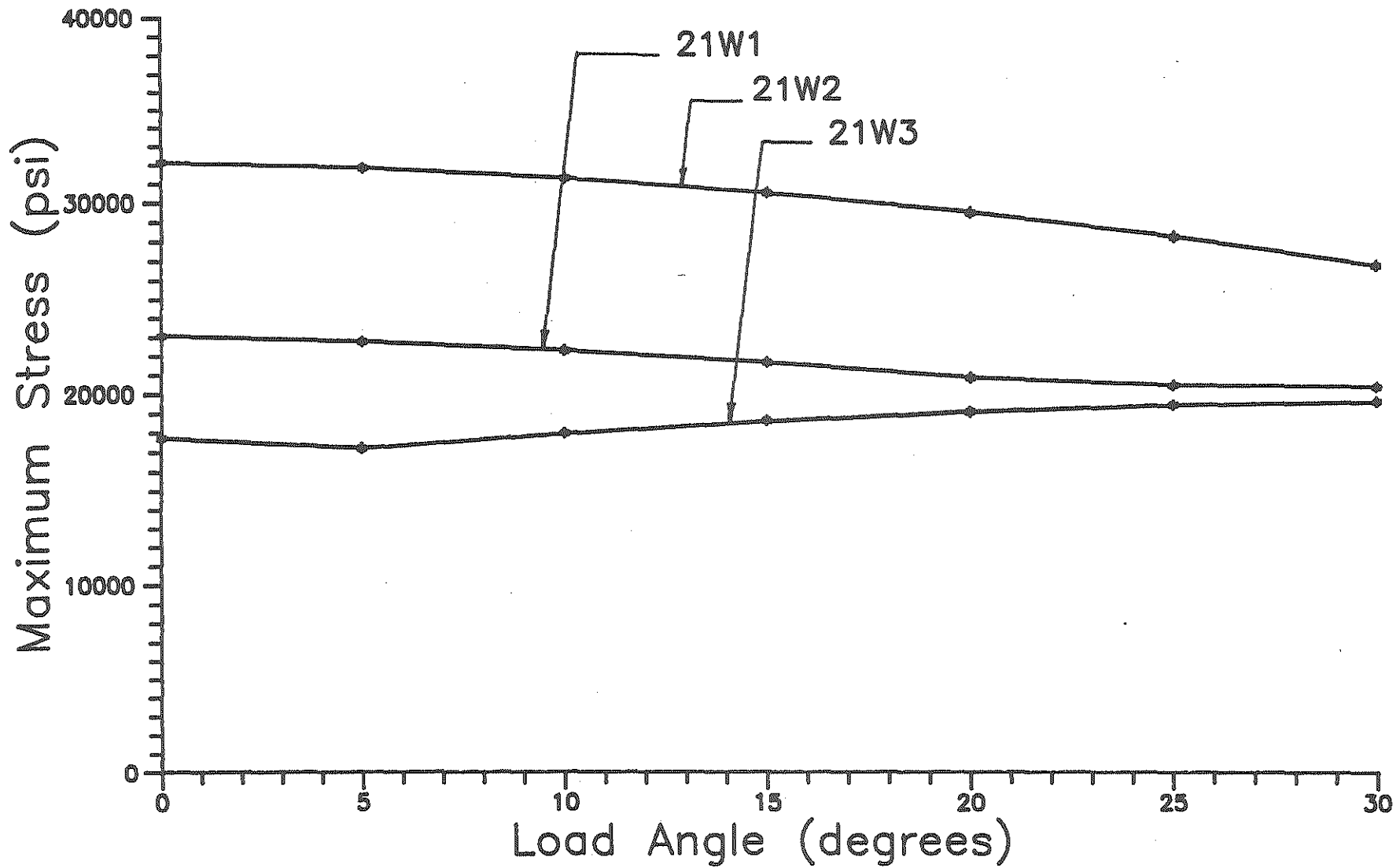


Fig. 43. 21-Floor Bus with Wall-Mounted Seats - Maximum Stresses in Longitudinal Chassis Cap Elements.

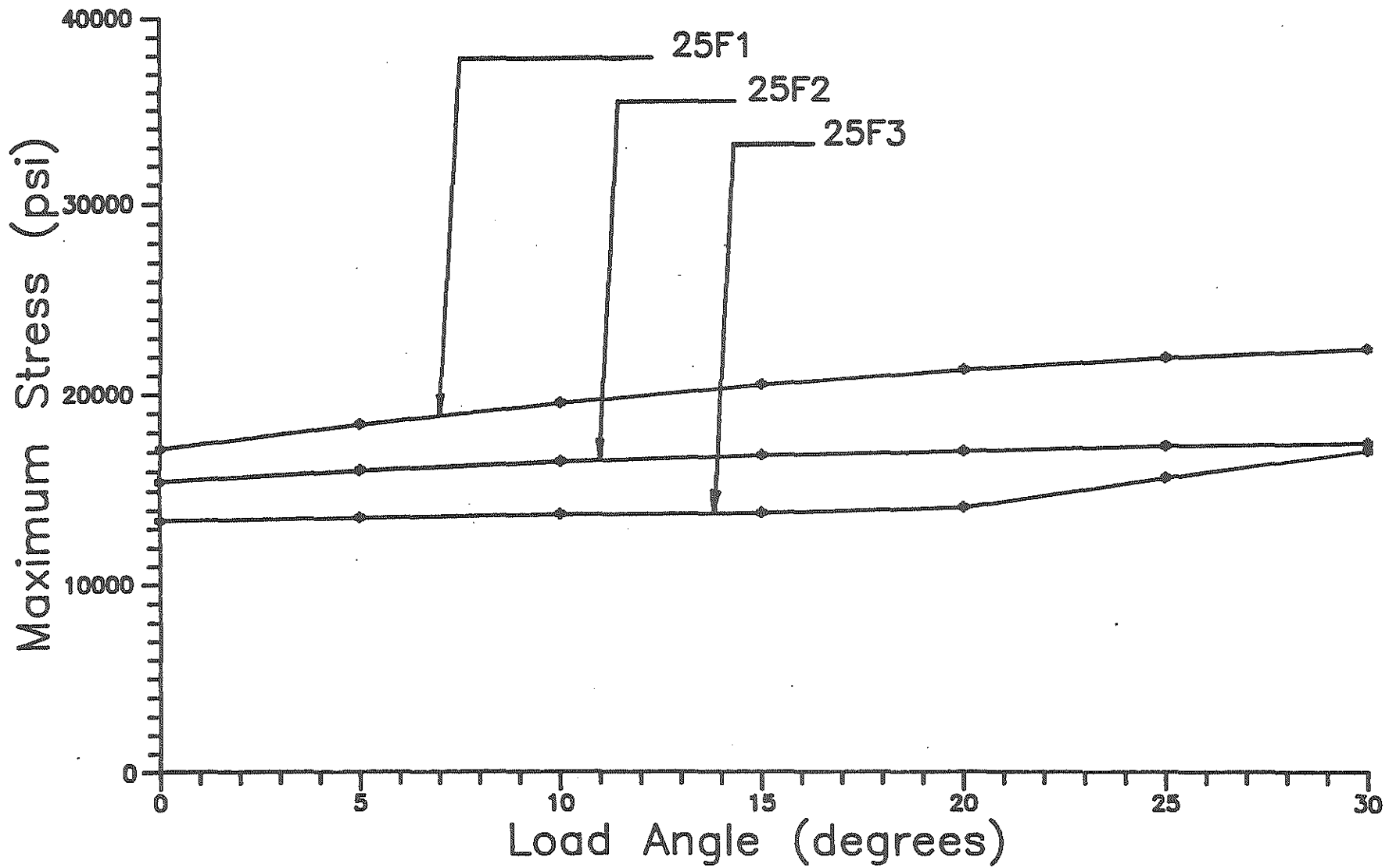


Fig. 44. 25-Foot Bus Floor-Mounted Seats — Maximum Stresses in Longitudinal Chassis Cap Elements.

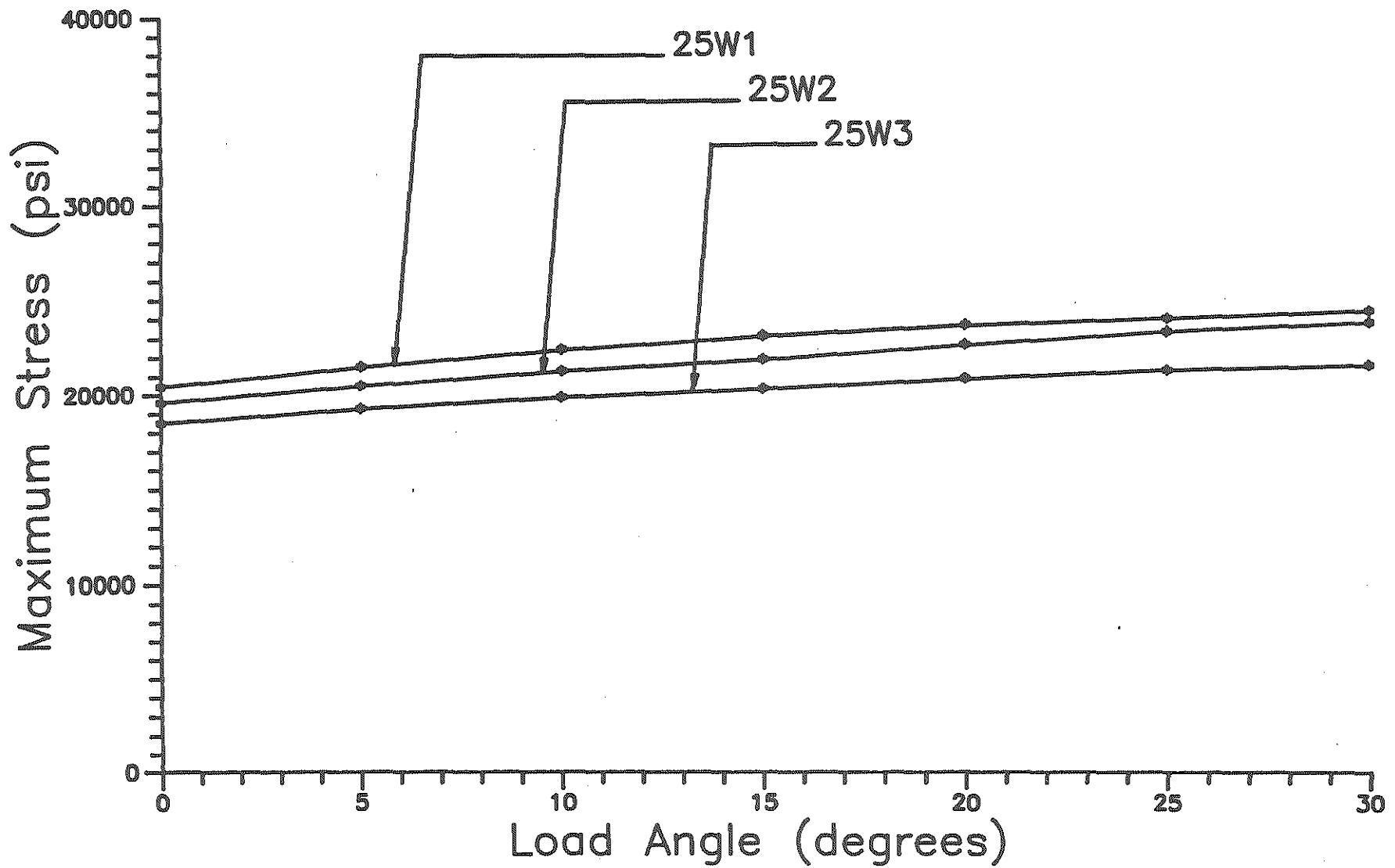


Fig. 45. 25-Foot Bus Wall-Mounted Seats - Maximum Stresses in Longitudinal Chassis Cap Elements.

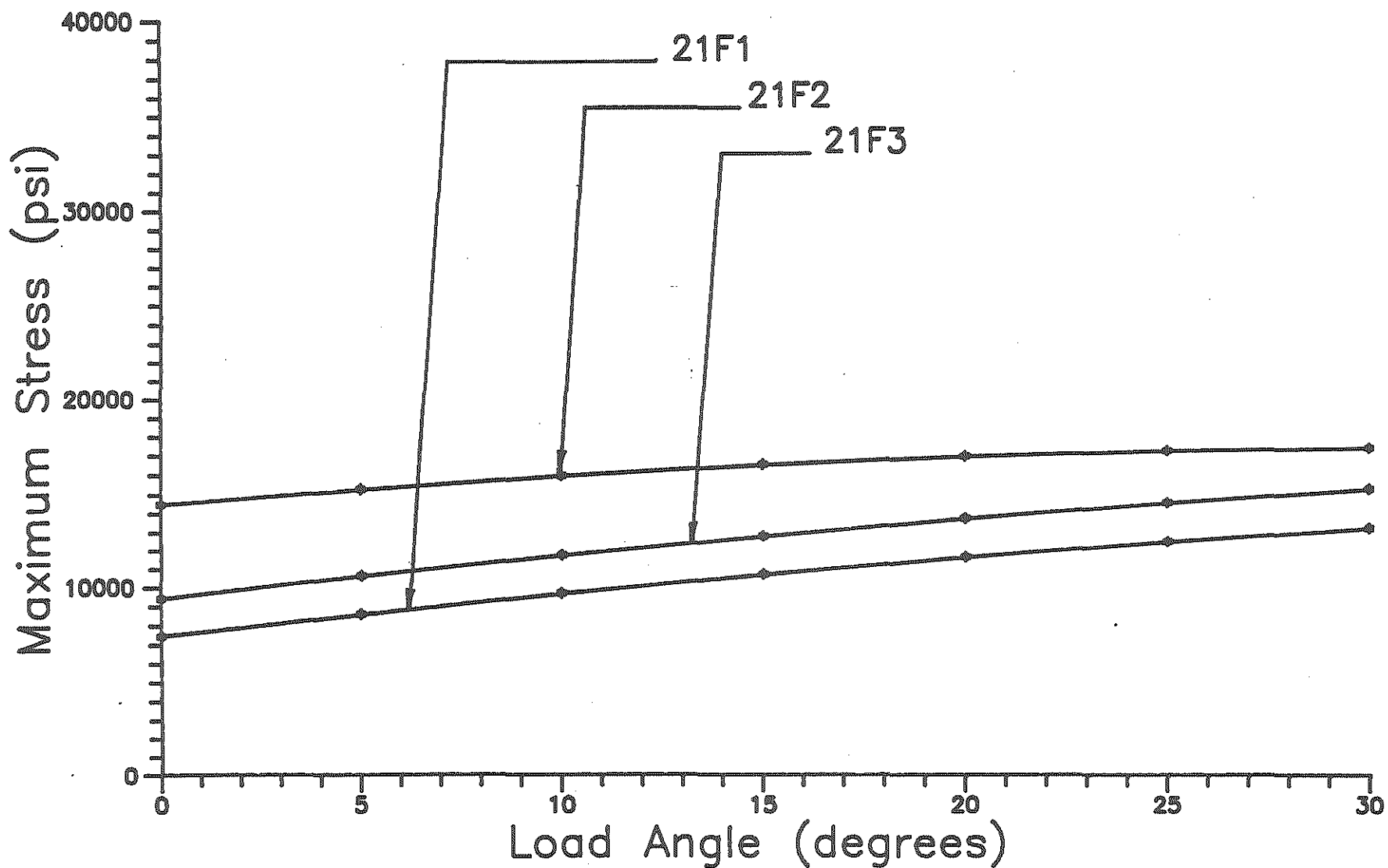
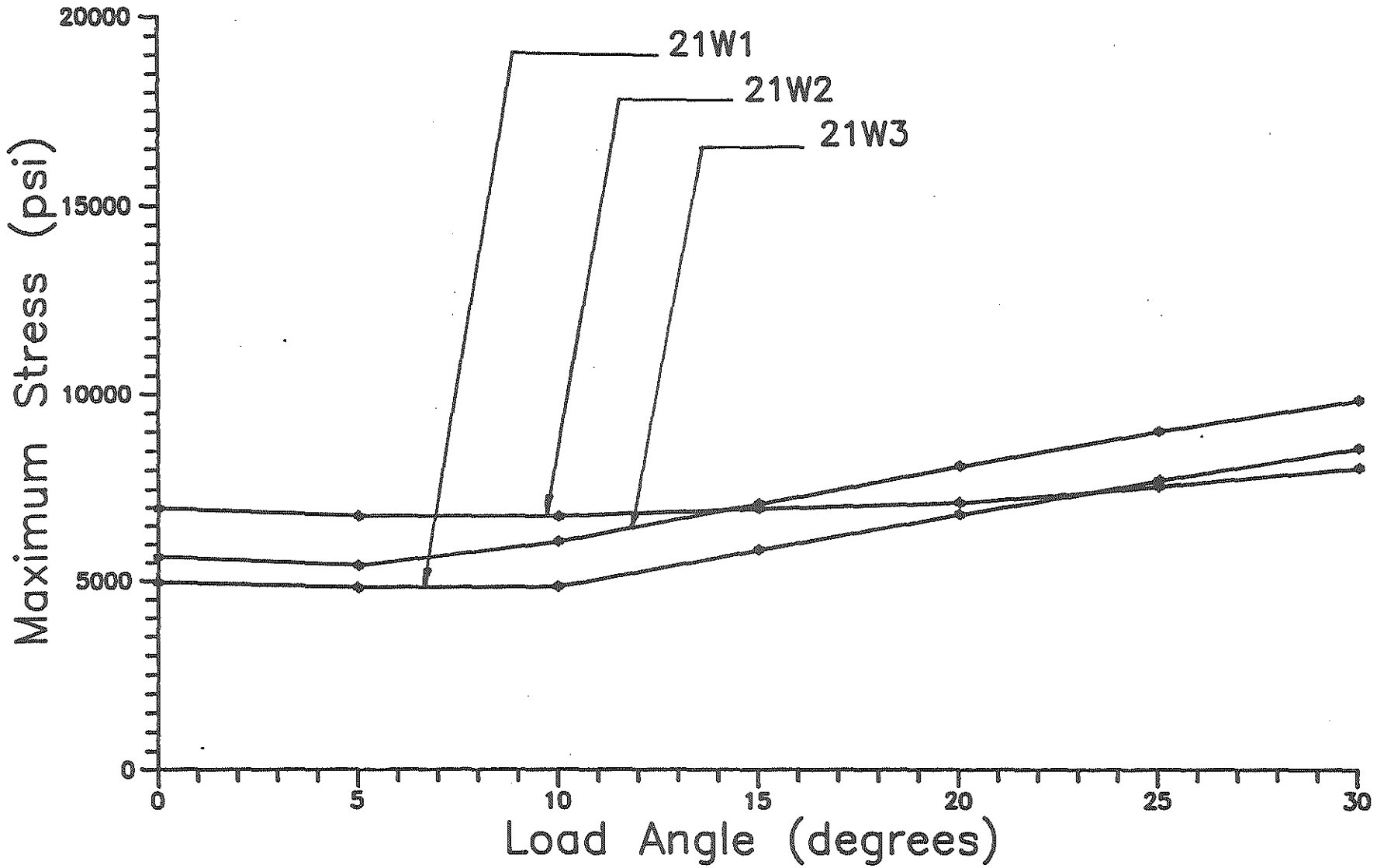


Fig. 46. 21-Foot Bus with Floor-Mounted Seats - Maximum Stresses in Lateral Chassis Elements.



-62-

Fig. 47. 21-Foot Bus with Wall-Mounted Seats - Maximum Stresses in Lateral Chassis Elements.

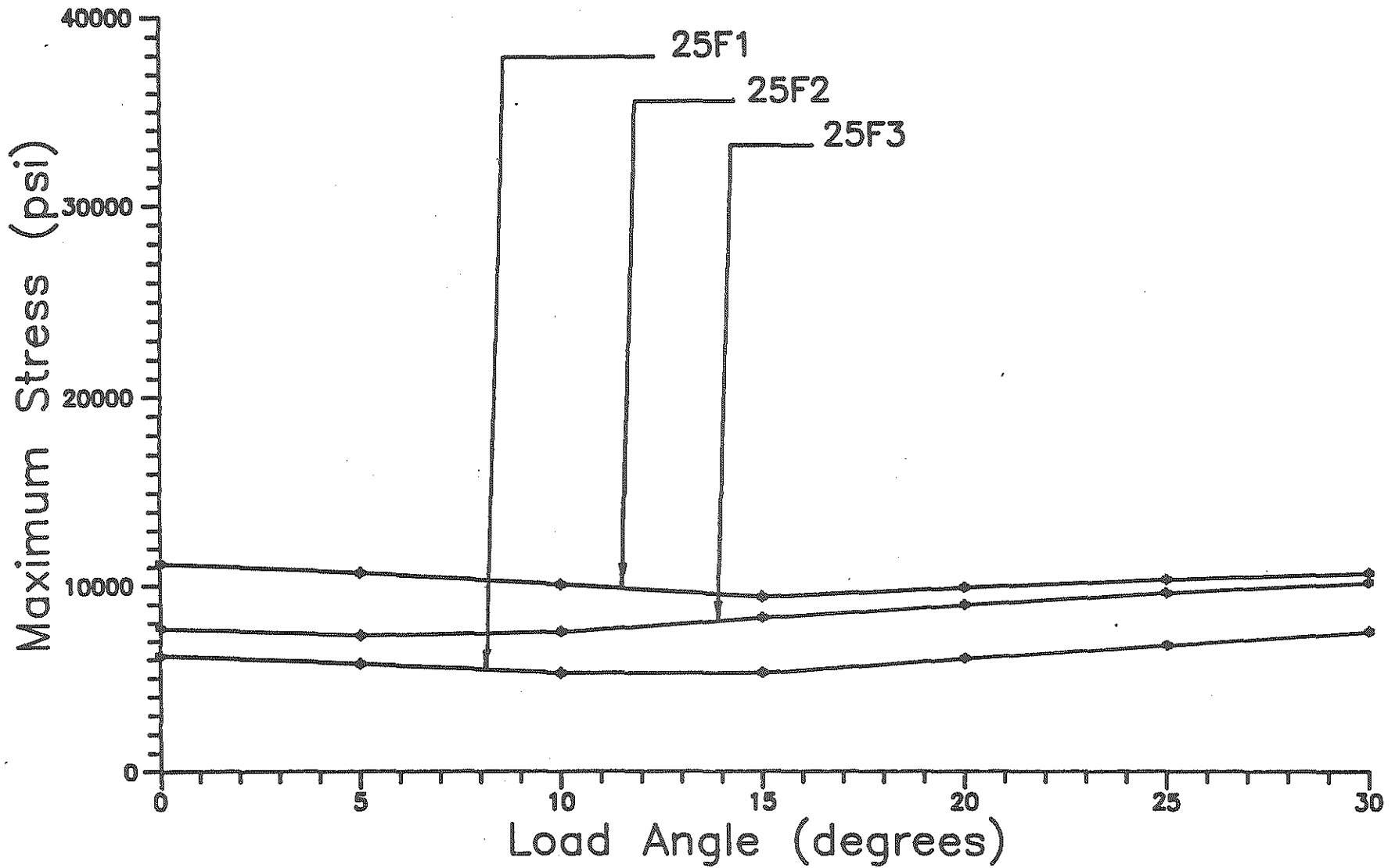


Fig. 48. 25-Foot Bus with Floor-Mounted Seats - Maximum Stresses in Lateral-Chassis Elements.

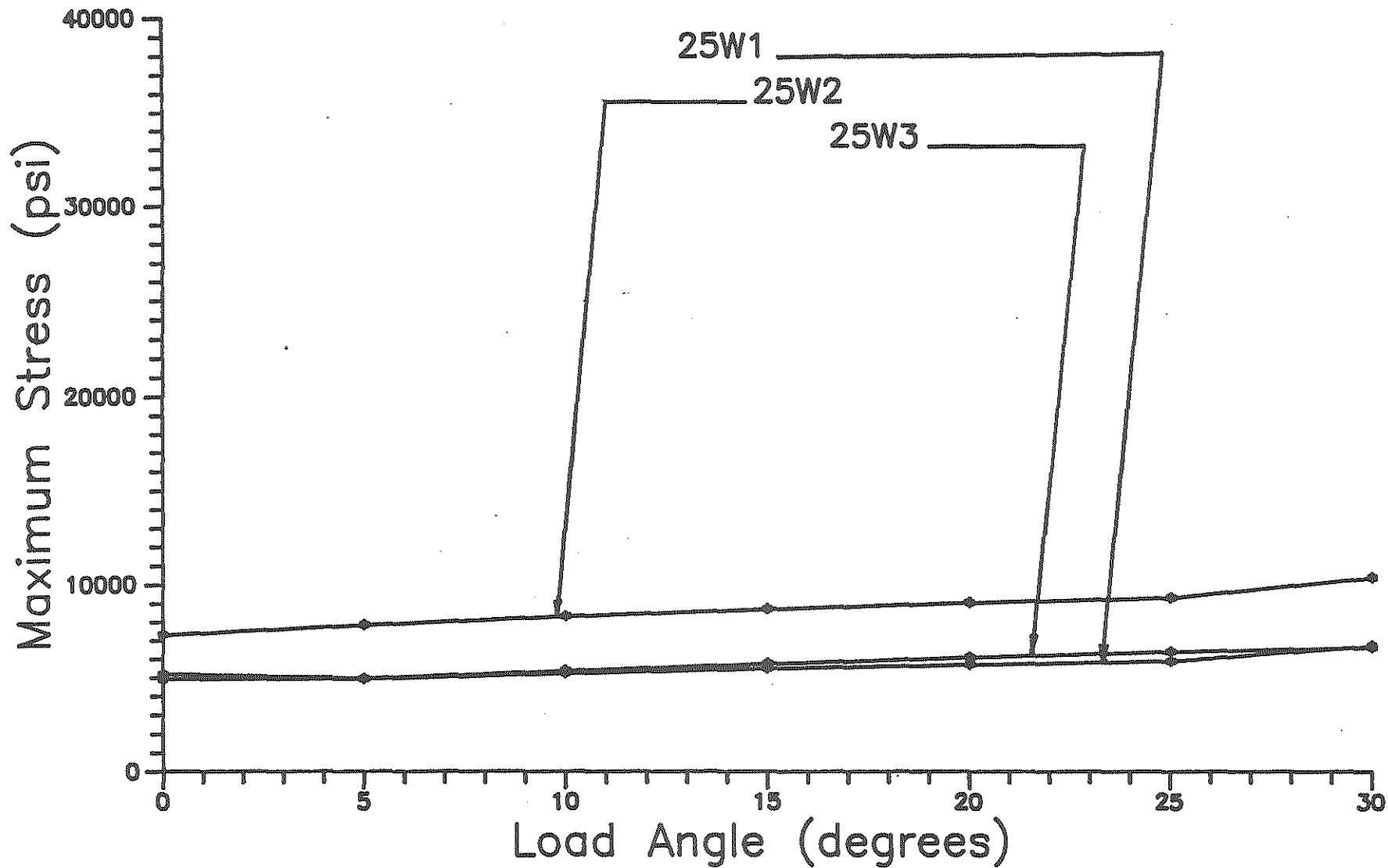


Fig. 49. 25-Foot Bus with Wall-Mounted Seats - Maximum Stresses in Lateral Chassis Elements.

CHAPTER 3

BUS MODELS WITH AND WITHOUT WHEELCHAIRS

MODELS AND ASSUMPTIONS

To assess the impact of wheelchairs, wheelchair restraints, and wheelchair lifts on the structural responses of medium-duty transit buses under rapid deceleration, two additional finite element models were developed based on modified versions of the 25-foot bus with wall-mounted seats and the 25-foot bus with floor-mounted seats as presented in Chapter 2. For each model, the following modifications were made to the original bus models:

1. The right sidewall (as shown in Fig. 50a) was modified (as illustrated in Fig. 50b) by removing the front window and inserting a representation of the wheelchair lift. The inertia of the wheelchair lift is represented by a single nodal point with a horizontal force of 8,000 pounds (400 pounds multiplied by a 20g bus deceleration). This nodal point was placed at the center of the opening for the wheelchair lift at one-third of the opening height and was connected by a series of pseudo-rigid elements to the points where the wheelchair lift is fastened to the bus sidewall and the bus floor. In modifying the right sidewall to accommodate the opening for the wheelchair lift, the width of the second window from the front was reduced from 45 inches to 35 inches.
2. The front four passenger seats on the left side of the bus and the front three seats on the right side were removed in order to make room for two wheelchairs with restraints. This leaves three seats at the left rear and right rear of each bus model. While the version of the 25-foot bus with two wheelchairs does have more than six passenger seats, all of these additional seats fold out of the way to make room for the wheelchairs. Thus none of these additional seats are included in the modified versions

of the 25-foot bus with wheelchairs.

3. Each wheelchair was modeled using a group of 10 pseudo-rigid elements as illustrated in Fig. 51. These pseudo-rigid elements connect the center of gravity of each wheelchair occupant with seven points on the floor and left sidewall: the two tie-down points for the rear tethers, the two points of contact for the main wheels of the wheelchair, the two points of contact for the front wheels of the wheelchair, and the point of attachment for the shoulder restraint which lies above the windows on the left bus sidewall.

LOAD CASES

To simulate the loads generated by passenger inertia under rapid bus deceleration, a force of 2,500 pounds was assumed for each bus passenger (12 total) and for each wheelchair occupant (2 total). As mentioned earlier, a force of 8,000 pounds was assumed for the wheelchair lift. All of these inertia forces were applied using seven angles of tilt from 0 to 30 degrees for the bus floor at maximum bus deceleration. These angles of tilt were simulated by "tilting" the forces as opposed to tilting the bus models. Full seat belt usage by all bus passengers was assumed.

ANALYSIS RESULTS

Plots of maximum element stress versus bus floor angle are presented in Figs. 52 to 61 for the plywood floor elements, the lateral frame elements, the longitudinal chassis elements, the body elements, the steel plate elements, the perimeter floor elements, the skirting elements, the wheel well elements, the longitudinal chassis cap elements, and the lateral chassis elements, respectively. Each of these figures contains four plots representing the results for the following four versions of the 25-foot bus:

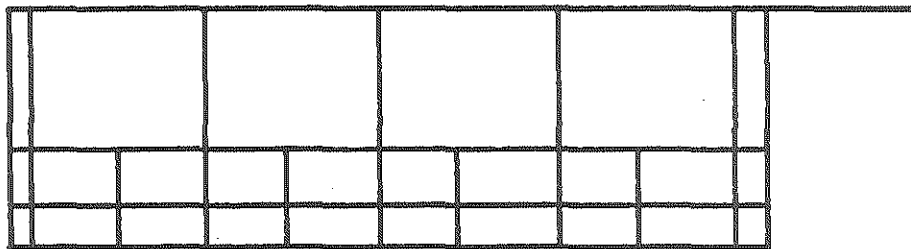
1. The version with 13 floor-mounted seats, no wheelchairs, and no wheelchair lift, which is the same version presented in Chapter 2 (FMS).

2. The version with six floor-mounted seats, two wheelchairs, and one wheelchair lift (FMS-WC).
3. The version with 13 wall-mounted seats, no wheelchairs, and no wheelchair lift, which is the same version presented in Chapter 2 (WMS).
4. The version with six wall-mounted seats, two wheelchairs, and one wheelchair lift (WMS-WC).

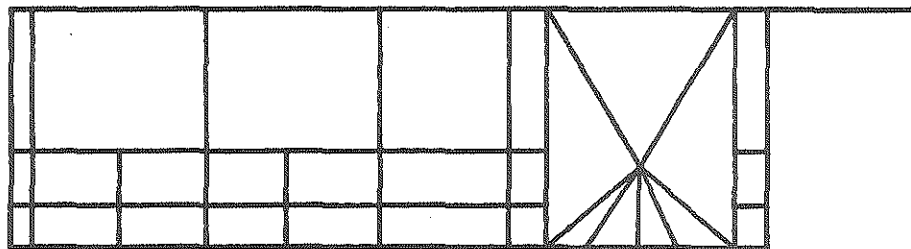
The results presented in Figs. 52 to 61 indicate relatively small differences between the bus responses with and without wheelchairs. The maximum stresses were generally larger for the cases with wheelchairs versus the corresponding cases without wheelchairs with the largest differences occurring in the models with wall-mounted seats.

The largest differences between the maximum element stresses with and without wheelchairs (and wheelchair lifts) for the versions of the 25-foot bus with floor-mounted seats were as follows: -0.4% for the plywood floor elements, +3.1% for the lateral frame elements, +5.2% for the longitudinal chassis elements, +3.4% for the body elements, +3.5% for the steel plate elements, +0.6% for the perimeter floor elements, -16.2% for the skirting elements, -3.8% for the wheel well elements, +0.6% for the longitudinal chassis cap elements, and +7.1% for the lateral chassis elements.

For the versions of the 25-foot bus with wall-mounted seats, the largest differences between the maximum element stresses with and without wheelchairs, (and wheelchair lifts) were as follows: +11.0% for the plywood floor elements, +11.4% for the lateral frame elements, +11.4% for the longitudinal chassis elements, -14.9% for the body elements, +3.0% for the steel plate elements, +7.4% for the perimeter floor elements, -2.1% for the skirting elements, +8.8% for the wheel well elements, -0.7% for the longitudinal chassis cap elements, and +21.1% for the lateral chassis elements.

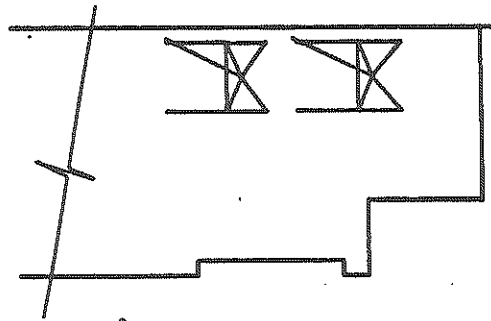


a) Original Sidewall

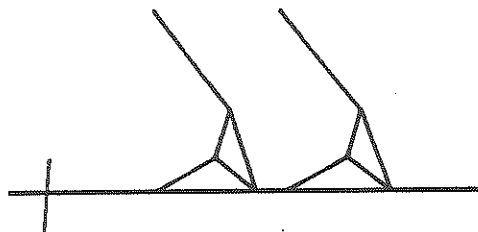


b) Modified Sidewall

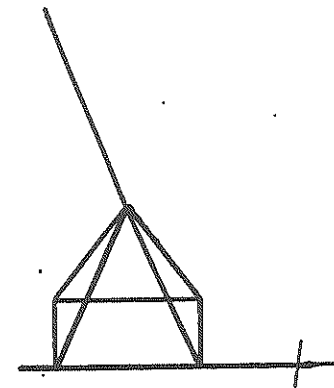
Fig. 50. 25-Foot Bus - Wheelchair Lift and Right Sidewall Model



a) Top View



b) Side View



c) Front View

Fig. 51. 25-Foot Bus - Wheelchair and Wheelchair Restraints Model

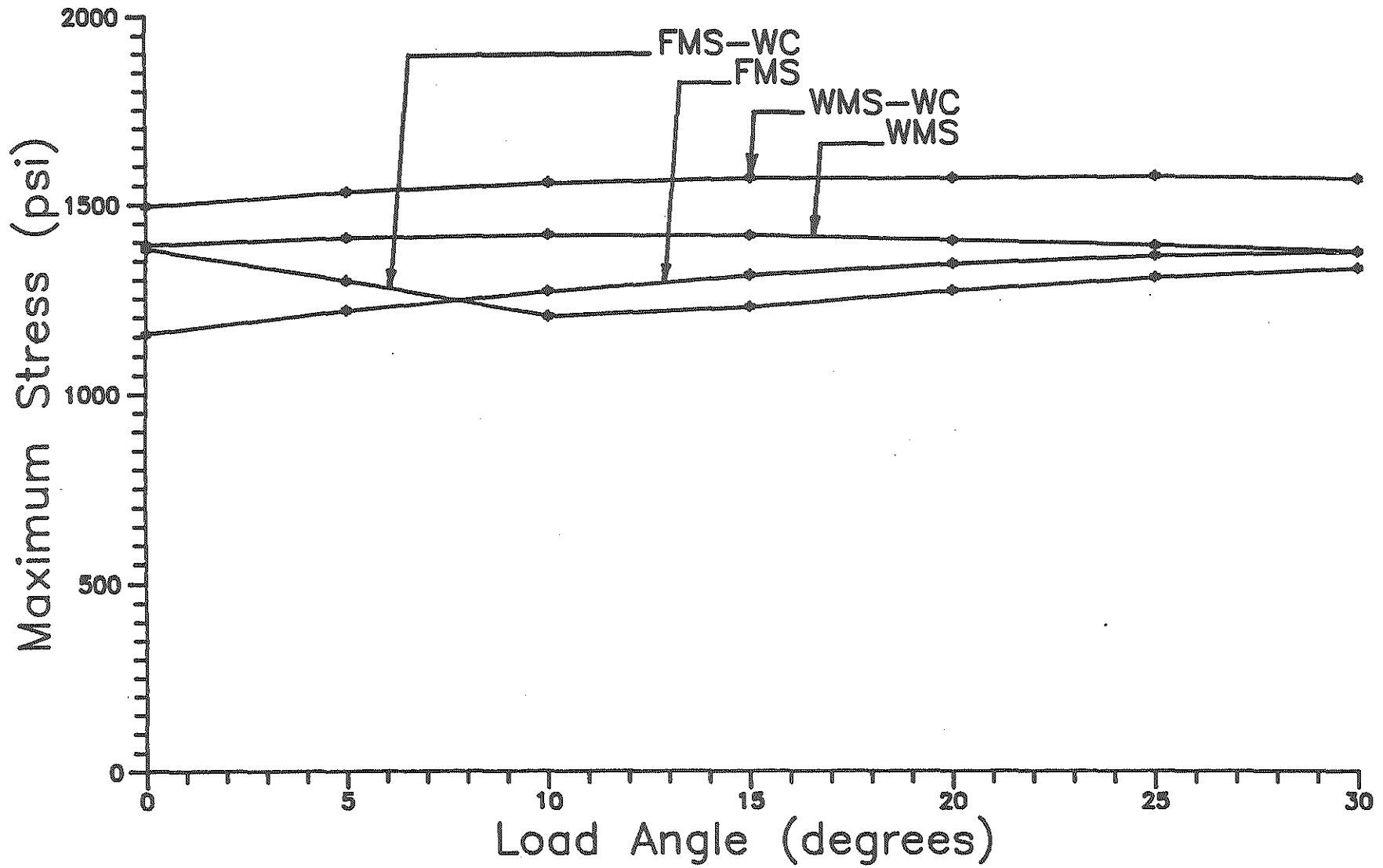


Fig. 52. 25-Foot Bus - Maximum Stresses in Plywood Floor Elements.

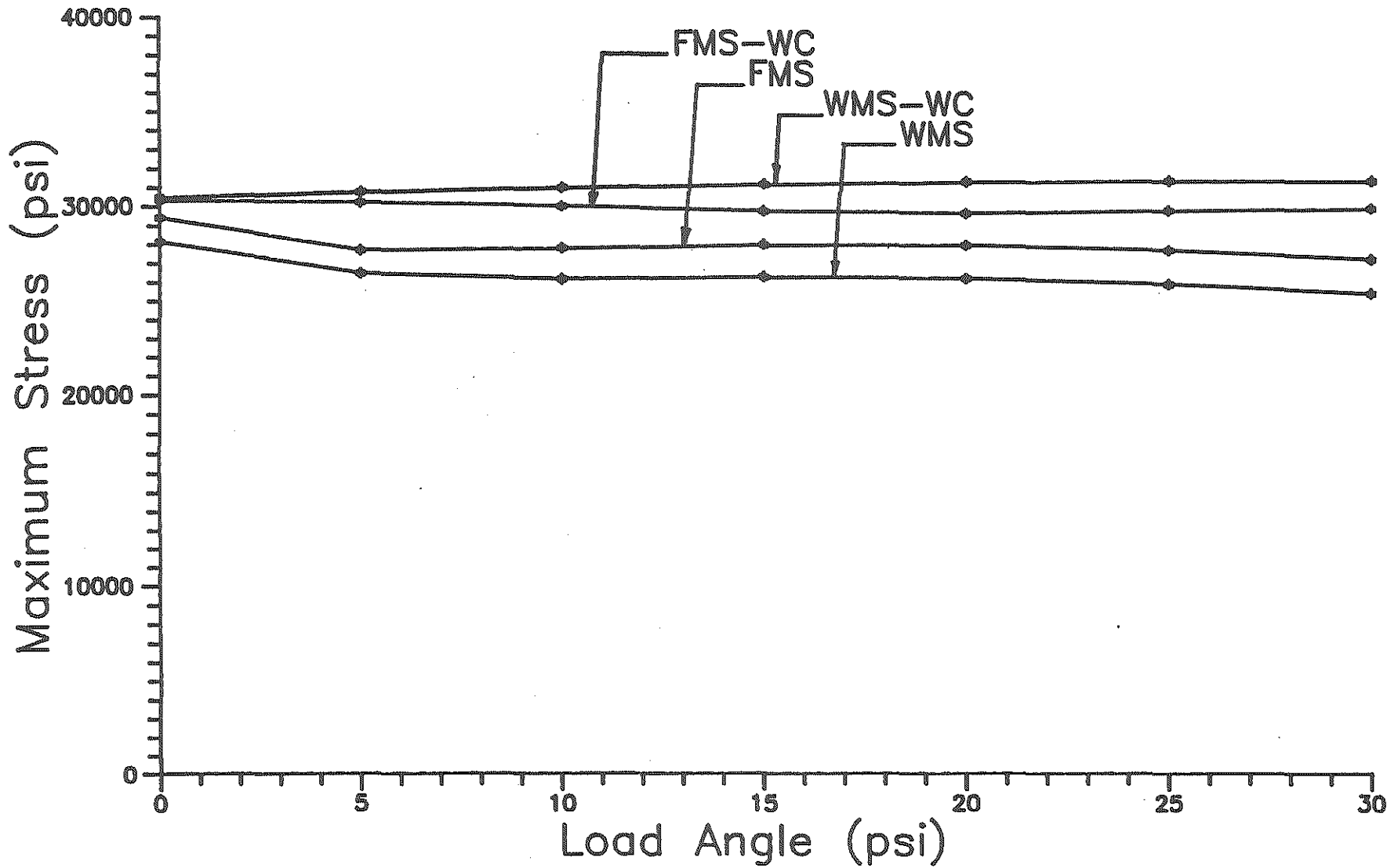


Fig. 53. 25-Foot Bus - Maximum Stresses in Lateral Frame Elements.

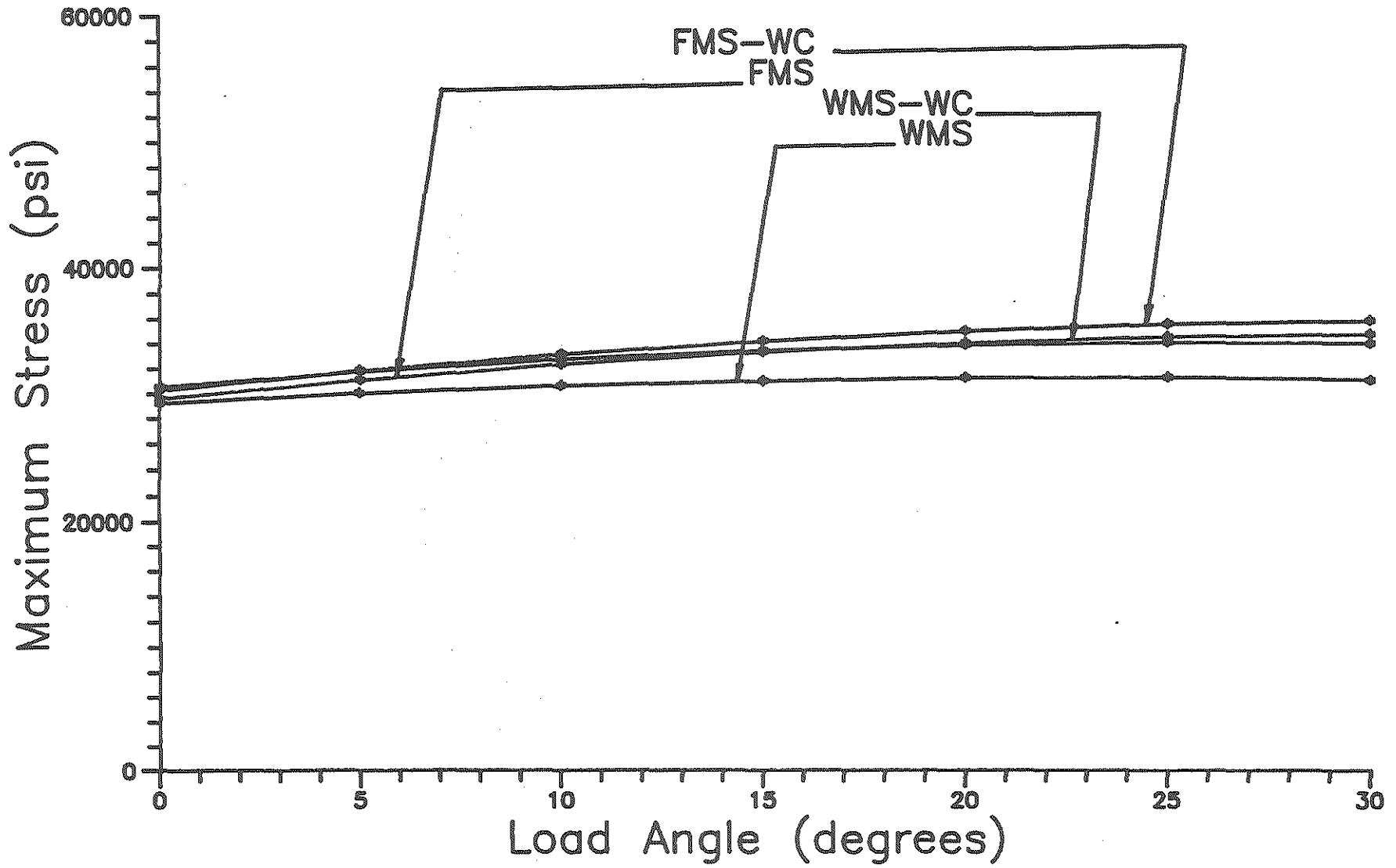


Fig. 54. 25-Foot Bus - Maximum Stresses in Longitudinal Chassis Elements.

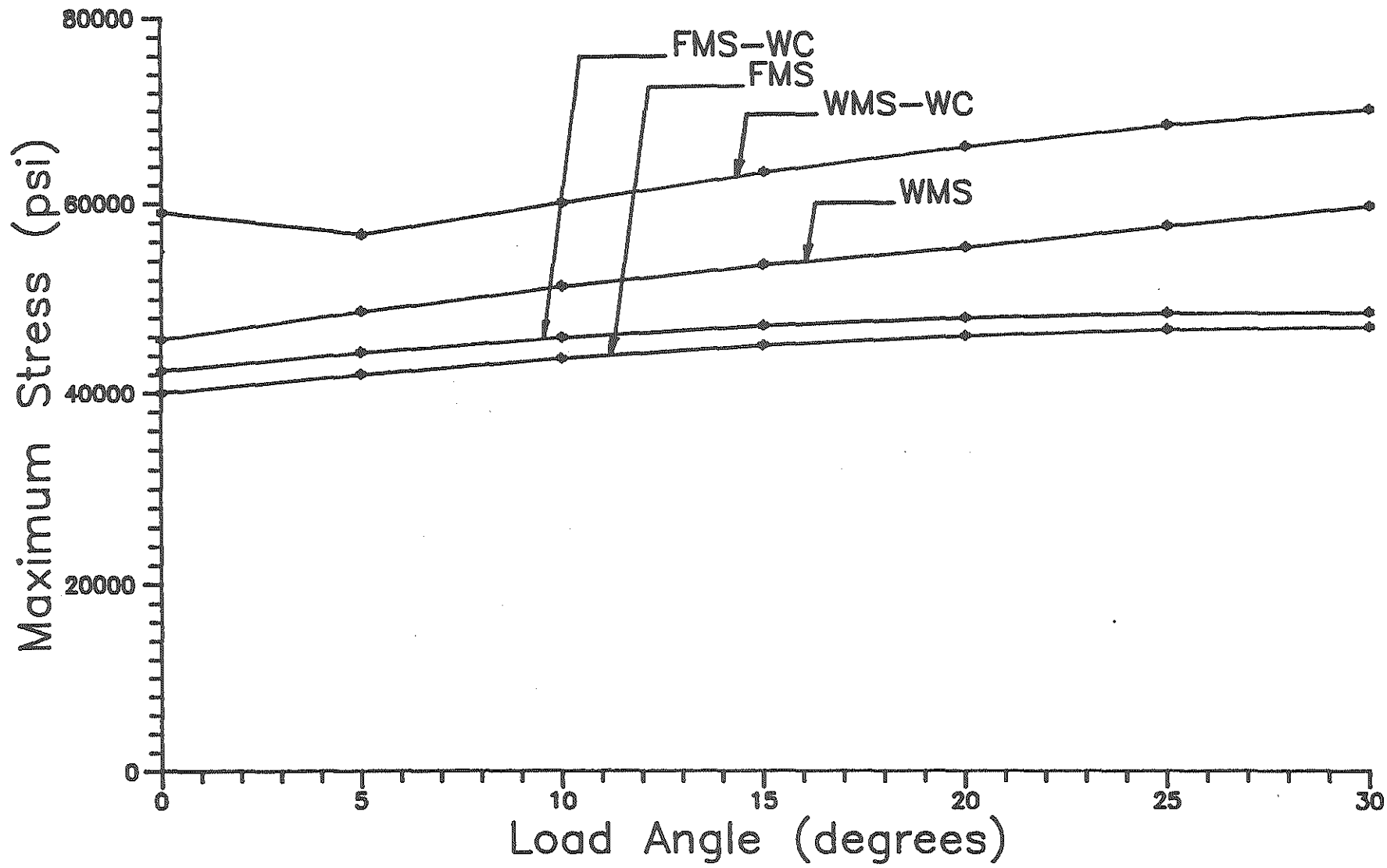


Fig. 55. 25-Foot Bus - Maximum Stresses in Body Elements.

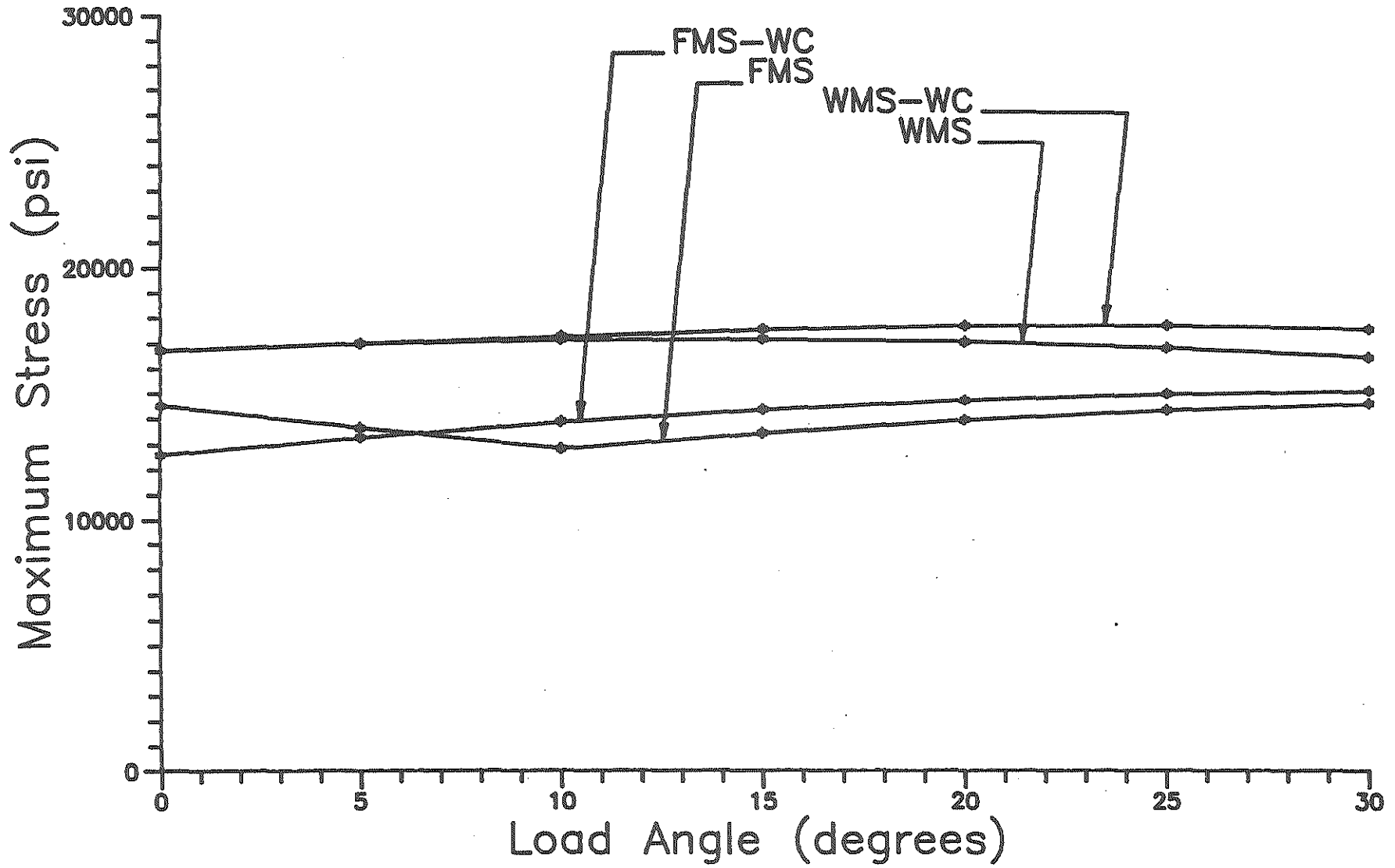


Fig. 56. 25-Foot Bus - Maximum Stresses in Steel Plate Elements.

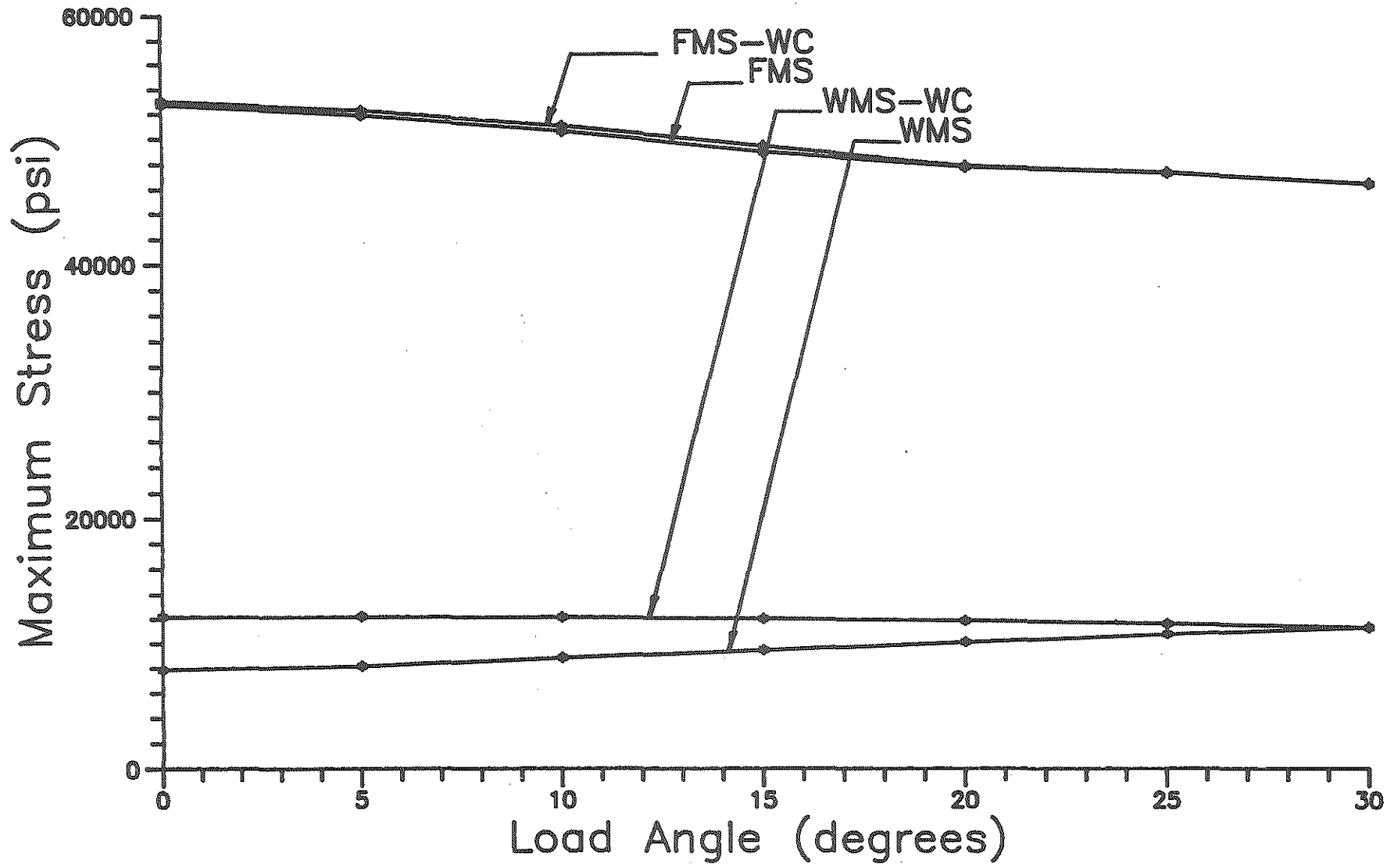


Fig. 57. 25-Foot Bus - Maximum Stresses in Perimeter Floor Elements.

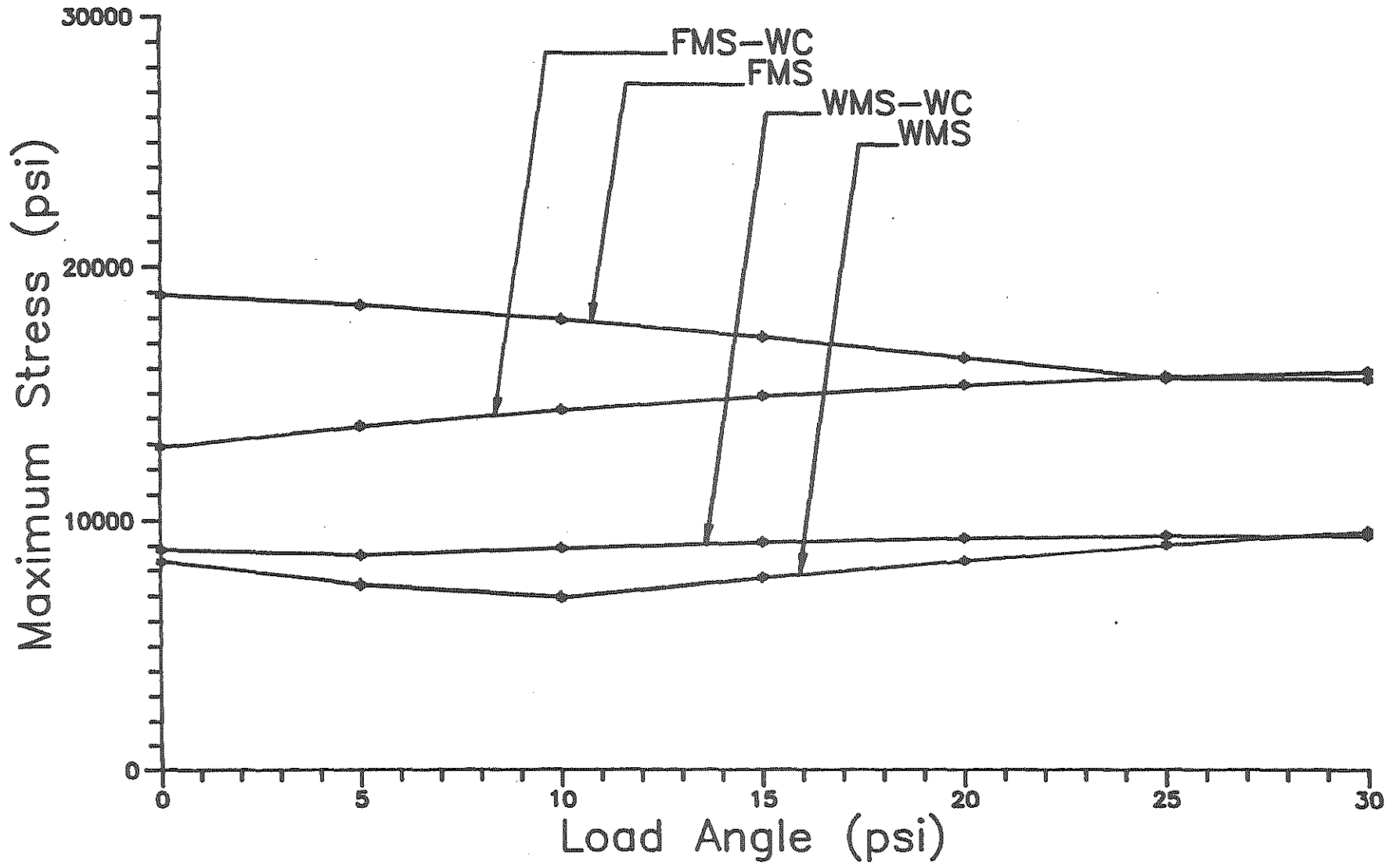


Fig. 58. 25-Foot Bus - Maximum Stresses in Skirting Elements.

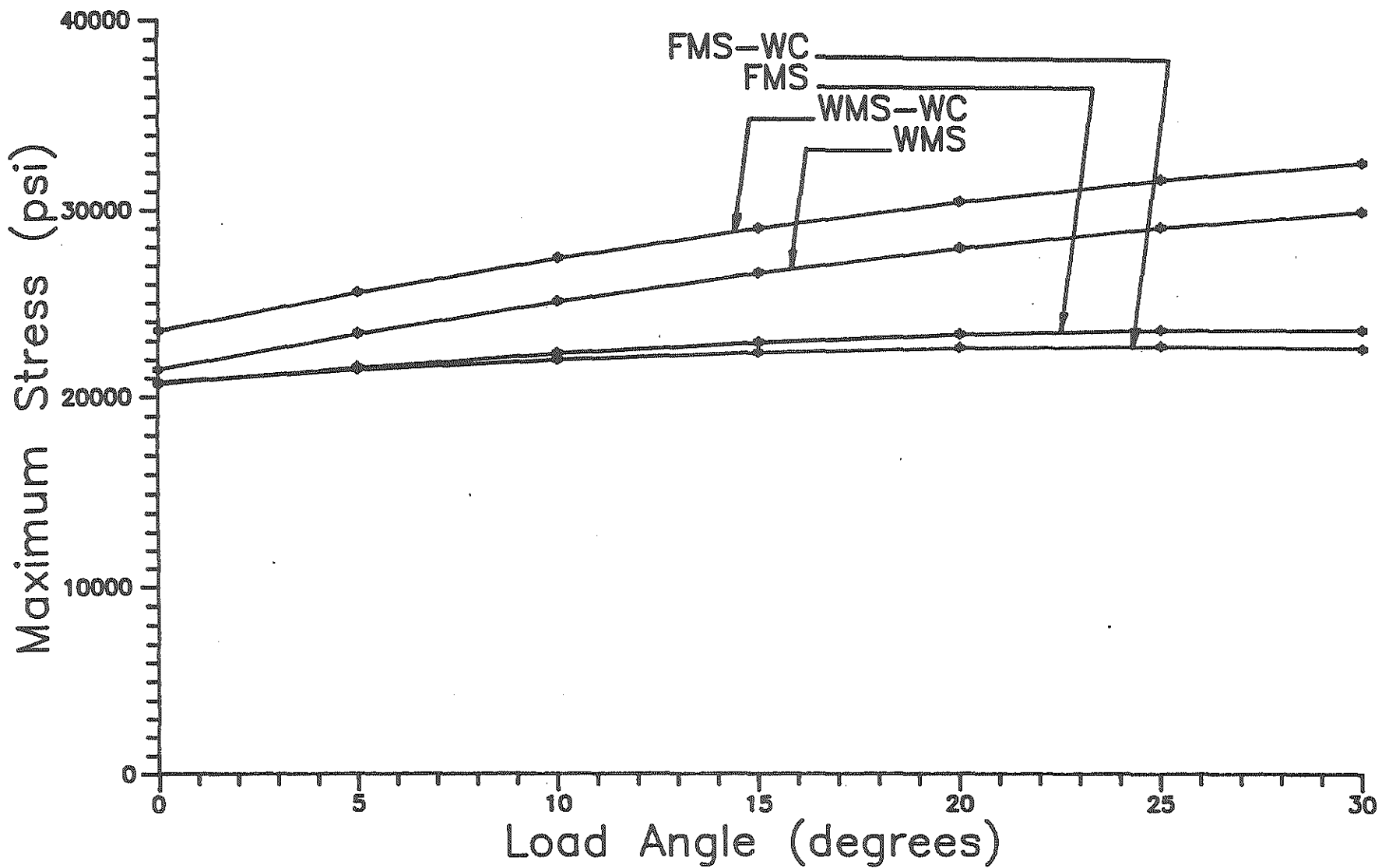


Fig. 59. 25-Foot Bus - Maximum Stresses in Wheel Well Elements.

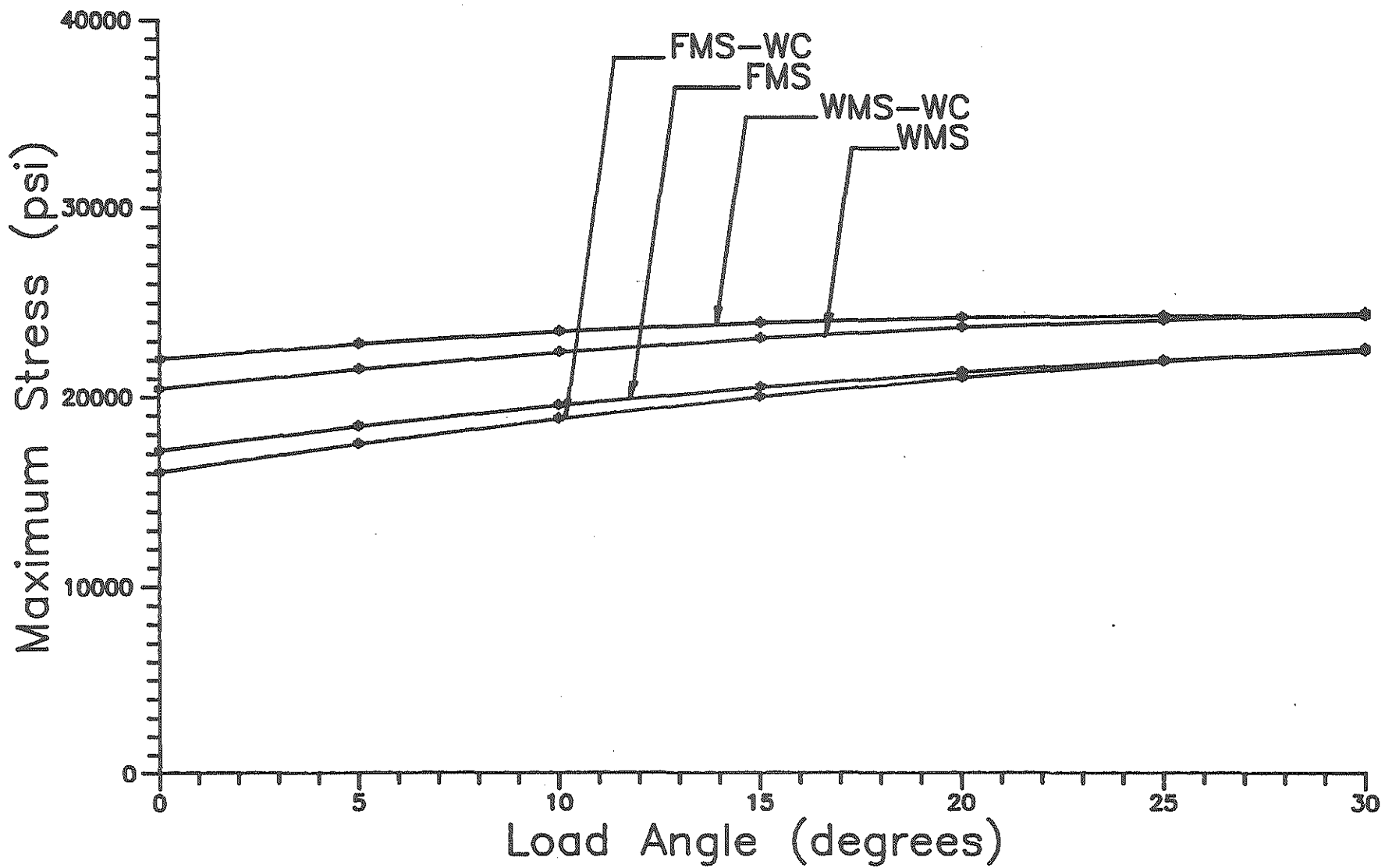


Fig. 60. 25-Foot Bus - Maximum Stresses in Longitudinal Chassis Cap Elements.

78

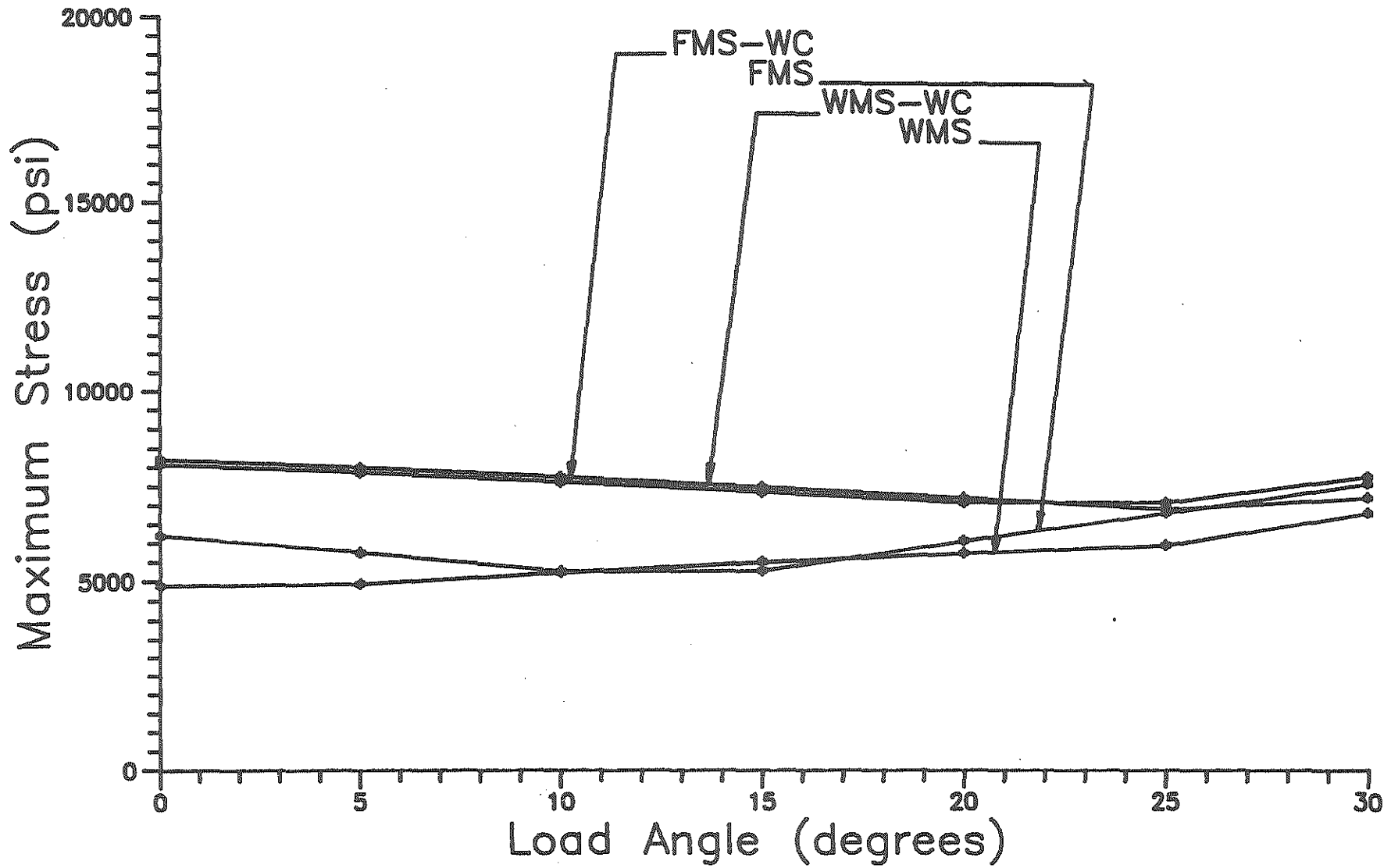


Fig. 61. 25-Foot Bus - Maximum Stresses in Lateral Chassis Elements.

CHAPTER 4

STATUS OF LABORATORY TESTING

In order to determine the ultimate strength capacity of the chassis-to-frame U-bolt connections in the 21-foot and 25-foot transit buses, laboratory tests were planned with testing activities to begin in Phase 2 of the project and with final connection testing to be completed in Phase 3. The following activities were finished during Phase 2 of the project:

1. Design of the load platform for the MTS machine.
2. Design of the test specimens.
3. Purchasing of construction materials.
4. Beginning construction of the load platform and five trial specimens.

The final designs for the load platform and the test specimens are illustrated by the front, side, and top views depicted in Figs. 62, 63, and 64. The load platform will consist of the following components:

1. An inverted tee-beam base which was fabricated from a hot-rolled WT 7 x 45 steel section and which will be bolted to the base of the MTS machine.
2. A 12-inch by 9-inch by 3/4-inch steel base plate which will be welded to the web of the tee-beam and which will be supported by four 6-inch by 5-inch by 1/2-inch steel plate stiffeners.
3. Two 5-inch by 3-inch by 3/16-inch hot-rolled rectangular steel tubes which will be welded to the tee-beam flange and which will each slope upward to support a 17-inch by 14-inch by 3/4-inch steel top plate.

Cross-section views of the load platform are shown in Figs. 65, 66, and 67, while a perspective view of the base of the load platform is shown in Fig. 68.

Perspective views of the test specimens and the initial design of the MTS connection detail for the test specimens are shown in Figs. 69 and 70. Each test specimen will consist of the following components:

1. Top and bottom 10-inch by 9-inch by $\frac{1}{2}$ -inch steel connection plates which will each be welded to a 48-inch segment of the longitudinal chassis channel member.
2. A 38-inch segment of the longitudinal chassis cap which will be fastened to the longitudinal chassis channel member with two or three U-bolts and with one or two shear tabs. Both the longitudinal chassis channel member and the longitudinal chassis cap were fabricated from cold-formed steel channel sections.
3. A 38-inch segment of $2\frac{1}{2}$ -inch by 1-inch oak which is sandwiched between the longitudinal chassis channel member and the longitudinal chassis cap.
4. An MTS connection detail which will be fastened to the longitudinal chassis cap and will serve to connect the test specimen with the loading head of the MTS machine.

After consultation with personnel in the College of Engineering's Mechanical Shop, the MTS connection detail is now in the process of being redesigned in order to reduce the construction costs for each specimen and in order to decrease the eccentricity of the applied load and hence to reduce the bending stresses in the test specimens.

All of the materials for the construction of the load platform and 30 test specimens were ordered in September 1991 and all of these materials have now been received by the mechanical shop. The longitudinal chassis channel members, the longitudinal chassis caps, the U-bolts, and the shear tabs were all ordered from the same vendors utilized by the bus manufacturer and using the same specifications as the bus manufacturer. The steel plates that were ordered for the original MTS connection detail (Fig. 70) will be traded with the mechanical shop for replacement materials once the new design for the MTS connection detail is completed.

Construction of the load platform and the five trial specimens is now in progress in the mechanical shop. However, because of a large backlog of work orders in the mechanical shop, the load platform and the five trial specimens will not be completed before January 1, 1992. The five trial specimens will be used to test various schemes for placement of the U-bolts, for placement of the shear tabs, and for the design and placement of the MTS connection detail. The final design details for the remaining 25 test specimens should be finished by February 1, 1992. The construction of the final 25 test specimens will most likely be completed by March 1, 1992, with the final tests utilizing these specimens finished by June 1, 1992.

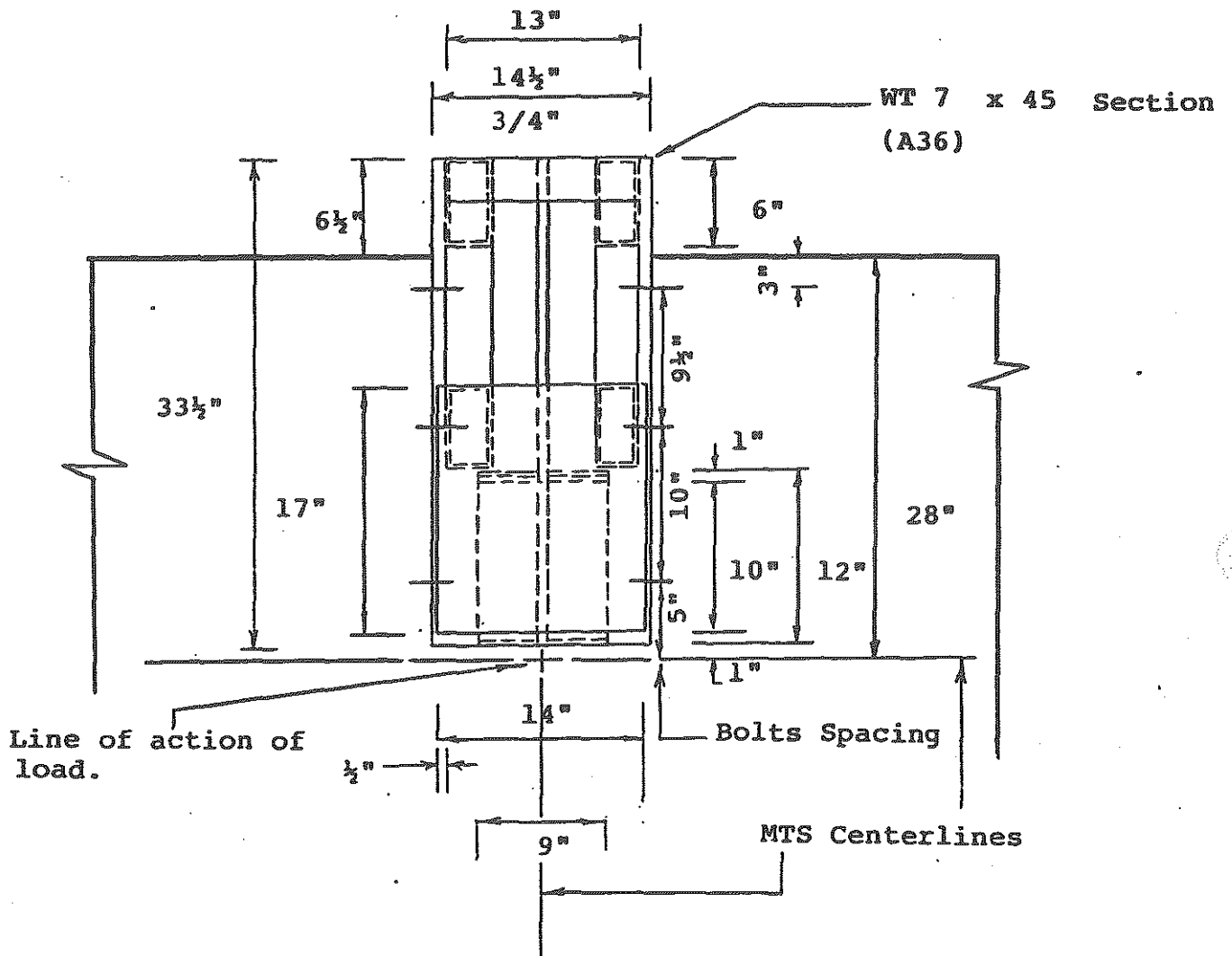
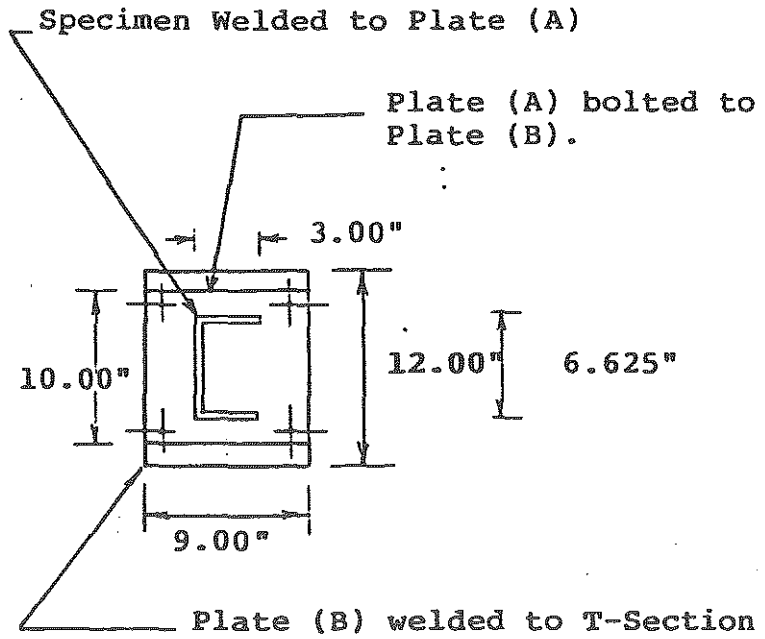


Fig. 64. Top View of Load Platform

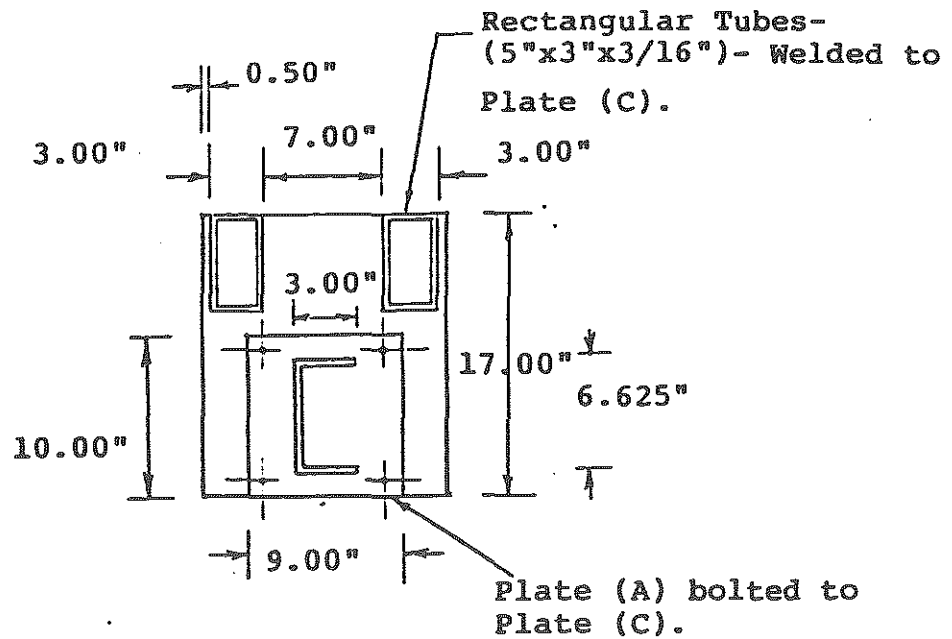


Section A-A

Plate (A) : (10"x9"x1/2") Welded to Longitudinal Chassis.

Plate (B) : (12"x9"x3/4")

Fig. 65. Section A-A of Load Platform



Section B-B

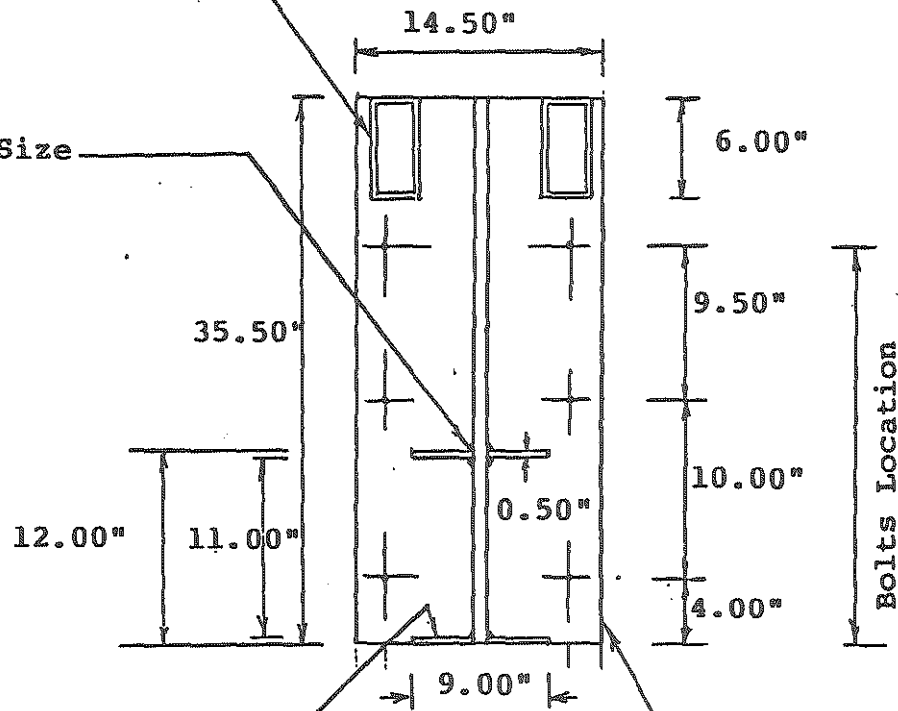
Plate (A) : (10"x9"x1/2") Welded to
Longitudinal Chassis.

Plate (C) : (17"x14"x3/4") Welded to
Rectangular Tubes.

Fig. 66. Section B-B of Load Platform

Rectangular Tube
(5"x3"x3/16")

Minimum Weld Size
(Full Length)



Stiffner
Plate
(6"x5"x1/2")

T-Section
(WT 7x45)

Section C-C

Fig. 67. Section C-C of Load Platform

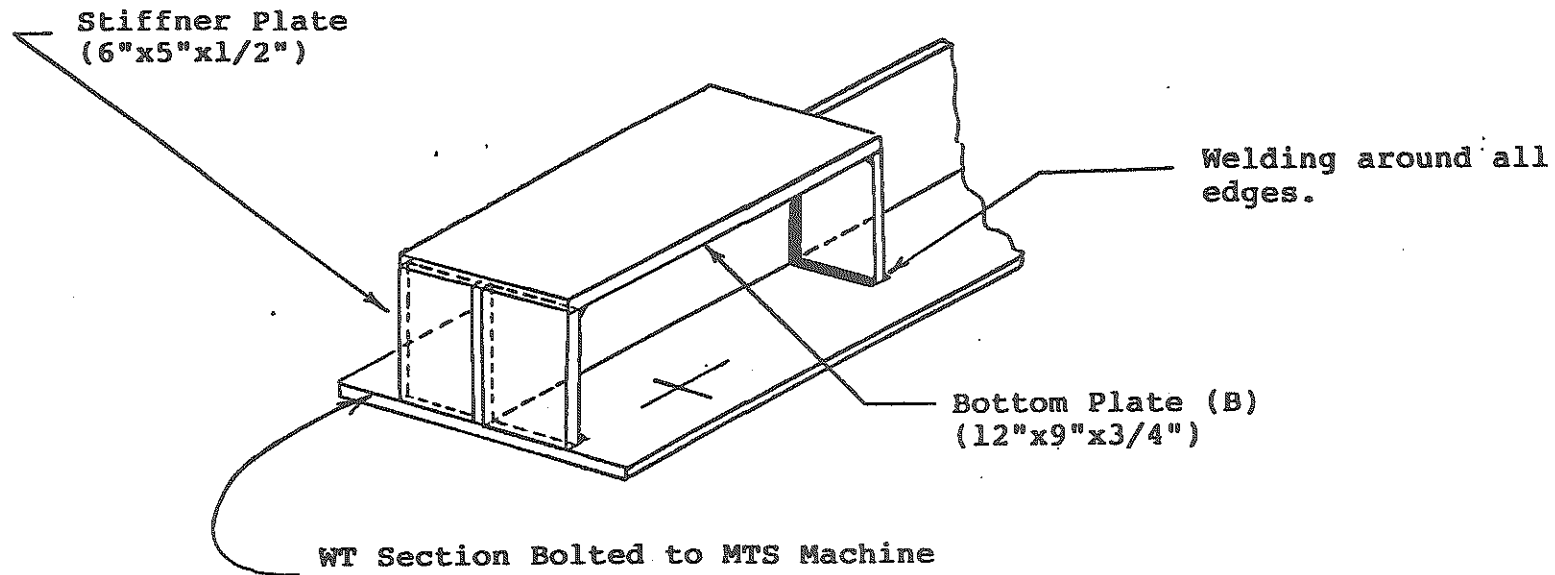


Fig. 68. Perspective View of Load Platform Base

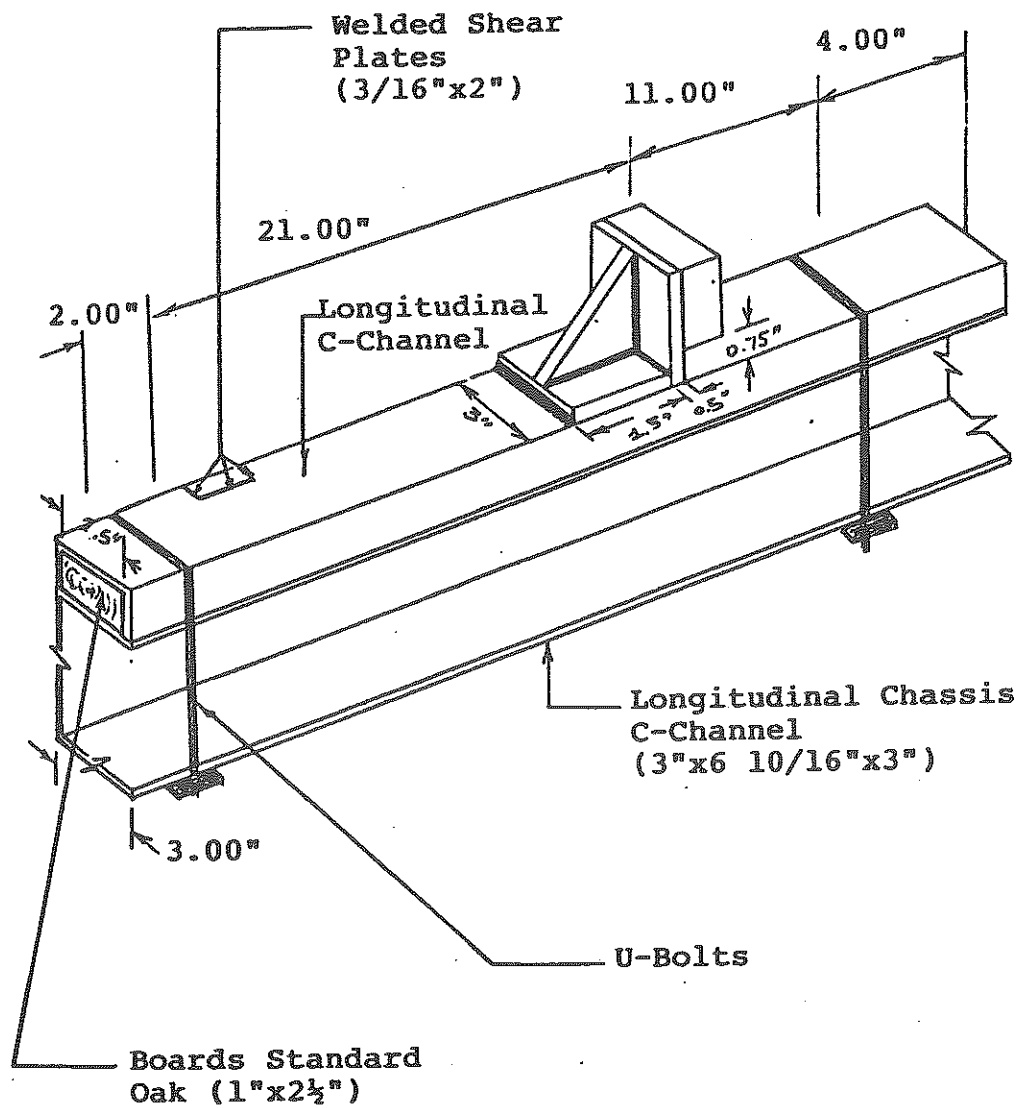
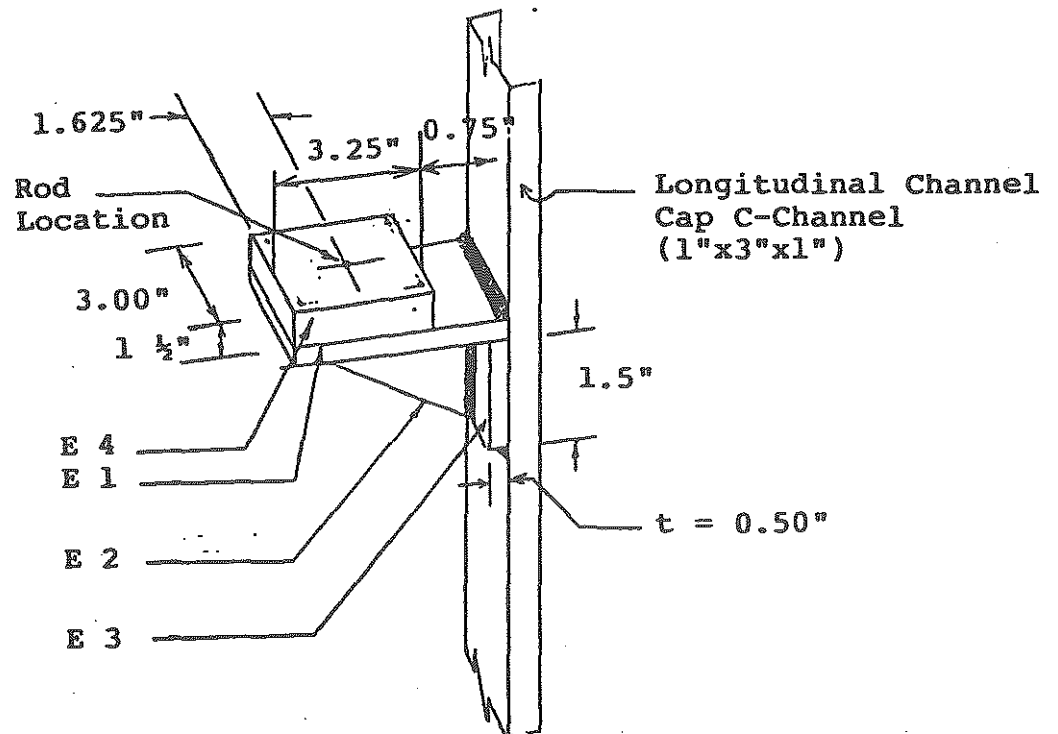


Fig. 69. Perspective View of Test Specimen



E1, E2, E3, E4 all have same thickness $t=0.50"$

Fig. 70. Perspective View of MTS Connection Detail

CHAPTER 5

SUMMARY AND CONCLUSIONS

SUMMARY

Bus Models With and Without Seat Belts

To assess the impact of rapid bus deceleration on the structure of a typical transit bus, four finite-element computer models were developed for the structure of two medium-duty transit buses: a 21-foot bus with 11 passenger seats and a 25-foot bus with 13 passenger seats. Two finite-element models were developed for each bus: one using floor-mounted seats and another using wall-mounted seats. Assumptions were made regarding the loading conditions in the event of rapid bus decelerations (front-end impacts). Parametric results for bus floor angles of 0, 5, 10, 15, 20, 25, and 30 degrees were derived for loading patterns with full seat belt usage, staggered seat belt usage, and front seat belt usage only. Conclusions pertaining to the results generated by these analyses are presented below.

Bus Models With and Without Seat Belts

To analyze the responses of the bus structure to wheelchairs, wheelchair restraints, and wheelchair lifts, two additional finite-element computer models of the 25-foot bus were developed: one with floor-mounted passenger seats and one with wall-mounted passenger seats. Both models were analyzed assuming full seat belt usage by bus passengers and including the inertia of the wheelchair occupants and the wheel chair lifts under rapid bus deceleration. Parametric results for floor angles of 0, 5, 10, 15, 20, 25, and 30 degrees at maximum bus deceleration were derived. Conclusions pertaining to the results generated by these additional analyses are also presented below.

Wall-Mounted Versus Floor-Mounted Seats

The following conclusions pertain to the bus responses with wall-mounted versus floor-mounted seats:

1. The maximum plywood floor element stresses were slightly higher (+1%) to substantially higher (+86%) with wall-mounted versus floor-mounted seats.
2. The lateral frame elements had slightly lower (-3%) to moderately lower (-30%) maximum stresses with wall-mounted versus floor-mounted seats.
3. In the 21-foot bus, the longitudinal chassis elements had maximum stresses that were moderately higher (+22%) to substantially higher (+41%) with wall-mounted seats versus floor-mounted seats.
4. The longitudinal chassis elements in the 25-foot bus had maximum stresses that were moderately lower (-22%) to moderately higher (+32%) with wall-mounted seats versus floor-mounted seats.
5. The body elements, steel plate elements, and longitudinal chassis cap elements had slightly higher (+4%) to very substantially higher (+278%) maximum stresses with wall-mounted versus floor-mounted seats.
6. The maximum stresses in the perimeter frame elements and the lateral chassis elements were slightly lower (-9%) to substantially lower (-77%) with wall-mounted versus floor-mounted seats.

With Versus Without Wheelchairs

In general, the maximum element stresses were higher with wheelchairs versus without wheelchairs. With floor-mounted seats, the differences between the cases with and without wheelchairs were generally small, with a maximum increase of +7.1% and a maximum decrease of -16.2%. With wall-mounted seats, however, the differences between the cases with and without wheelchairs were generally larger, with a maximum increase of +21.1% and a maximum decrease of -14.9%.

General Conclusions

The following general conclusions can be drawn regarding the responses of typical medium-duty transit buses to rapid deceleration:

1. With full seat belt usage, maximum member stresses should in general be lower compared with staggered seat belt usage or front seat belt usage only. The more-uniform distribution of passenger inertial loads resulting from full seat belt usage offers a clear advantage to the structure of the transit bus under rapid deceleration.
2. Maximum member stresses should in general be lower with floor-mounted versus wall-mounted seats. With their exterior legs attached directly to the perimeter of the frame, floor-mounted seats would seem to offer a distinct benefit to the bus structure under rapid deceleration.
3. The maximum stresses could be relatively high in the seat anchorage members with wall-mounted seats and in the perimeter frame members with floor-mounted seats. Thus these members could yield at relatively low levels of deceleration and could continue to yield and deform as deceleration increases. In this way, the authors believe that these secondary structural members may act as "passenger shock absorbers" in that their deformation (and hence their absorption of energy) could cushion the bus passengers, thus reducing the level of deceleration felt by the bus passengers.
4. In general, the differences should be relatively small between the maximum member stresses for shorter medium-duty transit buses and the corresponding maximum stresses for longer buses. While the shorter buses have fewer passengers and thus less passenger inertial load, the longer buses have more members thus providing more avenues for stress redistribution which results in lower member stresses per unit of load.

5. The presence of wheelchairs, wheelchair restraints, and wheelchair lifts could result in small to moderate increases in maximum member stresses, especially if wall-mounted seats are utilized. These increases in stress are most likely caused by stress concentrations in the vicinities of the wheelchairs and the wheelchair lifts.

ACKNOWLEDGEMENTS

This paper is the outcome of a research project currently being conducted at the Department of Civil Engineering, Wayne State University. The project is funded jointly by the U.S. Department of Transportation and the Michigan Department of Transportation (MDOT). The federal funding was obtained as a part of the Great Lakes Center for Truck Transportation Research (GLCTTR) at the University of Michigan Transportation Research Institute (UMTRI), Ann Arbor. Matching support was also provided by the Institute of Manufacturing Research and the Graduate School, Wayne State University.

The authors are grateful to all of the above agencies for providing the financial support for this study. The opinions and comments expressed in this paper are entirely those of the authors and do not necessarily reflect the policies and programs of the agencies mentioned above.

REFERENCES

1. D.M. Severy, H.M. Brink, and J.D. Baird. School Bus Passenger Protection. Automotive Engineering Congress. Society of Automotive Engineers, Detroit, Michigan, January 9-13, 1967, pp. 290-379.
2. D.J. LaBelle. Barrier Collision and Related Impact Sled Tests on Buses in Intercity Service. Proceedings of the Seventh Stapp Car Crash Conference. Institute of Transportation and Traffic Engineering, Charles C. Thomas Publisher, Springfield, Illinois, 1965, pp. 46-53.
3. K. Rompe and H.J. Kruger. Possibilities of Development in Bus Safety. International Journal of Vehicle Design - The Journal of Vehicle Engineering Components, Vol. 7, Nos. 5/6, September 1986, pp. 178-191.
4. C.R. Ursell. A Study Relating to Seat Belts for Use in Buses. Report No. HS-802 253. U.S. Department of Transportation, Washington, D.C., January 1977.
5. G.N. Farr. School Bus Safety Study, Volume 1. Report No. TP 6222 E. Traffic Safety Standards and Research, Transport Canada, Ottawa, Ontario, Canada, January 1985.
6. D.A. Alianello and W.E. Levan. Crash Testing of Thomas Minotour Vehicle, 1986 Thomas Bus, Intermediate School Bus. Calspan Report No. 7481-1. Calspan Corporation, Buffalo, New York, June 1986.
7. F.G.J. Van Asperen and H.J.M. Voets. Optimization of the Dynamic Behavior of a City Bus Structure. Proceedings of the International Conference on the Bus '86. The Institution of Mechanical Engineers, Mechanical Engineering Publications, Ltd., London, England, September 9-10, 1986.
8. R.A. Dusseau, S. Khasnabis, and T.J. Dombrowski. Impact of Seat Belts on the Structure of a Typical Transit Bus. Transportation Research Record. Transportation Research Board, Washington, D.C., 1991.

9. S. Khasnabis, R.A. Dusseau, and T.J. Dombrowski. Safety Implications of Seat Belts on Transit Buses. Transportation Research Record.
Transportation Research Board, Washington, D.C., 1991.
10. Motor Vehicle Safety Standard No. 222: School Bus Seating and Crash Protection. Federal Motor Vehicle Safety Standards and Regulations.
National Highway Traffic Safety Administration, U.S. Department of Transportation, Washington, D.C., January 28, 1976.

SAFETY AND STRUCTURAL IMPLICATIONS
OF SEAT BELTS ON TRANSIT BUSES

PHASE III - FINAL REPORT

By

Ralph Alan Dusseau

Associate Professor

Department of Civil and Environmental Engineering

Snehamay Khasnabis

Professor

Department of Civil and Environmental Engineering

Terence Smith

Graduate Research Assistant

Department of Civil and Environmental Engineering

Wayne State University

Detroit, MI 48202

December 1992

This study was jointly sponsored by the Michigan Department of Transportation and the U.S. Department of Transportation through the Great Lakes Center for Truck Transportation Research at the University of Michigan, Ann Arbor.

TABLE OF CONTENTS

	<u>PAGE</u>
List of Figures.....	iii
Chapter 1: Introduction.....	1
Chapter 2: Laboratory Testing.....	3
Section 2.1: Introduction.....	3
Subsection 2.1.1: Phase II Activities.....	3
Subsection 2.1.2: Phase III Testing.....	5
Section 2.2: Test Specimen Configurations.....	5
Section 2.3: Laboratory Test Results.....	7
Section 2.4: Calculated Test Results.....	9
Subsection 2.4.1: Coefficient of Friction.....	9
Subsection 2.4.2: Minimum Shear Force Capacity....	10
Subsection 2.4.3: Critical Bus Decelerations.....	12
Chapter 3: Computer Modeling.....	15
Chapter 4: Summary, Conclusions, and Recommendations.....	16
Section 4.1 Summary.....	16
Section 4.2 Conclusions.....	16
Section 4.3 Recommendations.....	17
Acknowledgments.....	19
Appendix: Notation.....	20
Tables.....	21
TABLE 1. Laboratory Test Results.....	21
TABLE 2. Calculated Test Results.....	22
Figures.....	23

LIST OF FIGURES

- Figure 1. Schematic Diagram of Load Platform and Specimen
- Figure 2. Plot for Specimen 45-2-N
- Figure 3. Plot for Specimen 45-2-Y
- Figure 4. Plot for Specimen 45-3-N
- Figure 5. Plot for Specimen 45-3-Y
- Figure 6. Plot for Specimen 50-2-N
- Figure 7. Plot for Specimen 50-2-Y
- Figure 8. Plot for Specimen 50-3-N
- Figure 9. Plot for Specimen 50-3-Y
- Figure 10. Plot for Specimen 55-2-N
- Figure 11. Plot for Specimen 55-2-Y
- Figure 12. Plot for Specimen 55-3-N
- Figure 13. Plot for Specimen 55-3-Y
- Figure 14. Plot for Specimen 60-2-N
- Figure 15. Plot for Specimen 60-2-Y
- Figure 16. Plot for Specimen 60-3-N
- Figure 17. Plot for Specimen 60-3-Y
- Figure 18. Plot for Specimen 65-2-N
- Figure 19. Plot for Specimen 65-2-Y
- Figure 20. Plot for Specimen 65-3-N
- Figure 21. Plot for Specimen 65-3-Y
- Figure 22. Plot for Specimen 70-2-N
- Figure 23. Plot for Specimen 70-2-Y
- Figure 24. Plot for Specimen 70-3-N
- Figure 25. Plot for Specimen 70-3-Y
- Figure 26. U-bolt Deformation Diagram

CHAPTER 1

INTRODUCTION

This report is the result of a study conducted at the Department of Civil and Environmental Engineering, Wayne State University to assess the safety and structural implications of seat belts on transit buses. Phase III of this investigation, jointly funded by the U.S. Department of Transportation and the Michigan Department of Transportation, had two primary tasks:

1. To perform laboratory tests to determine the ultimate shear strength capacity of the bus frame-to-chassis U-bolt connections (both with and without shear tabs) that were used in the 1989 and 1990 CTS buses.
2. To develop and analyze computer models of the structural system consisting of one track-mounted bus seat, and including representative sections of the bus floor, sidewalls, and frame.

Because the design of track-mounted seats has not yet been completed by the bus manufacturer, a decision was made (after consultation with MDOT officials) to perform the following task during Phase III in lieu of Task 2 listed above:

3. To perform preliminary activities related to the development of a finite-element computer model for the 1992 CTS 25-foot bus.

Moreover, the time that would have been devoted to Task 3 during Phase IV of the project will instead be used to perform Task 2 assuming that the design of the track-mounted seats is completed by the bus manufacturer. If this design is not completed during

Phase IV, then another task related to the CTS buses will be performed.

The remaining portion of this Phase III Final Report is presented in three additional chapters. A report on the results of the laboratory tests that were conducted as part of Task 1 listed above is presented in Chapter 2. A brief report on the status of the finite-element modeling and analysis activities that are described under Task 3 listed above is included in Chapter 3. The summary of Phase III activities and the conclusions and recommendations for Phase III with regard to the laboratory tests that were conducted are presented in Chapter 4.

CHAPTER 2

LABORATORY TESTING

2.1 INTRODUCTION

To determine the ultimate shear strength capacity of the frame-to-chassis U-bolt connections in the 1989 and 1990 CTS buses, laboratory tests were conducted with testing activities beginning in Phase 2 of the project and with final connection testing completed in Phase 3. These tests utilized the MTS machine in the Department of Civil and Environmental Engineering at Wayne State University.

2.1.1 Phase II Activities

The following activities were finished during Phase 2 of the project:

1. Design of the load platform for the MTS machine.
2. Design of the test specimens.
3. Design of the MTS connection detail.
4. Purchasing construction materials.

The final design for the load platform consisted of the following components:

1. An inverted tee-beam base which was fabricated from a hot-rolled WT 7 x 45 steel section and was bolted to the base of the MTS machine.
2. A 12-inch by 9-inch by 3/4-inch steel base plate which was welded to the web of the tee-beam and which was supported by four 6-inch by 5-inch by 1/2-inch steel plate stiffeners.
3. Two 5-inch by 3-inch by 3/16-inch hot-rolled

rectangular steel tubes which were welded to the tee-beam flange and which slope upward to support a 17-inch by 14-inch by 3/4-inch steel top plate.

4. Top and bottom 10-inch by 9-inch by 1/2-inch steel connection plates which were bolted to the top and bottom plates of the load frame and were connected by two 1-inch by 1-inch square tubes.

The final design for the test specimens consisted of the following components:

1. A 48-inch segment of the longitudinal chassis channel members which was bolted to the top and bottom steel connection plates.
2. A 38-inch segment of the longitudinal channel cap members which was fastened to the segment of the longitudinal chassis channel member with two or three U-bolts and with or without shear tabs.
3. A 38-inch segment of 2 1/2-inch by 1-inch oak which was sandwiched between the chassis channel segment and the channel cap segment.

An MTS connection detail was designed to connect the chassis cap segment of the test specimen with a 2.5-inch steel rod that was connected to the loading head of the MTS machine. A schematic diagram of the load frame, test specimen, and connection detail is shown in Fig. 1.

All of the materials for the construction of the load platform, the 30 test specimens, and the MTS connection detail were ordered and received in the Summer and Fall of 1991. The

chassis channel segments, the channel cap segments, the U-bolts, and the shear tabs were all ordered from the same vendors utilized by the bus manufacturer and using the same specifications as the bus manufacturer.

2.1.2 Phase III Testing

During Phase III, each specimen was mounted and then tested in the MTS machine. Shearing forces representing the inertia of the bus body and passengers were applied to the test specimens through the MTS connection detail and were increased until failure of the specimens occurred. For each test specimen, the maximum shear forces applied and the relative displacements between the channel cap segment (which represents the bus frame) and chassis channel segment were monitored during load application. Thus, the failure mode for each specimen was determined. Six of the 30 test specimens were used for preliminary tests to determine the limits on the parameters that were to be varied in the primary tests. The results of these six preliminary tests are not presented herein, but the findings for the remaining 24 tests are presented and all 24 of these primary tests were videotaped.

2.2 TEST SPECIMEN CONFIGURATIONS

Three parameters were considered in deriving the specimens to be tested: U-bolt torque, number of U-bolts, and utilization of shear tabs. The U-bolt torque used by the bus manufacturer for tightening the nuts on all CTS bus U-bolts is 55 foot-pounds (ft-lb). Because we believed that bolt torque could play a role in maximum shear capacity, six different bolt torques were used in the tests: 45, 50, 55, 60, 65, and 70 ft-lb. Four different

specimens were tested at each of these bolt torques:

1. A specimen having two U-bolts without shear tabs.
2. A specimen having two U-bolts with shear tabs.
3. A specimen having three U-bolts without shear tabs.
4. A specimen having three U-bolts with shear tabs.

Thus, a total of 24 primary specimens were tested.

For each test specimen, loads were applied using a "displacement controls" procedure in which the displacements of the channel cap segment relative to the chassis channel segment were increased at uniform rates. For the 12 test specimens without shear tabs, the rate of application was one inch per minute for the entire six inches of motion allowed. While this rate of application is considerably slower than what an actual bus might experience under emergency conditions, a faster rate of application would have made it much more difficult to adequately record all test results (both measured and videotaped). Two of the six preliminary tests were conducted at much greater rates of application. The results of these two tests indicated that much faster rates of application would result in very little if any change in the test results.

For the 12 specimens with shear tabs, the rate of application was $\frac{1}{4}$ inch per minute for the first inch of motion and then one inch per minute for the remaining five inches of motion. The very slow initial rate of application was chosen in order to be able to adequately record the failure mechanism for the shear tabs which were expected to fail within the first inch of motion. The rate of application for the remaining five inches of motion, which

should occur after failure of the shear tabs, was the same as the one inch per minute rate of application used for the 12 specimens without shear tabs.

2.3 LABORATORY TEST RESULTS

The final plots of shear force versus relative displacement are depicted in Figs. 2 to 25 for the 24 primary test specimens. The specimen names (such as 45-2-N or 70-3-Y) refer to the bolt torque (45 to 70 ft-lb), the number of U-bolts per specimen (2 or 3), and the use of shear tabs (N = no and Y = yes).

For the 12 specimens without shear tabs (Figs. 2, 4, 6, 8, 10, 12, 14, 16, 18, 20, 22, and 24), the curves were characterized by a gradual buildup of force to a maximum value. This gradual buildup of force ended at a relative displacement of one to two inches when one or more U-bolts slipped. This slippage occurred at the bottom of the U-bolt(s) where the base plate(s) of the U-bolt(s) slid along the bottom flange of the chassis channel segment. In most cases, further cycles of force buildup and slippage then occurred, but in none of the cases did the shear force exceed the value derived before the slippage of the first U-bolt(s). This is a clear indication that the U-bolts reached and exceeded their yield stresses during the initial buildup of forces and were thus longer and offered less resistance during subsequent cycles. Moreover, the results for all 12 test specimens indicated no apparent correlation between U-bolt torque and the maximum shear force capacity. Thus, the maximum shear force capacity for these specimens was a function of the yield stress of the U-bolts and not the initial stress in the U-bolts.

For the 12 specimens with shear tabs (Figs. 3, 5, 7, 9, 11, 13, 15, 17, 19, 21, 23, and 25), the curves were characterized by a rapid buildup of force to a maximum value. This rapid buildup of force ended when the welds on the shear tabs failed which happened before a relative displacement of one inch had occurred. This was followed by a gradual buildup of force similar to the specimens without shear tabs which ended with slippage of the first U-bolt(s). The remainder of the curves were very similar to curves for the specimens without shear tabs. Because the failure mechanism for these specimens was the shear tab welds, the results for all 12 test specimens indicated no apparent correlation between U-bolt torque and the maximum shear force capacity.

Table 1 presents a summary of the results for each test specimen with averages (AV-2-N, AV-2-Y, AV-3-N, and AV-3-Y) for the four different types of specimens listed in Section 2.2 above. The results that are listed in Table 1 for each test include the maximum shear force (F_s) in kips (1000 pounds) that was recorded prior to slippage of the first U-bolt(s), the maximum relative displacement (δ_s) in inches before the first U-bolt(s) slipped, the angle of tilt (α) in degrees for all of the U-bolts when the first U-bolt(s) slipped, and the maximum shear force (F_{st}) in kips resisted by the shear tabs for the 12 specimens with shear tabs.

2.4 CALCULATED TEST RESULTS

Table 2 presents the results derived by hand calculations which were based on the test results. These hand calculations are described in more detail below.

2.4.1 Coefficient of Friction

As indicated in Table 1, the angle of tilt (α) of the U-bolts when the first U-bolt(s) slipped was between 9.3 and 12.9 degrees for each specimen. Assuming the total force in the U-bolt shanks was a constant value (P) due to yielding of the U-bolt shanks, then (as depicted in Fig. 26) the total normal force (N) transferred by the shanks through the base plates of the U-bolts to the bottom flange of the chassis channel segment would be:

$$N = P \cdot \cos \alpha \quad (1)$$

Slippage between the oak filler and the top flange of the chassis channel segment began almost immediately upon application of loading. Thus, the shear resistance along this surface and hence the coefficient of friction between the oak and the steel would appear to be very small. Therefore, the shear resistance between the oak filler and the top flange of the chassis channel section is not included in the calculations that follow. Hence, the maximum resisting shear force (F_s) was attributed to friction between the base plates of the U-bolts and the bottom flange of the chassis channel segment. This maximum resisting shear force (F_s) can be calculated as follows:

$$F_s = \mu_s \cdot N = \mu_s \cdot P \cdot \cos \alpha \quad (2)$$

where μ_s is the steel-to-steel coefficient of friction between the base plates of the U-bolts and the bottom flange of the chassis channel segment. Just prior to slippage of the first U-bolt(s), the total shear force (F_t) transferred from the channel cap segment through the U-bolt shanks to the U-bolt base plates would be:

$$F_t = P \sin \alpha \quad (3)$$

At the time of slippage of the first U-bolt(s):

$$F_t = F_s \quad (4)$$

And thus:

$$\mu_s P \cos \alpha = P \sin \alpha \quad (5)$$

or:

$$\mu_s = \sin \alpha / \cos \alpha \quad (6)$$

The values of μ_s derived for each test specimen using Equation 6 are listed in Table 2 and range from 0.164 to 0.229 with an average of about 0.20. The values of μ_s were relatively close to 0.20 for most of the 24 test specimens.

2.4.2 Minimum Shear Force Capacity

As indicated in Table 1 (and as discussed in Subsection 2.4.1 above), all 24 test specimens recorded U-bolt tilts before first U-bolt slippage of 9.3 to 12.9 degrees. In order to achieve these angles of tilt, elongations of the 7-inch U-bolt shanks of 0.093 to 0.181 inches would be required. These represent steel strains between 0.0133 to 0.0259 which would all be far in excess of the value required to cause yielding of the steel (0.00114). Thus, it can safely be assumed that when the first U-bolt(s) slipped, the stress in all of the U-bolt shanks had reached the yield stress. Inspections of the U-bolts after each test indicated that yielding did occur in the U-bolt shanks in the areas at or slightly above the locations of the U-bolt nuts.

Based on information supplied by the fabricators, the steel used to make the U-bolts should have a minimum yield stress of 33 kips per square inch (ksi). The diameter of the U-bolt shanks was

found to be 0.525 inches at the base of the threads. Thus, the minimum area of each U-bolt shank should be 0.2165 square inches (si). Using this area and a minimum yield stress (Fy) of 33 ksi, the minimum yield force capacity (Ps) of each U-bolt shank should be:

$$P_s = A_b * F_y = (0.2165) * (33) = 7.145 \text{ kips per shank} \quad (8)$$

The minimum calculated shear force capacity (Fc) of each test specimen would then be:

$$F_c = n * P_s * \sin \alpha. \quad (9)$$

where n is the total number of U-bolt shanks. For specimens with two U-bolts (n = 4):

$$F_c = 28.6 * \sin \alpha \quad (10)$$

For specimens with three U-bolts (n = 6):

$$F_c = 42.9 * \sin \alpha \quad (11)$$

The minimum calculated shear force capacity (Fc) for each test specimen is listed in Table 2. The percent difference between the actual shear capacity (Fs) of each test specimen and the minimum calculated value (Fc) is also presented in Table 2. These percentages represent the reserve strength of each specimen which may be attributable to one or more of the following:

1. The differences in the steel-to-steel coefficients of friction which have a direct impact on the U-bolt angle of tilt (α).
2. Some of the U-bolt shanks, especially those with strains at or above 0.02, may have reached the strain hardening stage of stress which would result in axial stresses above the yield stress of 33 ksi.

3. The actual yield stresses for some of the U-bolts may have been somewhat higher than the minimum of 33 ksi which is guaranteed by the manufacturer.
4. Higher grades of steel may have been used to fabricate some of the U-bolts.
5. Some U-bolts or U-bolt shanks may have had small initial angles of tilt before the application of loading began.
6. Deformation of some U-bolt heads, shanks, and threads may have occurred as the U-bolts bit into the channel caps during initial stressing and during testing.
7. Excess bending of the bottom flanges of some of the chassis channel segments may have occurred due to stressing of the U-bolts both initially and during testing.

It should be noted, however, that every attempt was made to avoid anomalies such as item 5 listed above.

2.4.3 Critical Bus Decelerations

While the shear tab in one test specimen did fail at 8.1 kips due to the poor quality of the shear tab welds, the average results from Table 1 indicate that the maximum shear capacity per shear tab should be approximately 21 kips, while the maximum shear capacity per U-bolt should be about 3.5 kips. For the 1989 and 1990 CTS 25-foot buses, the number of shear tabs per bus was two, while the number of U-bolts was 14. Thus, the maximum shear capacity (F_v) of the frame-to-chassis connections in each 1989 and 1990 CTS 25-foot bus should be approximately 42 kips (2 shear tabs

at 21 kips per shear tab) for the shear tabs and 49 kips (14 U-bolts at 3.5 kips per U-bolt) for the U-bolts. Assuming an average passenger weight of 125 lbs (0.125 kips) and assuming the total weight of the bus body, frame, seats, etc. in the bus passenger compartment to be at least 1,000 pounds (1 kip), then the minimum bus decelerations (Dcr) required to cause failure of the shear tab welds and the U-bolts could be calculated using:

$$\begin{aligned} Dcr &= Fv / [(26 \text{ pass.}) (0.125 \text{ kips per pass.}) + 1 \text{ kip}] \quad (12) \\ &= Fv / 4.25 \end{aligned}$$

The resulting minimum bus decelerations would be 10.0g and 11.5g, respectively, for the shear tab welds and the U-bolts, where "g" is the gravitational acceleration constant (32.2 feet per second²). Assuming a bus velocity, V, of 55 miles per hour (mph) or 81 feet per second (fps), these levels of deceleration (10.0g and 11.5g) would translate into stopping distances, Lst, calculated as follows:

$$\begin{aligned} Lst &= V^2 / (2 g Dcr) \quad (13) \\ &= (81)^2 / (2 (32.2) Dcr) \\ &= 102 / Dcr \end{aligned}$$

The resulting stopping distances would be 10.2 feet and 8.9 feet, respectively, for failure of the shear tab welds and slippage of the U-bolts. This would clearly require a serious collision. As a comparison, assuming an emergency braking distance (without collision) of 300 feet at 55 mph, the level of deceleration required would only be 0.34g.

It should be noted that for each of the 12 test specimens with shear tabs, the welds that were used to fasten the shear tabs

to the channel cap segments and to the chassis channel segments were wrap-around welds with total weld lengths of approximately 4 inches per side of connection (channel cap side or chassis channel side). Some of the shear tab welds that were observed on a new 1992 CTS 25-foot bus during a field trip to the bus manufacturer were end-welds only, with total lengths of approximately 2 inches per side. Thus, with end-welds only, the expected capacity of the shear tabs would drop to 10.5 kips or less per tab for a total of 21.0 kips or less per bus. This would translate into a minimum bus deceleration for shear tab weld failure of 5g or less.

CHAPTER 3

COMPUTER MODELING

As discussed in Chapter 1, because the bus manufacturer has not yet completed the design of track-mounted seats for the CTS buses, the time that would have been spent during Phase III in the development of a detailed model with track-mounted seats was instead spent performing several preliminary activities related to the development of a finite-element computer model for the 1992 CTS 25-foot bus. These activities included the sizing of the structural members (determination of member shape, length, width, height, thickness, etc.), the calculation of member properties (cross-sectional areas, moments of inertia, etc.), and the calculation of nodal coordinates (x, y, and z). These activities are a time-consuming but necessary precursor to the finite-element modeling and analysis that will be performed during Phase IV of the project. Because the results of these preliminary activities consist of calculations and computer input data which are rather detailed, very repetitive, quite extensive, and largely uninformative in nature, the results of these preliminary activities for the 1992 CTS 25-foot bus have not been included in this Phase III Final Report. It should be noted that these types of preliminary results for the 1989 and 1990 CTS buses were not included in the final reports for Phases I or II of the project.

CHAPTER 4

SUMMARY, CONCLUSIONS, AND RECOMMENDATIONS

4.1 SUMMARY

Laboratory tests were conducted to determine the ultimate shear capacity of the bus frame-to-chassis U-bolt connections in the 1989 and 1990 CTS buses. These tests were conducted on 24 primary specimens:

1. With U-bolt torques of 45, 50, 55, 60, 65, and 70 ft-lb.
2. With two and three U-bolts.
3. With and without shear tabs.

Preliminary activities related to the Phase IV finite-element modeling and analysis of the new 1992 CTS 25-foot bus were also performed.

4.2 CONCLUSIONS

For the 12 test specimens without shear tabs, no correlation was found between the U-bolt torque and the maximum shear capacity. An average maximum shear capacity of about 3.5 kips per U-bolt was derived. For each specimen, the maximum shear capacity was reached between one and two inches of relative displacement after a gradual buildup of shear force. Failure happened when slippage occurred between the base plates of one or more U-bolts and the bottom flange of the chassis channel segments.

For the 12 specimens with shear tabs, no correlation was found between the U-bolt torque and the maximum shear capacity. The results indicated that the maximum shear capacity that was attributable to the shear tabs was about 21 kips per shear tab with full wrap-around welds. This maximum shear capacity was

reached within the first one inch of relative displacement after a rapid buildup of shear force. After failure of the shear tabs, the shear capacity dropped sharply and then began to gradually increase to a secondary maximum value that was comparable to the maximum shear forces derived for the 12 corresponding test specimens without shear tabs.

4.3 RECOMMENDATIONS

Because the torque that is used to tighten the U-bolts has no apparent effect on the maximum shear capacity of the bus frame-to-chassis connections, no change in the 55 foot-pounds of torque that is currently used by the bus manufacturer is recommended. In addition, based on the test results presented herein, the number of U-bolts (14) used in the 1989 and 1990 CTS 25-foot buses should be adequate to resist a maximum bus deceleration of 11.5g with a corresponding relative bus body to chassis displacement of about 1.5 inches. We would like to note, however, that some additional U-bolt shear capacity could be achieved if the base plates of the U-bolts were welded to the bottom flanges of the chassis channel members. The potential increase in U-bolt shear capacity resulting from U-bolt base plate-to-bottom flange welds will be investigated as part of the Phase IV laboratory tests.

With regard to the shear tabs and shear tab welds, the original design (which utilized two shear tabs per bus) should be adequate up to 10.0g of bus deceleration if full wrap-around welds were used as designated in the bus design plans for the 1989 and 1990 CTS buses. If a maximum bus deceleration of at least 10.0g

is to be reached in the new 1992 CTS buses before the shear tabs fail, then full wrap-around welds should also be designated for these new buses. A recent inspection of a 1992 CTS bus, however, indicated, that end-welds only are currently being used for these new buses. Thus, the maximum bus deceleration before shear tab failure will probably be 5g or less for these new buses. The actual shear capacity of these weaker shear tab welds will be investigate as part of the Phase IV laboratory tests.

The authors believe that the final determination as to what the critical bus decelerations should be for the shear tabs and/or the U-bolts must be carefully considered given the tradeoff between higher shear tab and/or U-bolt capacity and the resulting higher decelerations and stresses that would be felt by the individual bus passengers versus lower shear tab and/or U-bolt capacity and the potential for longitudinal collapse of the bus passenger compartment.

ACKNOWLEDGMENTS

This paper is the outcome of a research project currently being conducted at the Department of Civil and Environmental Engineering, Wayne State University. The project is jointly funded by the U.S. Department of Transportation and the Michigan Department of Transportation. The federal funding was obtained as a part of the Great Lakes Center for Truck Transportation Research at the University of Michigan Transportation Research Institute, Ann Arbor. Additional support was also provided by the Institute for Manufacturing Research and the Graduate School, Wayne State University.

The authors are grateful to all of the above agencies for providing the financial support for this study. The opinions and comments expressed in this paper are entirely those of the authors, however, and do not necessarily reflect the policies and programs of the agencies mentioned above.

APPENDIX: NOTATION

- α = maximum angle of tilt of U-bolts at first U-bolt slippage, degrees
- P = maximum total axial force in U-bolt shanks at first U-bolt slippage, kips
- N = maximum total normal force transferred by U-bolt base plates to bottom flange of chassis channel segment at first U-bolt slippage, kips
- F_s = maximum total resisting shear force due to friction between base plates of U-bolts and bottom flange of chassis channel segment at first U-bolt slippage, kips
- F_{st} = maximum shear force at shear tab failure, kips
- μ_s = steel-to-steel coefficient of friction between U-bolt base plates and bottom flange of chassis channel segment
- F_t = maximum total shear force transferred from U-bolt shanks to U-bolt base plates at first U-bolt slippage, kips
- A_b = cross-sectional area of one U-bolt shank, square inches
- P_s = axial force in one U-bolt shank after yielding, kips
- F_c = minimum calculated shear force capacity of all U-bolts, kips
- n = total number of U-bolt shanks per test specimen
- D_{cr} = minimum (critical) bus deceleration required to cause shear failure (shear tab weld failure or U-bolt slippage), g
- F_v = total shear force capacity of frame-to-chassis connections for each 25-foot bus (due to shear tabs or U-bolts), kips
- g = gravitational acceleration constant (32.2 feet per second)
- L_{st} = stopping distance required to generate critical bus deceleration (D_{cr}) at a velocity of 55 miles per hour, feet

TABLE 1. Laboratory Test Results

U-bolt Torque, lb-ft T	Number of U-bolts N	Shear Tabs? yes or no	Test Specimen Name	Test Results at First U-bolt Slippage			Maximum Shear Tab Force, kips F _{st}
				Maximum Shear Force, kips F _s	Maximum Relative Translation, inches δ _s	Maximum U-bolt Angle of Tilt, degrees α	
45	2	no	45-2-N	6.90	1.55	12.5	NA
		yes	45-2-Y	7.50	1.40	11.3	8.1
	3	no	45-3-N	10.50	1.40	11.3	NA
		yes	45-3-Y	10.00	1.60	12.9	25.8
50	2	no	50-2-N	8.10	1.40	11.3	NA
		yes	50-2-Y	6.80	1.50	12.1	22.1
	3	no	50-3-N	8.60	1.40	11.3	NA
		yes	50-3-Y	9.50	1.35	10.9	22.0
55	2	no	55-2-N	7.10	1.35	10.9	NA
		yes	55-2-Y	7.90	1.40	11.3	21.8
	3	no	55-3-N	10.00	1.30	10.5	NA
		yes	55-3-Y	12.80	1.15	9.3	21.4
60	2	no	60-2-N	6.30	1.45	11.7	NA
		yes	60-2-Y	7.10	1.45	11.7	21.0
	3	no	60-3-N	10.30	1.40	11.3	NA
		yes	60-3-Y	10.00	1.45	11.7	20.2
65	2	no	65-2-N	6.70	1.30	10.5	NA
		yes	65-2-Y	7.90	1.60	12.9	18.5
	3	no	65-3-N	11.30	1.45	11.7	NA
		yes	65-3-Y	9.20	1.30	10.5	21.6
70	2	no	70-2-N	8.30	1.30	10.5	NA
		yes	70-2-Y	8.40	1.55	12.5	21.5
	3	no	70-3-N	10.20	1.30	10.5	NA
		yes	70-3-Y	10.10	1.40	11.3	19.2
Ave.	2	no	AV-2-N	7.23	1.39	11.2	NA
		yes	AV-2-Y	7.60	1.48	12.0	21.0
	3	no	AV-3-N	10.15	1.38	11.1	NA
		yes	AV-3-Y	10.27	1.38	11.1	21.7

TABLE 2. Calculated Test Results

U-bolt Torque, lb-ft T	Number of U-bolts N	Shear Tabs? yes or no	Test Specimen Name	Steel-To-Steel Coefficient of Friction, μ_s	U-bolt Shear Forces		
					Minimum Calculated, kips Fc	Maximum Measured, kips Fs	Percent Difference*
45	2	no	45-2-N	0.222	6.18	6.90	+ 11.7
		yes	45-2-Y	0.200	5.60	7.50	+ 33.9
	3	no	45-3-N	0.200	8.40	10.50	+ 25.0
		yes	45-3-Y	0.229	9.57	10.00	+ 4.5
50	2	no	50-2-N	0.200	5.60	8.10	+ 44.6
		yes	50-2-Y	0.214	5.99	6.80	+ 13.5
	3	no	50-3-N	0.200	8.40	8.60	+ 2.4
		yes	50-3-Y	0.193	8.11	9.50	+ 17.1
55	2	no	55-2-N	0.193	5.40	7.10	+ 31.5
		yes	55-2-Y	0.200	5.60	7.90	+ 41.1
	3	no	55-3-N	0.185	7.81	10.00	+ 28.0
		yes	55-3-Y	0.164	6.93	12.80	+ 84.7
60	2	no	60-2-N	0.207	5.79	6.30	+ 8.8
		yes	60-2-Y	0.207	5.79	7.10	+ 22.6
	3	no	60-3-N	0.200	8.40	10.30	+ 22.6
		yes	60-3-Y	0.207	8.69	10.00	+ 15.1
65	2	no	65-2-N	0.185	5.21	6.70	+ 28.6
		yes	65-2-Y	0.229	6.38	7.90	+ 23.8
	3	no	65-3-N	0.207	8.69	11.30	+ 30.0
		yes	65-3-Y	0.185	7.81	9.20	+ 17.8
70	2	no	70-2-N	0.185	5.21	8.30	+ 59.3
		yes	70-2-Y	0.222	6.18	8.40	+ 35.9
	3	no	70-3-N	0.185	7.81	10.20	+ 30.6
		yes	70-3-Y	0.200	8.40	10.10	+ 20.2
Ave.	2	no	AV-2-N	0.199	5.56	7.23	+ 30.8
		yes	AV-2-Y	0.212	5.92	7.60	+ 28.5
	3	no	AV-3-N	0.196	8.25	10.15	+ 23.1
		yes	AV-3-Y	0.196	8.25	10.27	+ 26.6

* 100 [(Fs / Fc) - 1]

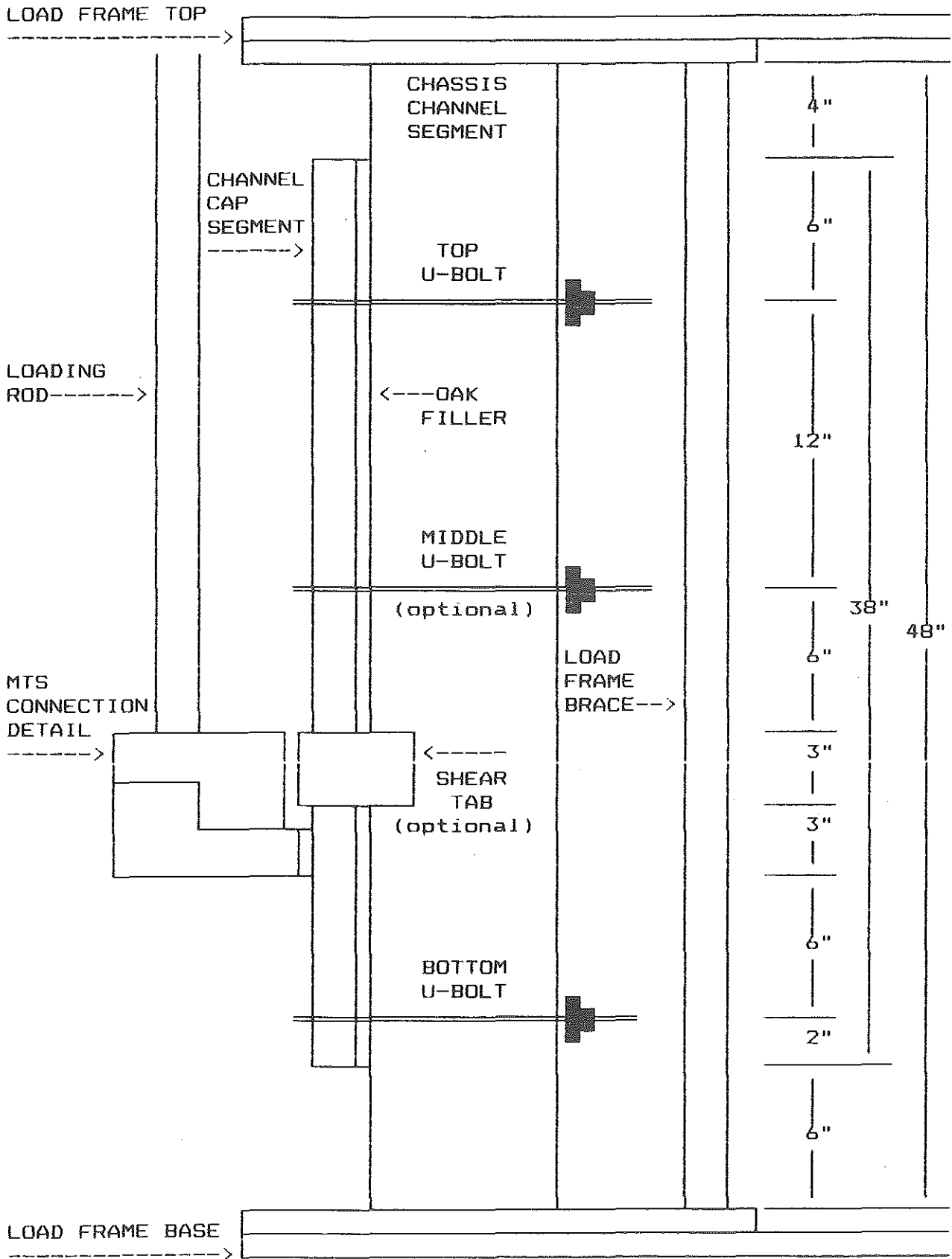


FIG. 1. SCHEMATIC DIAGRAM OF LOAD PLATFORM AND SPECIMEN

FIG.2: PLOT FOR SPECIMEN 45-2-N

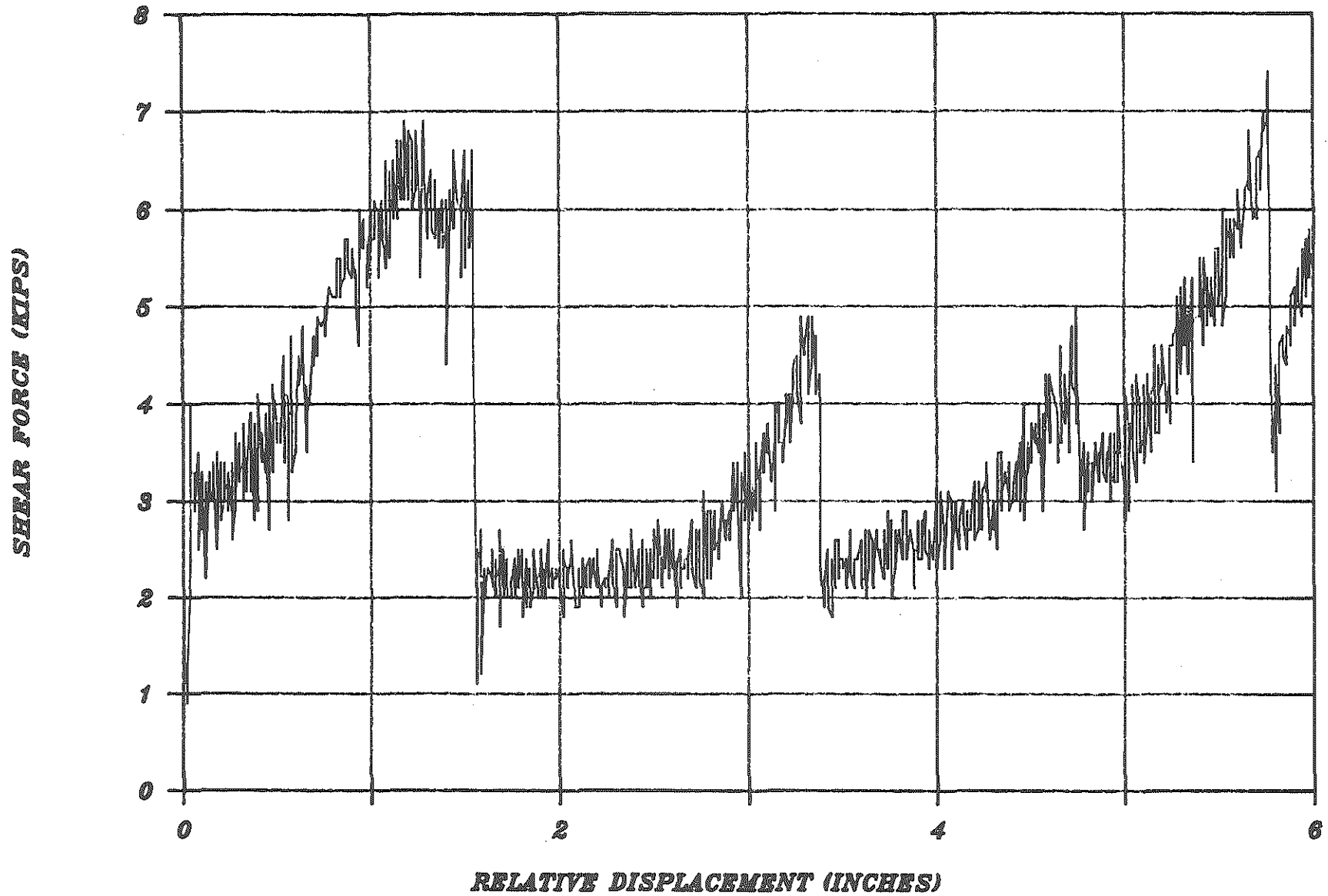


FIG.3: PLOT FOR SPECIMEN 45-2-Y

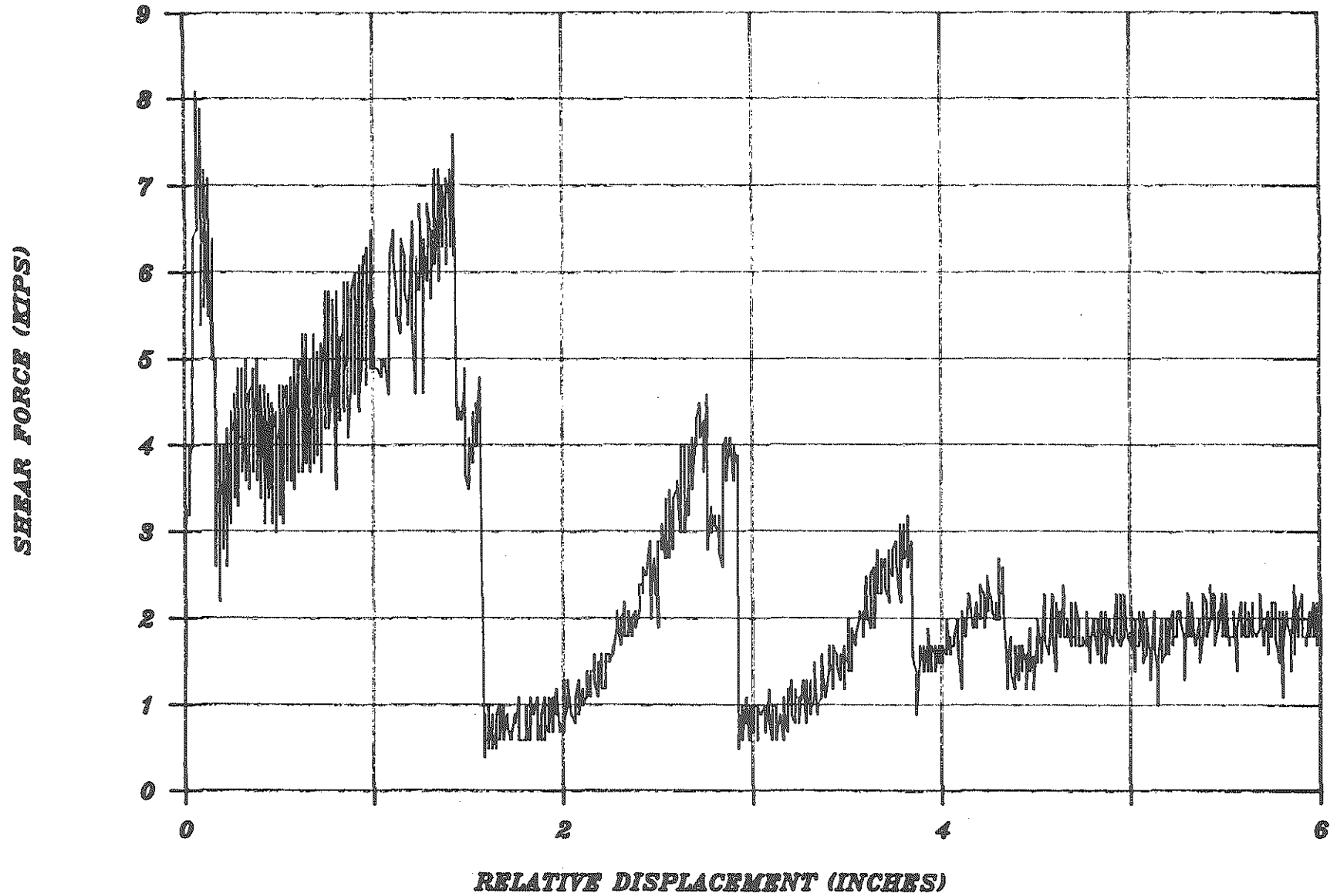


FIG.4: PLOT FOR SPECIMEN 45-3-N

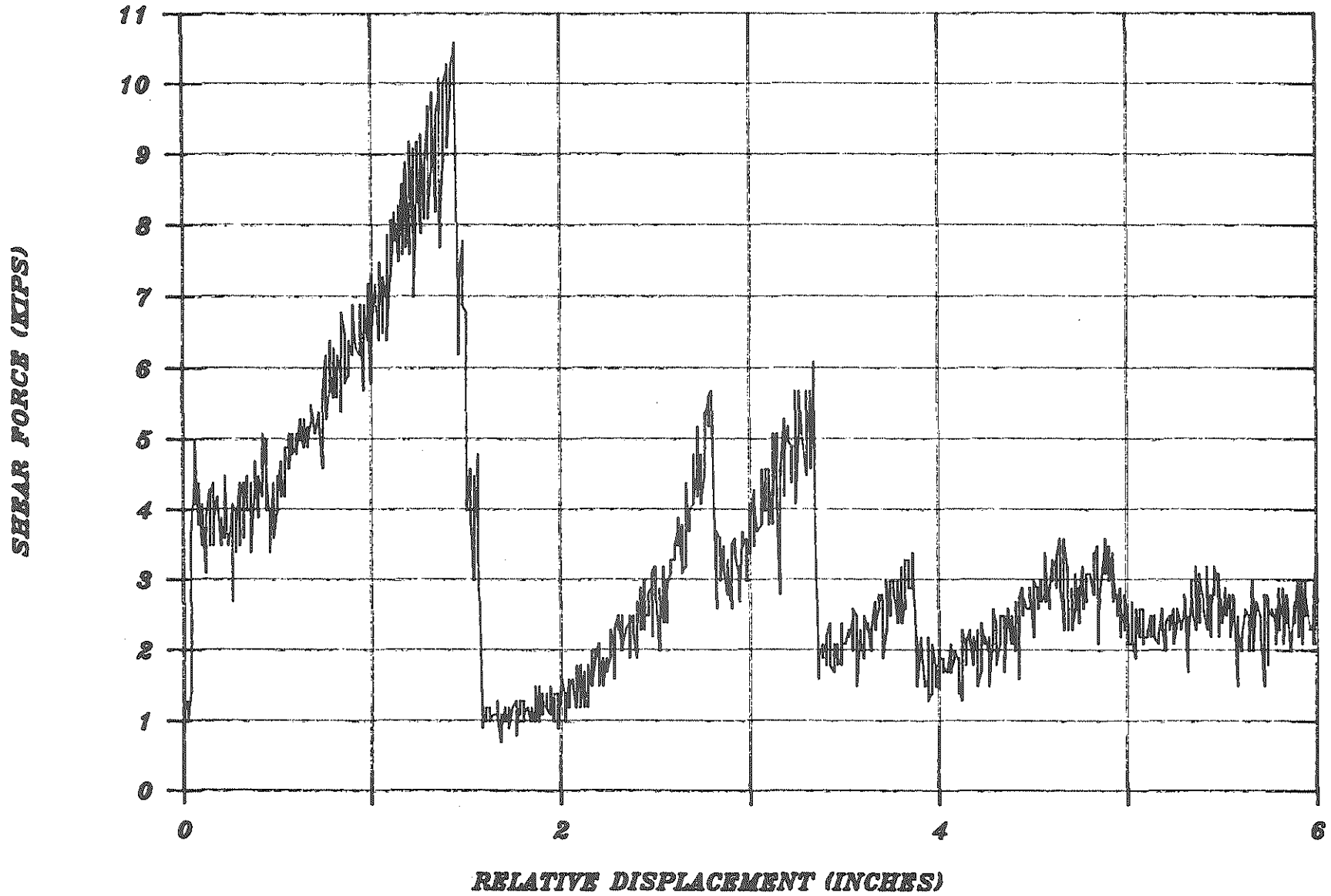


FIG.5: PLOT FOR SPECIMEN 45-3-Y

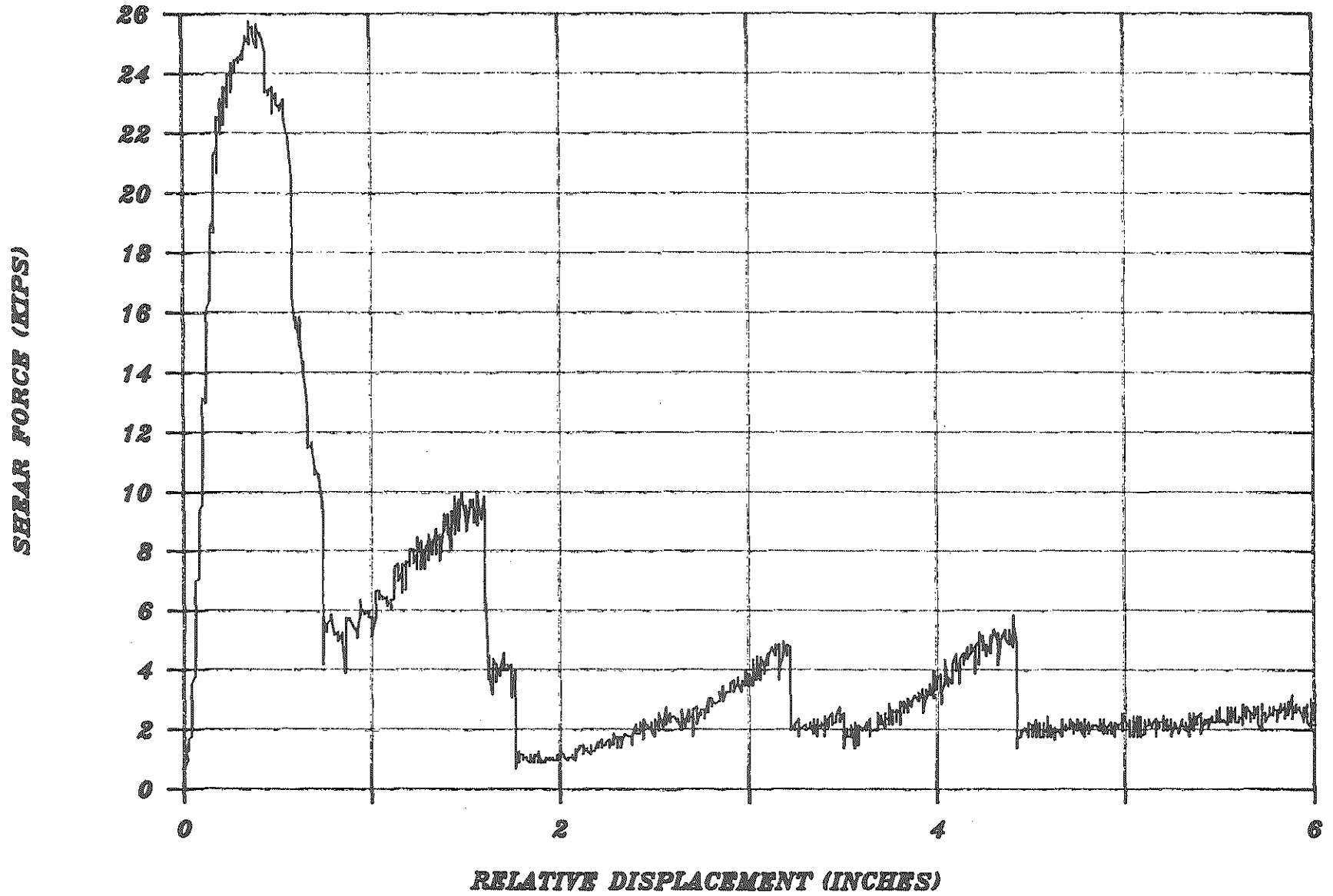


FIG. 6: PLOT FOR SPECIMEN 50-2-N

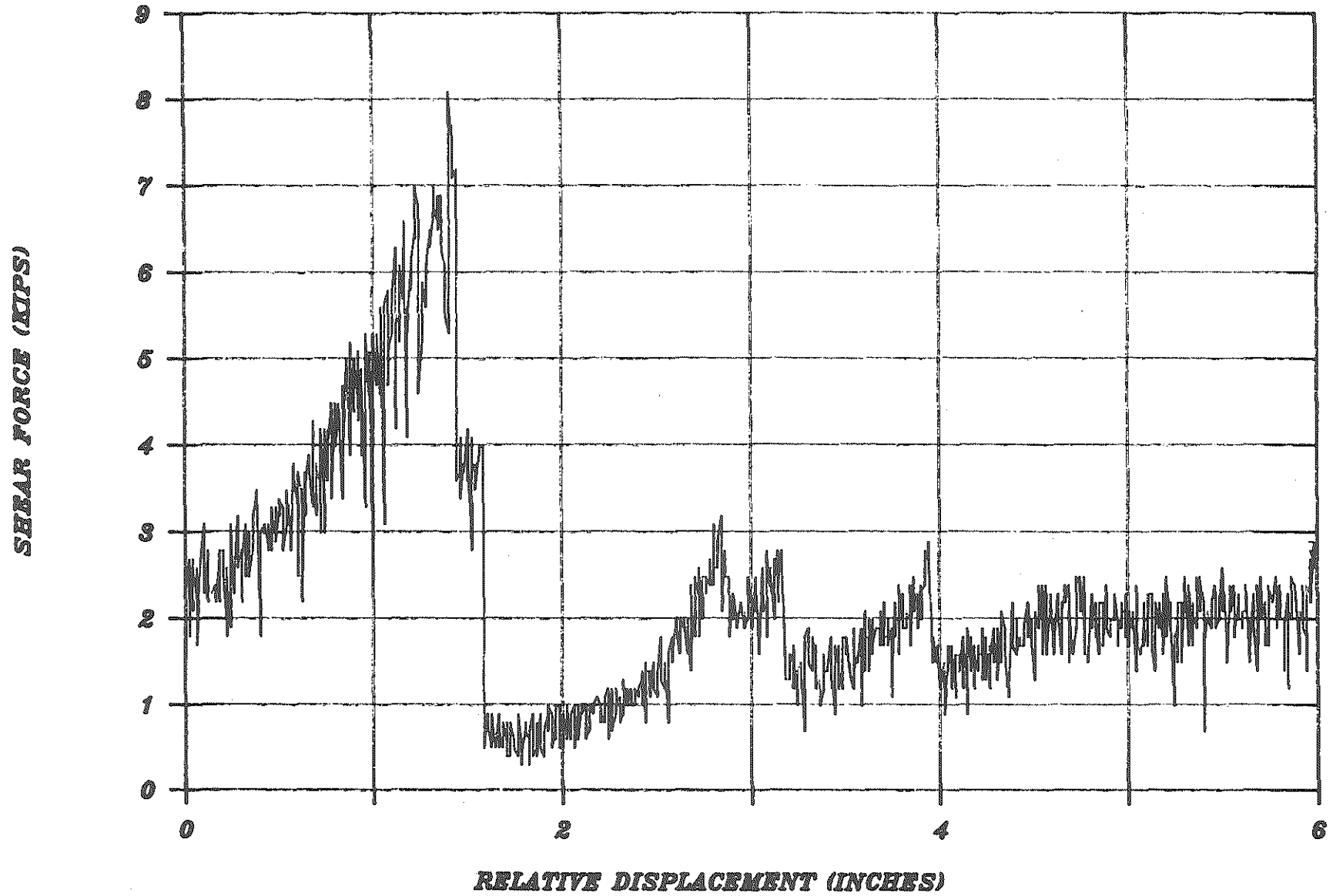


FIG.7: PLOT FOR SPECIMEN 50-2-Y

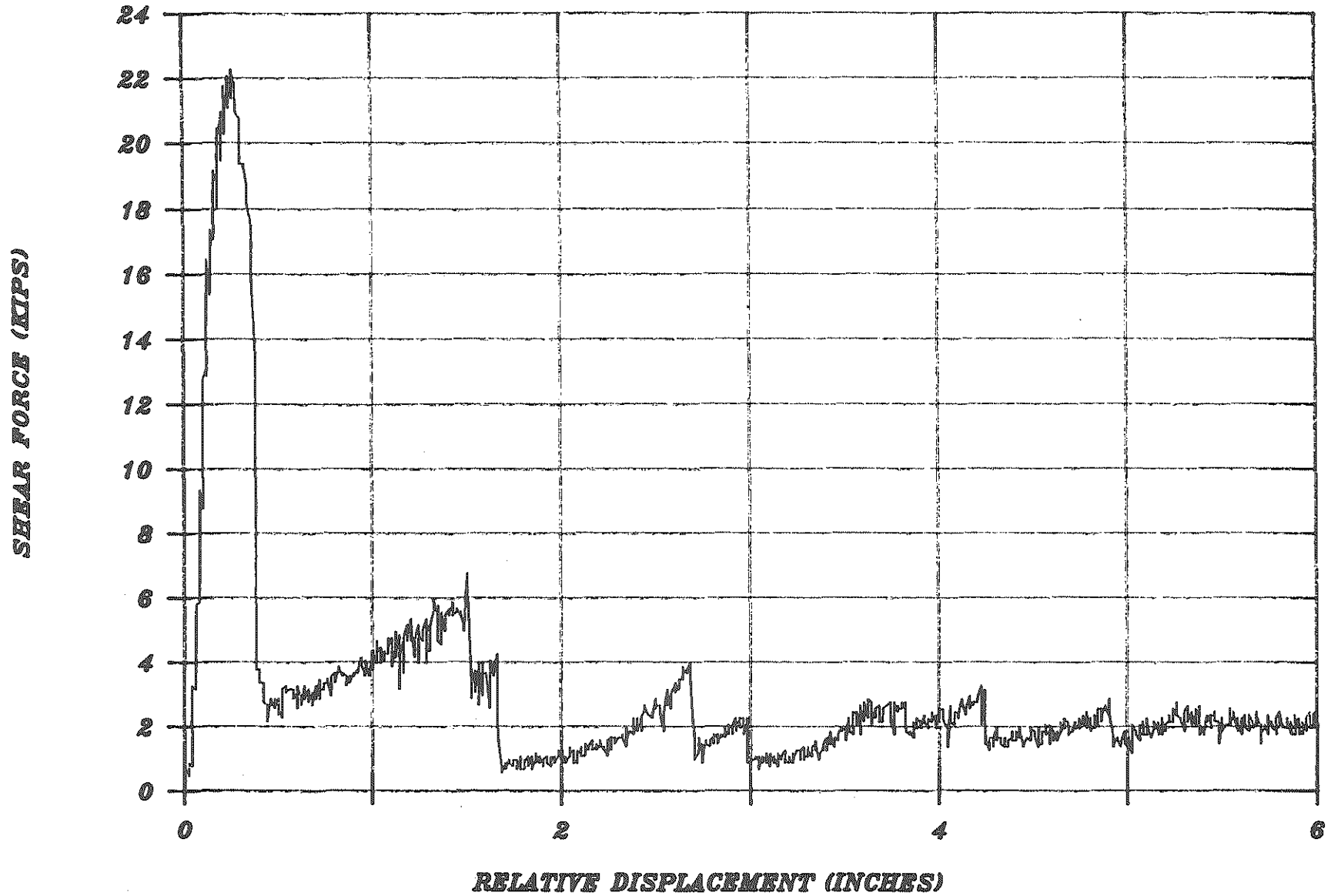


FIG. 8: PLOT FOR SPECIMEN 50-3-N

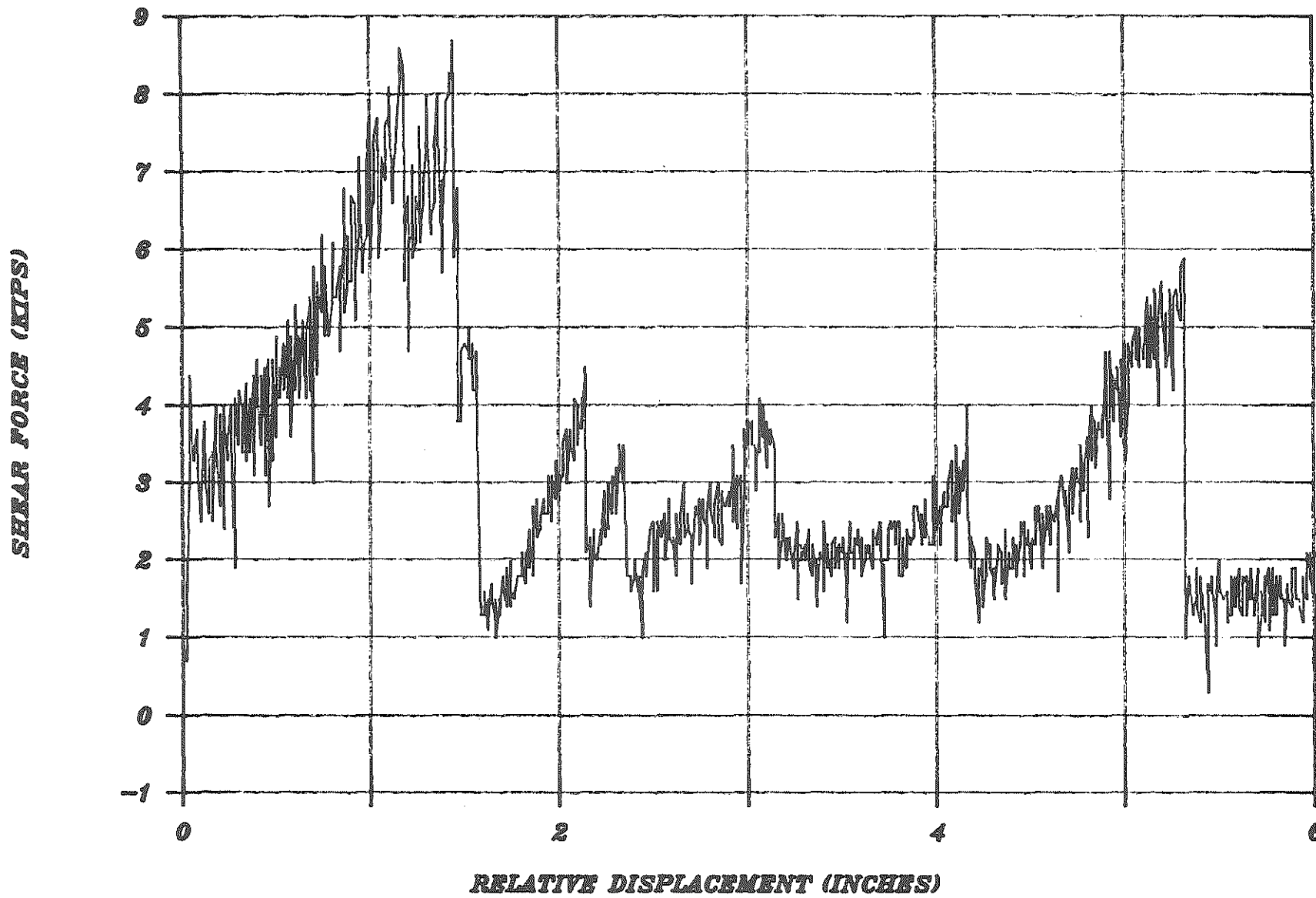


FIG. 9: PLOT FOR SPECIMEN 50-3-Y

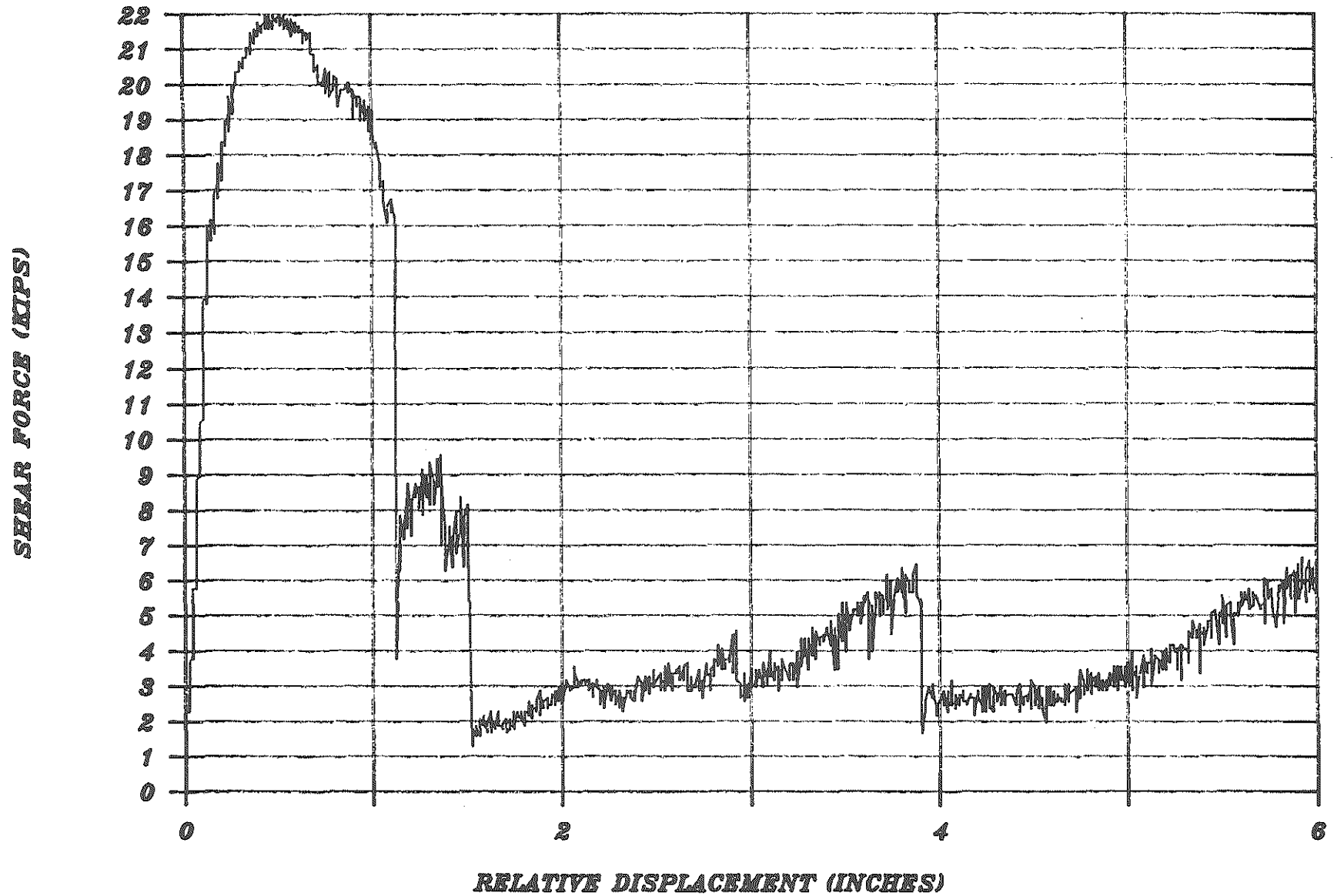


FIG. 10: PLOT FOR SPECIMEN 55-2-N

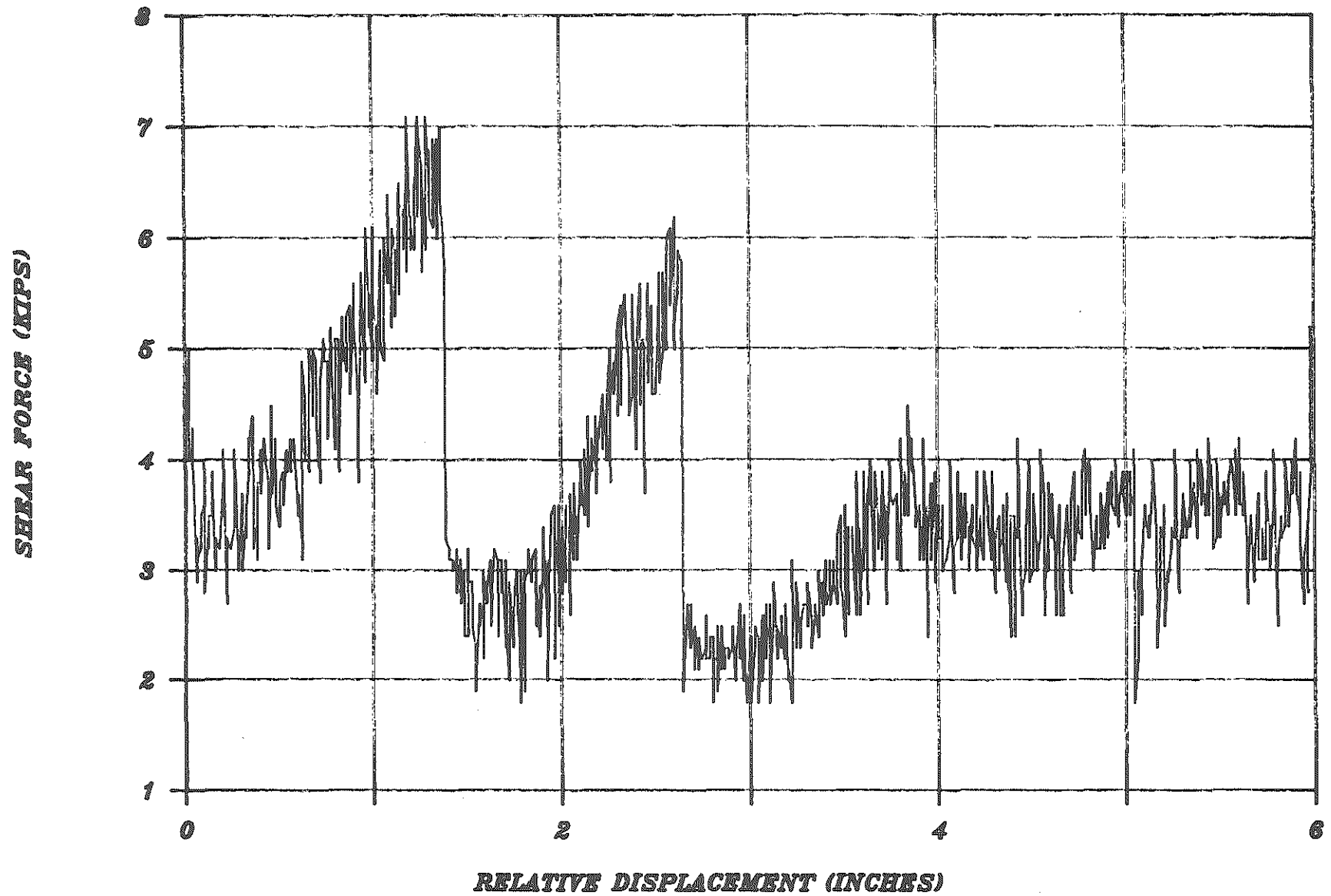


FIG. 11: PLOT FOR SPECIMEN 55-2-Y

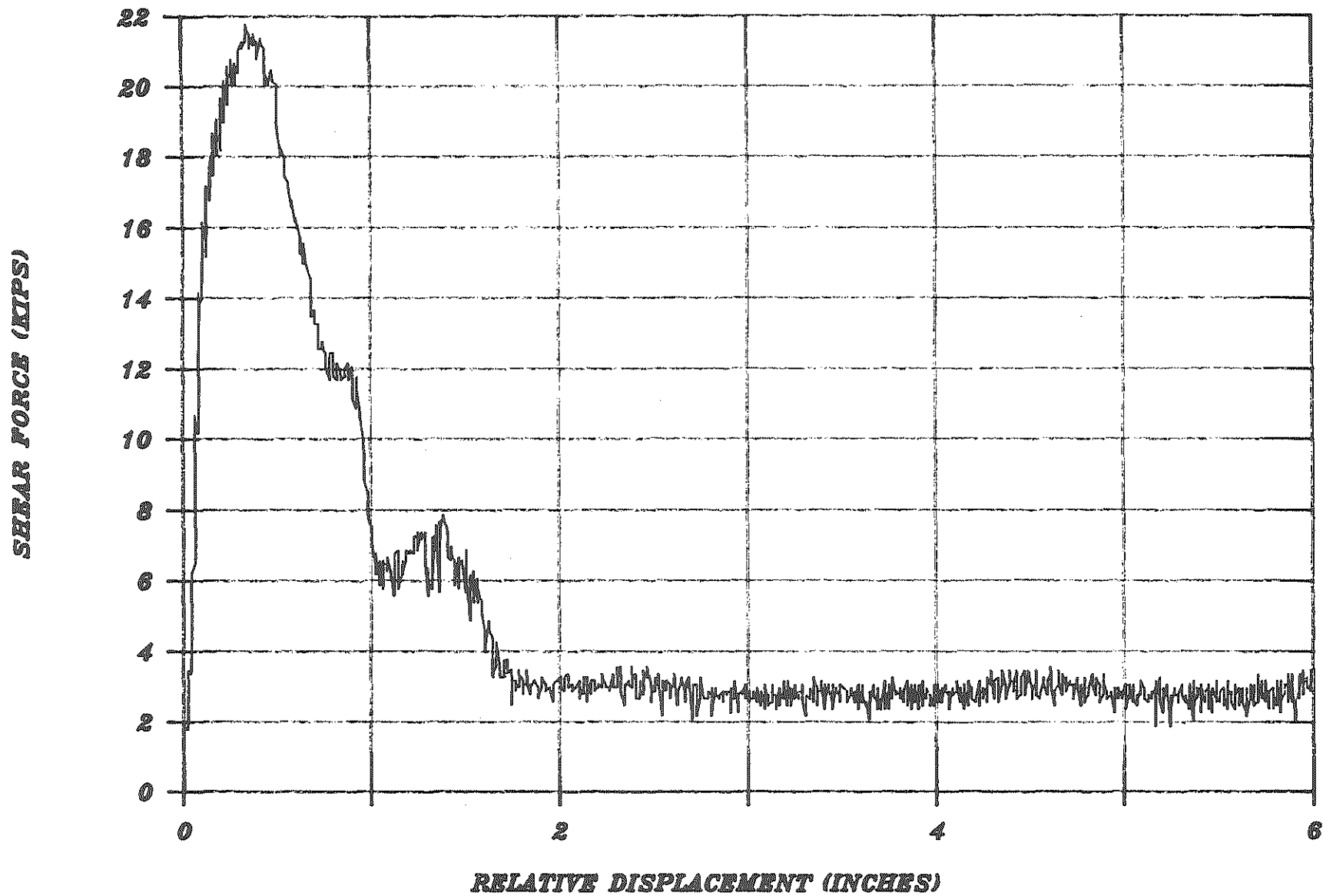


FIG. 12: PLOT FOR SPECIMEN 55-3-N

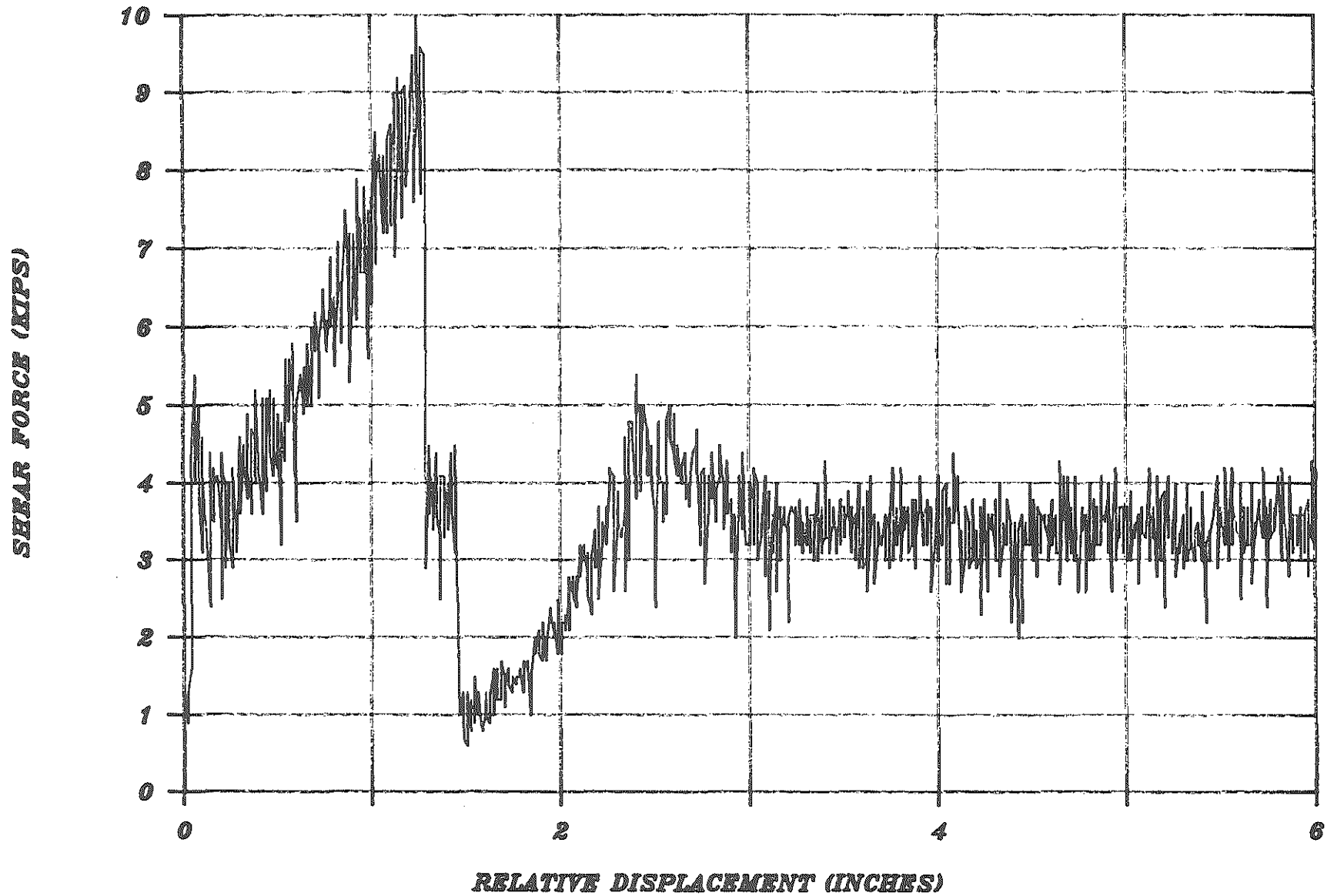


FIG. 13: PLOT FOR SPECIMEN 55-3-Y

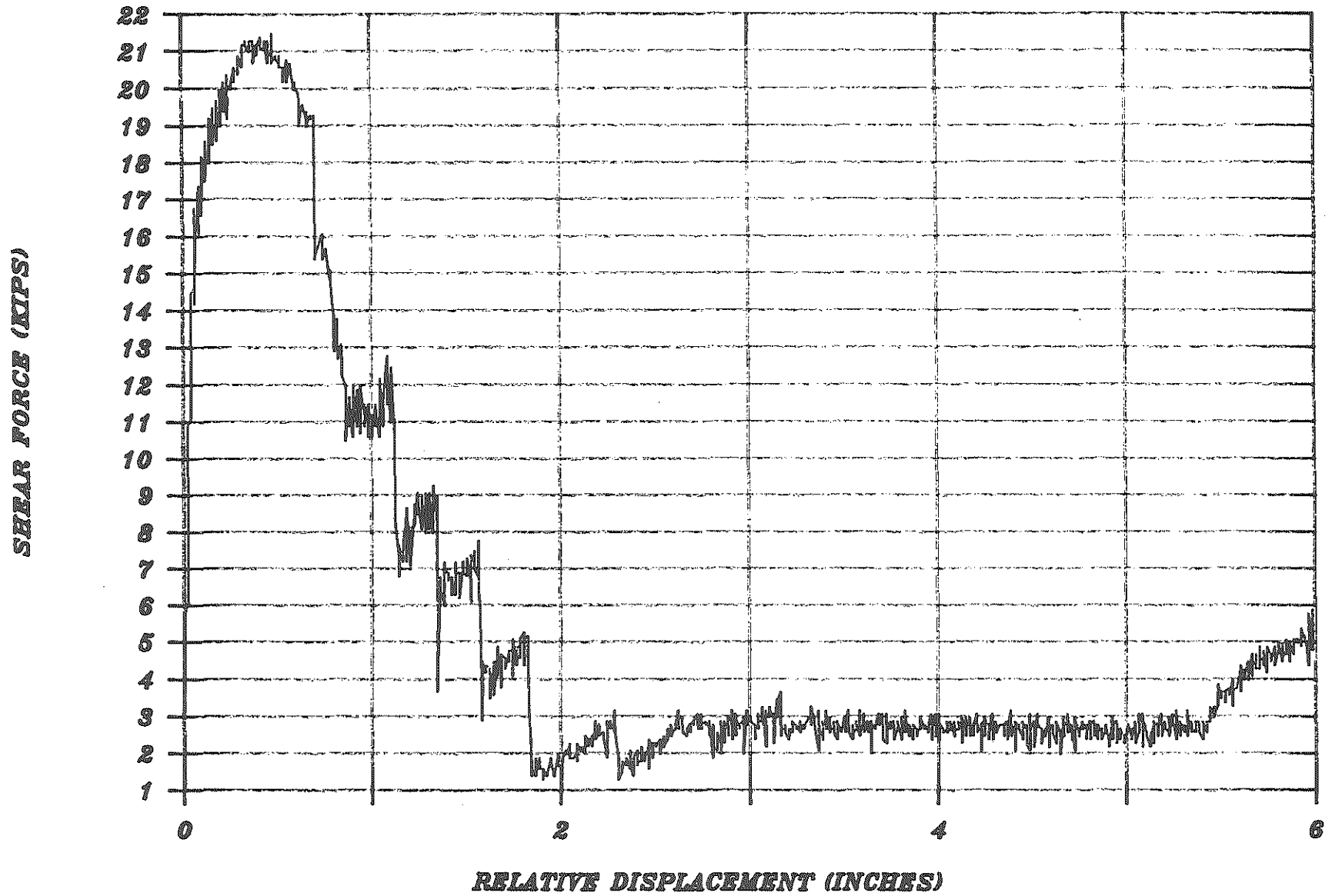


FIG. 14: PLOT FOR SPECIMEN 60-2-N

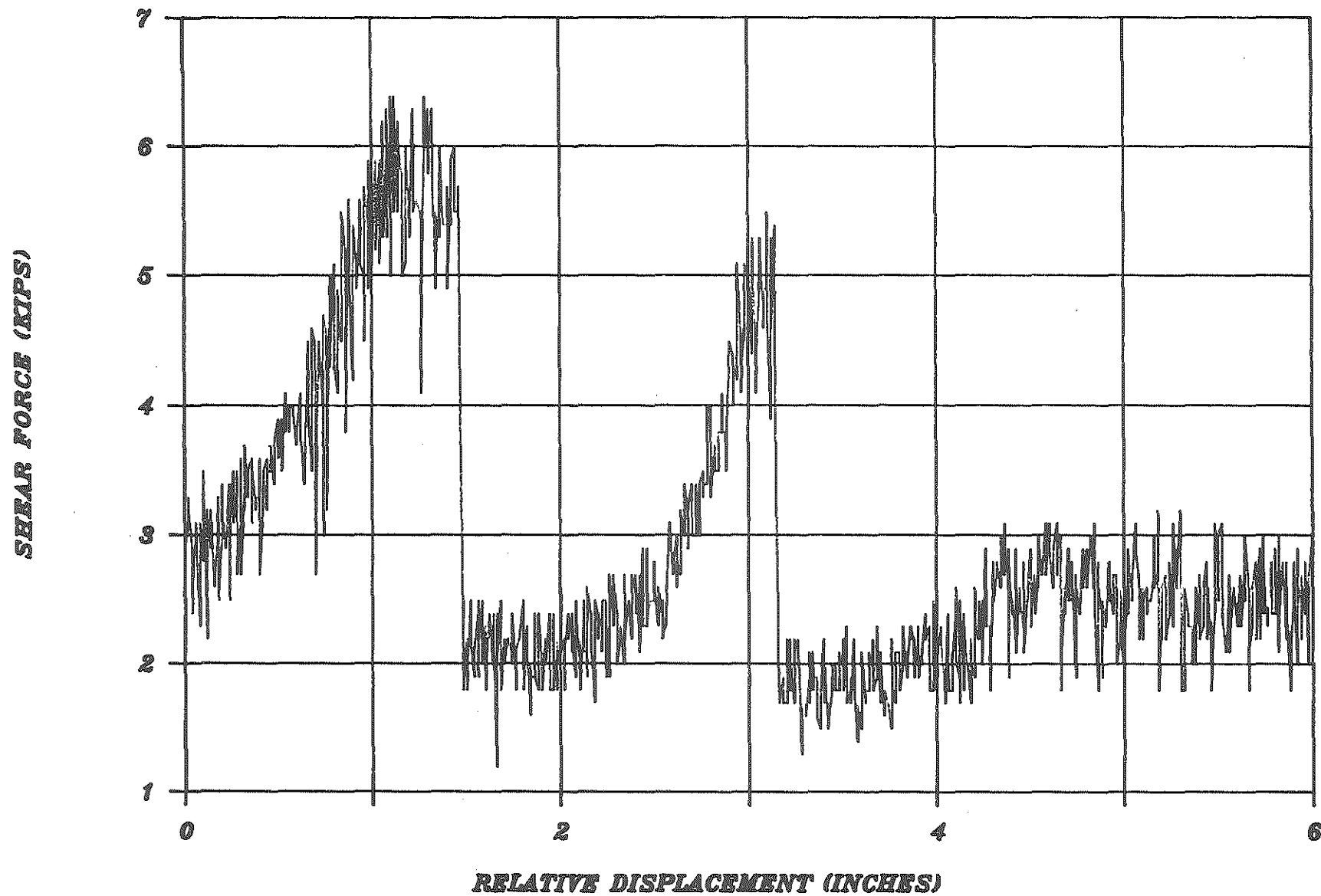


FIG.15: PLOT FOR SPECIMEN 60-2-Y

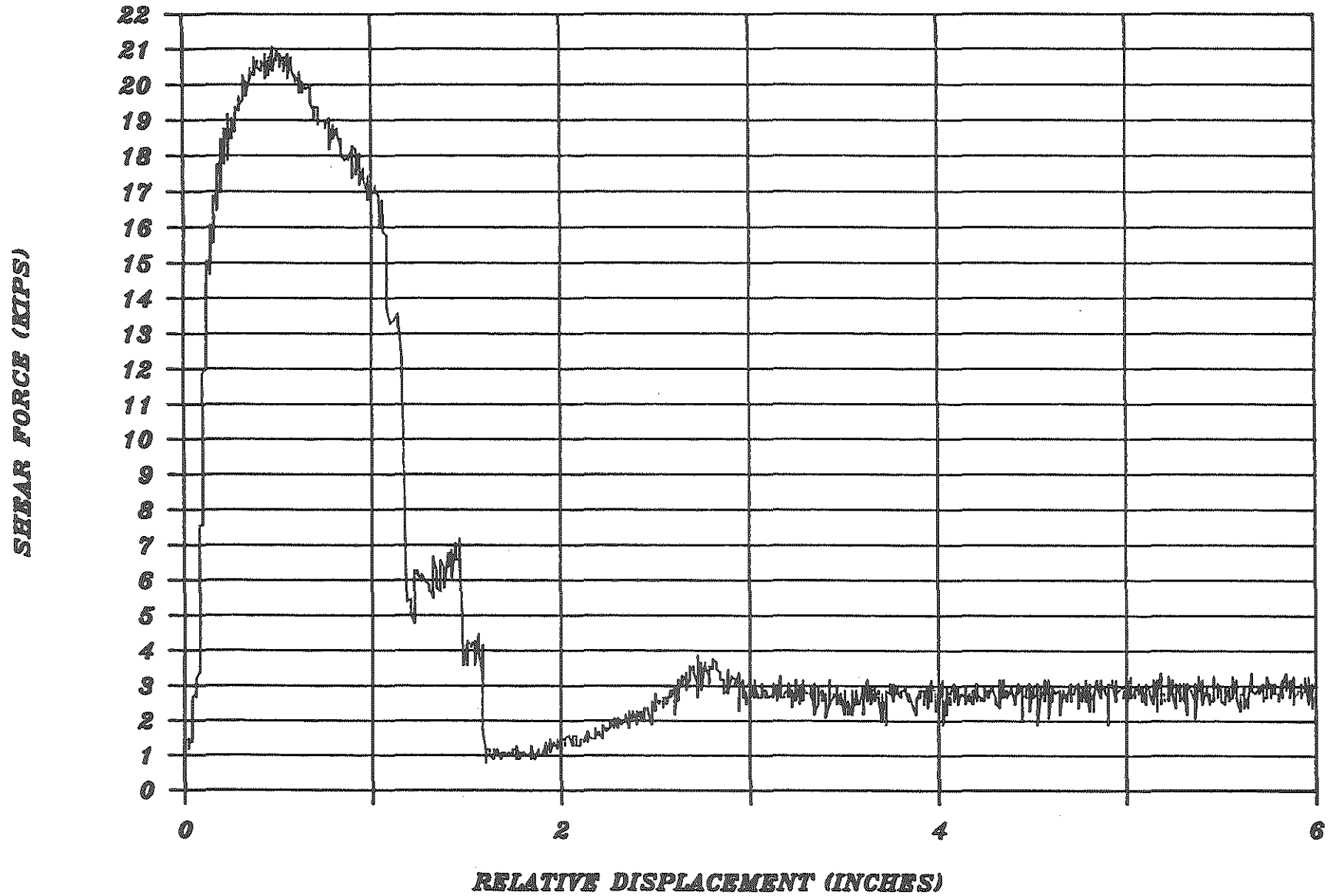


FIG. 16: PLOT FOR SPECIMEN 60-3-N

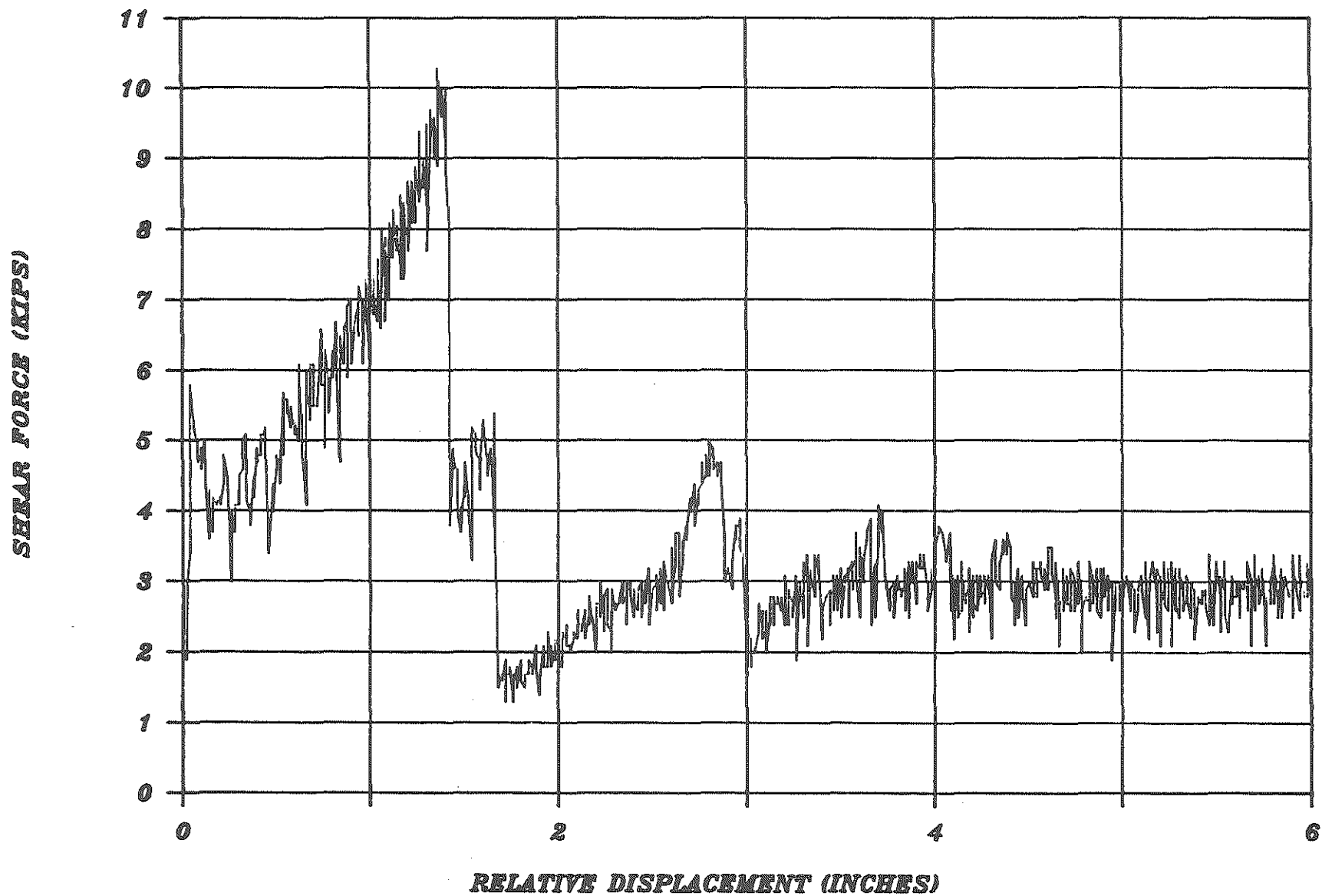


FIG.17: PLOT FOR SPECIMEN 60-3-Y

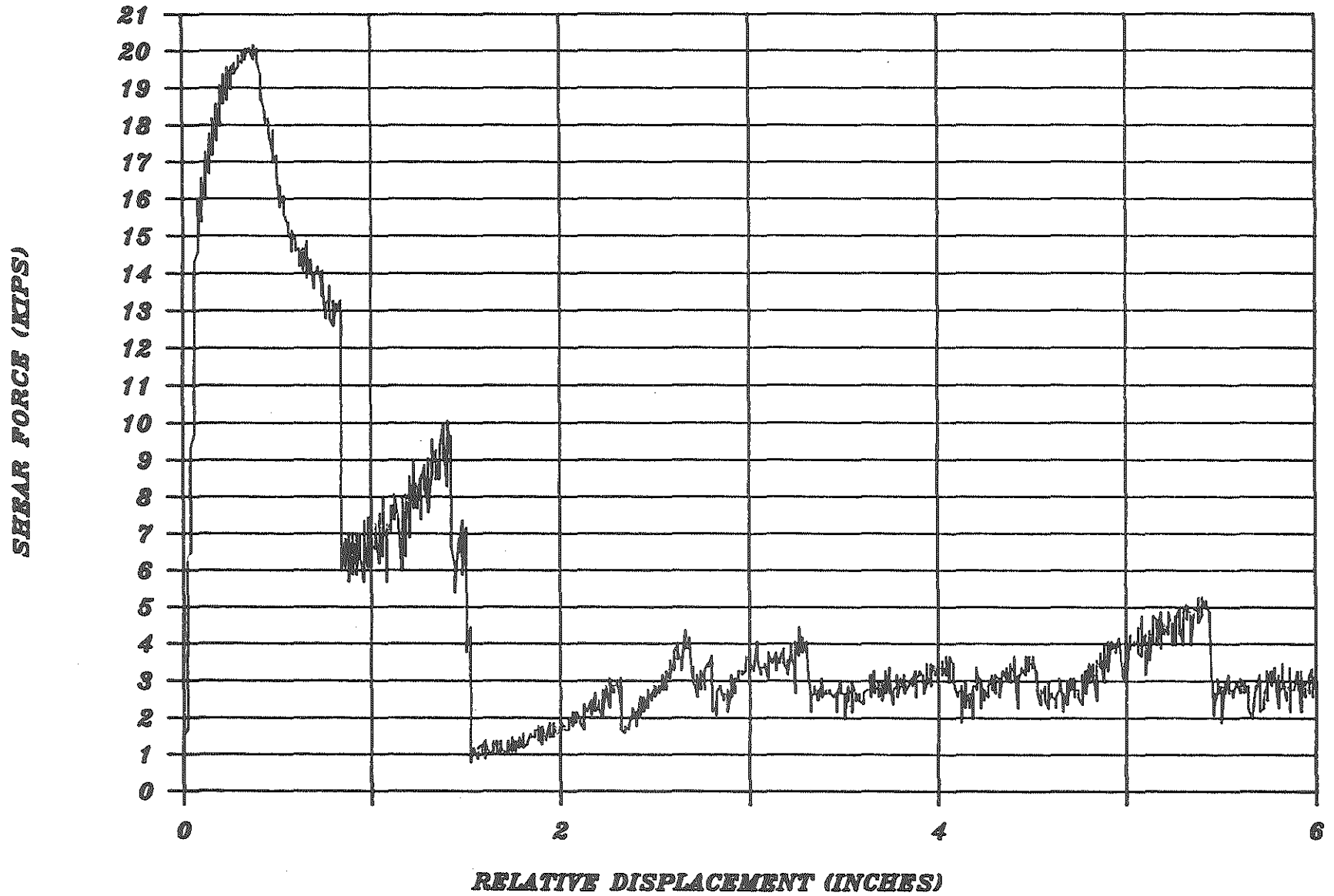


FIG. 18: PLOT FOR SPECIMEN 65-2-N

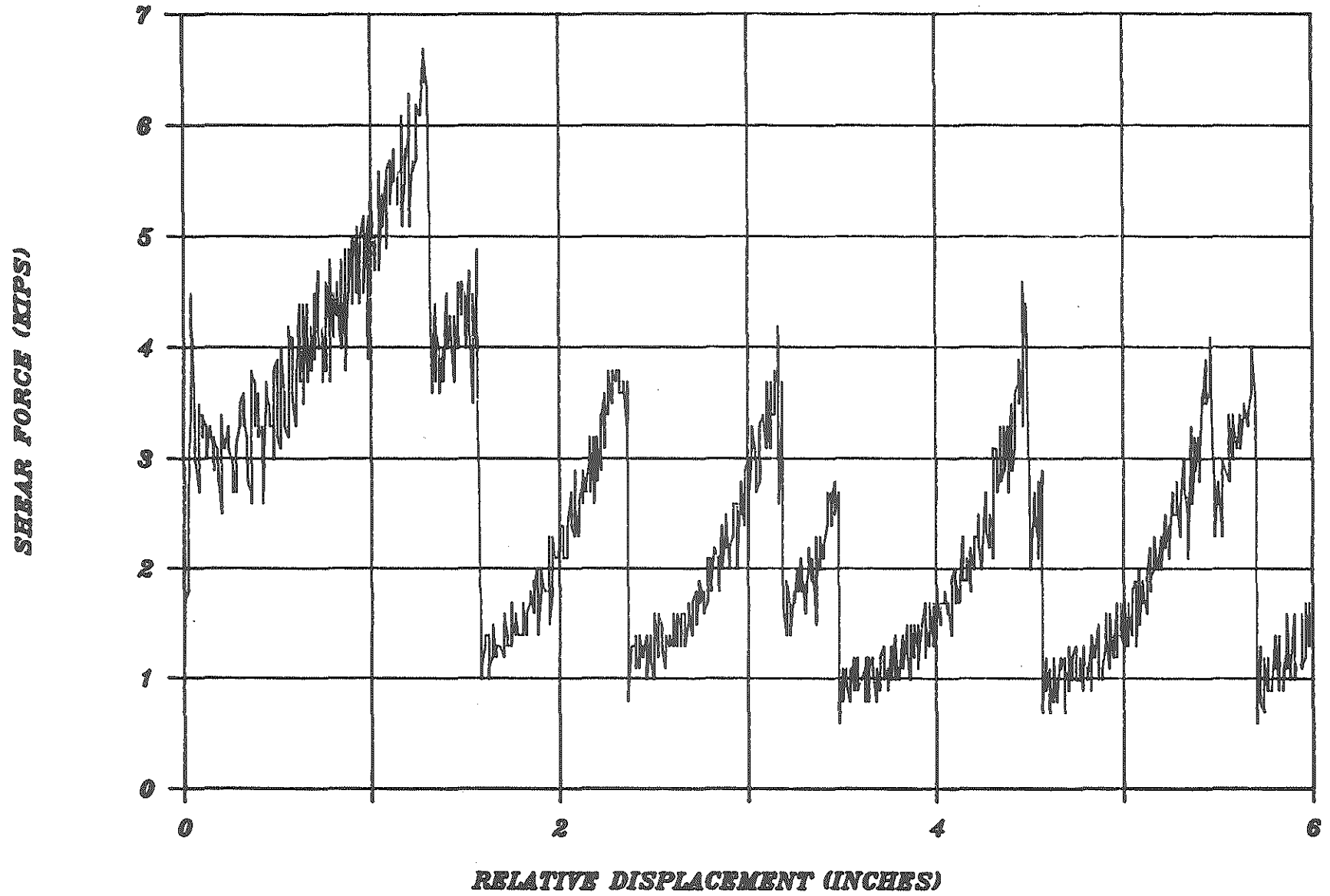


FIG. 19: PLOT FOR SPECIMEN 65-2-Y

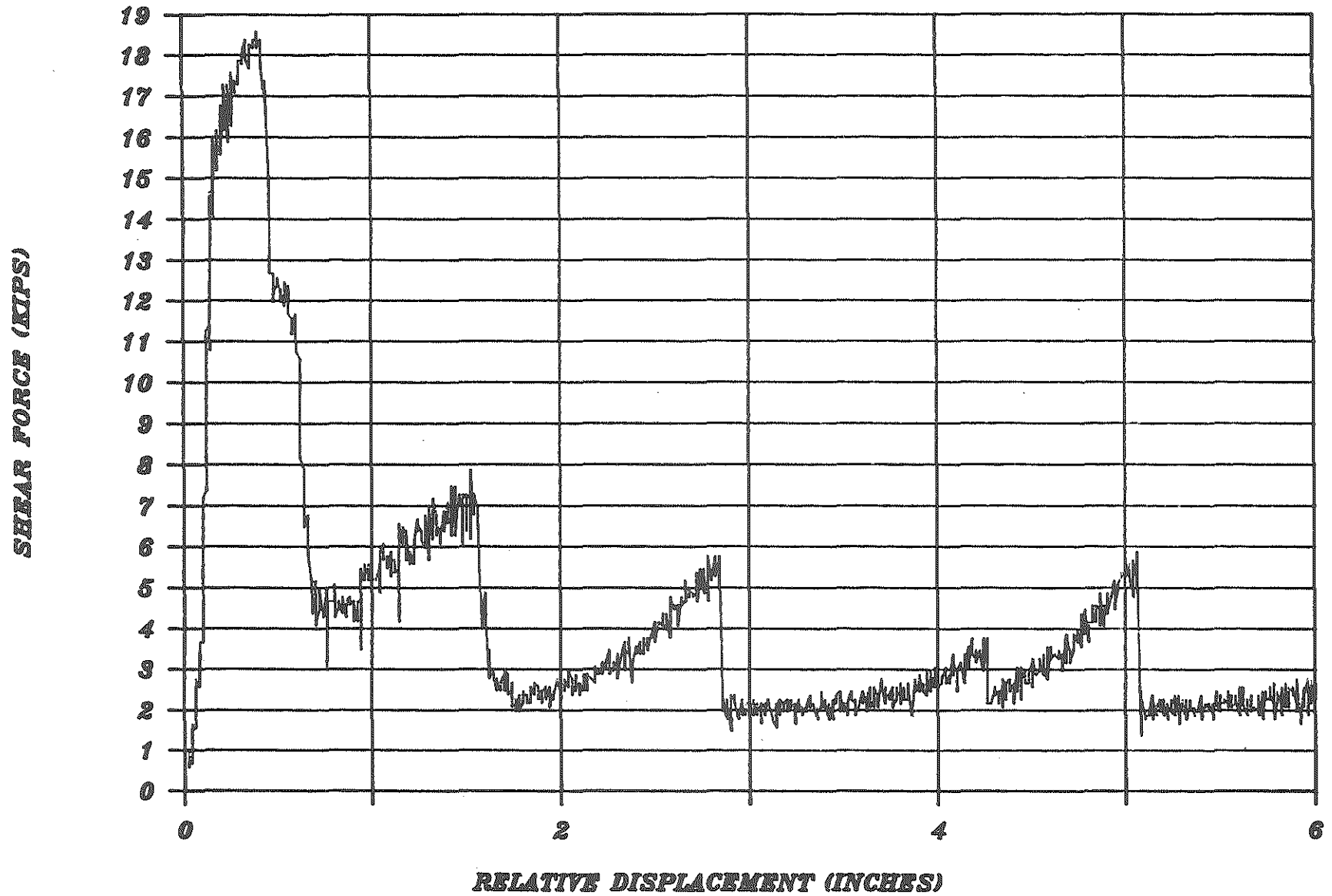


FIG.21: PLOT FOR SPECIMEN 65-3-Y

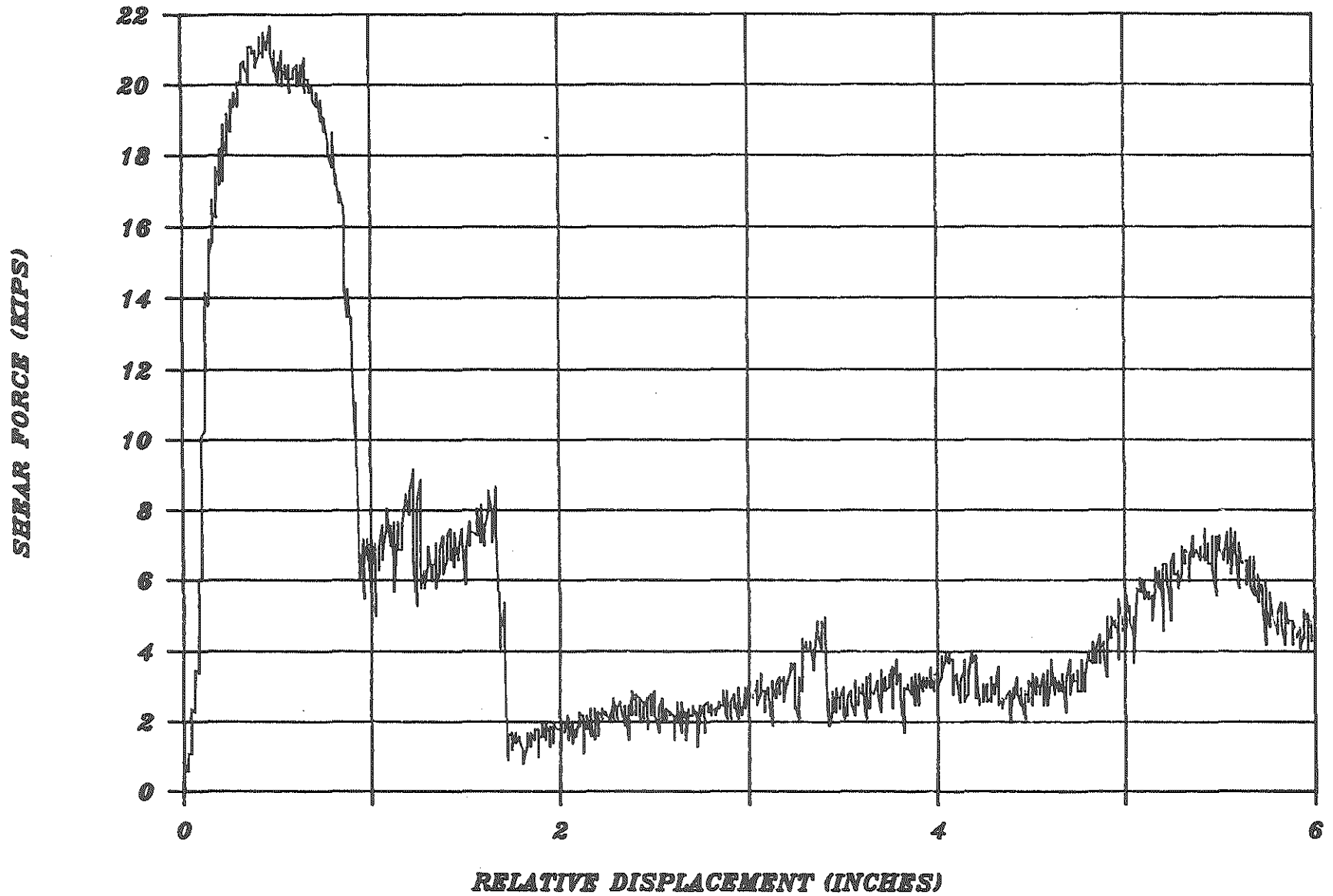


FIG.20: PLOT FOR SPECIMEN 65-3-N

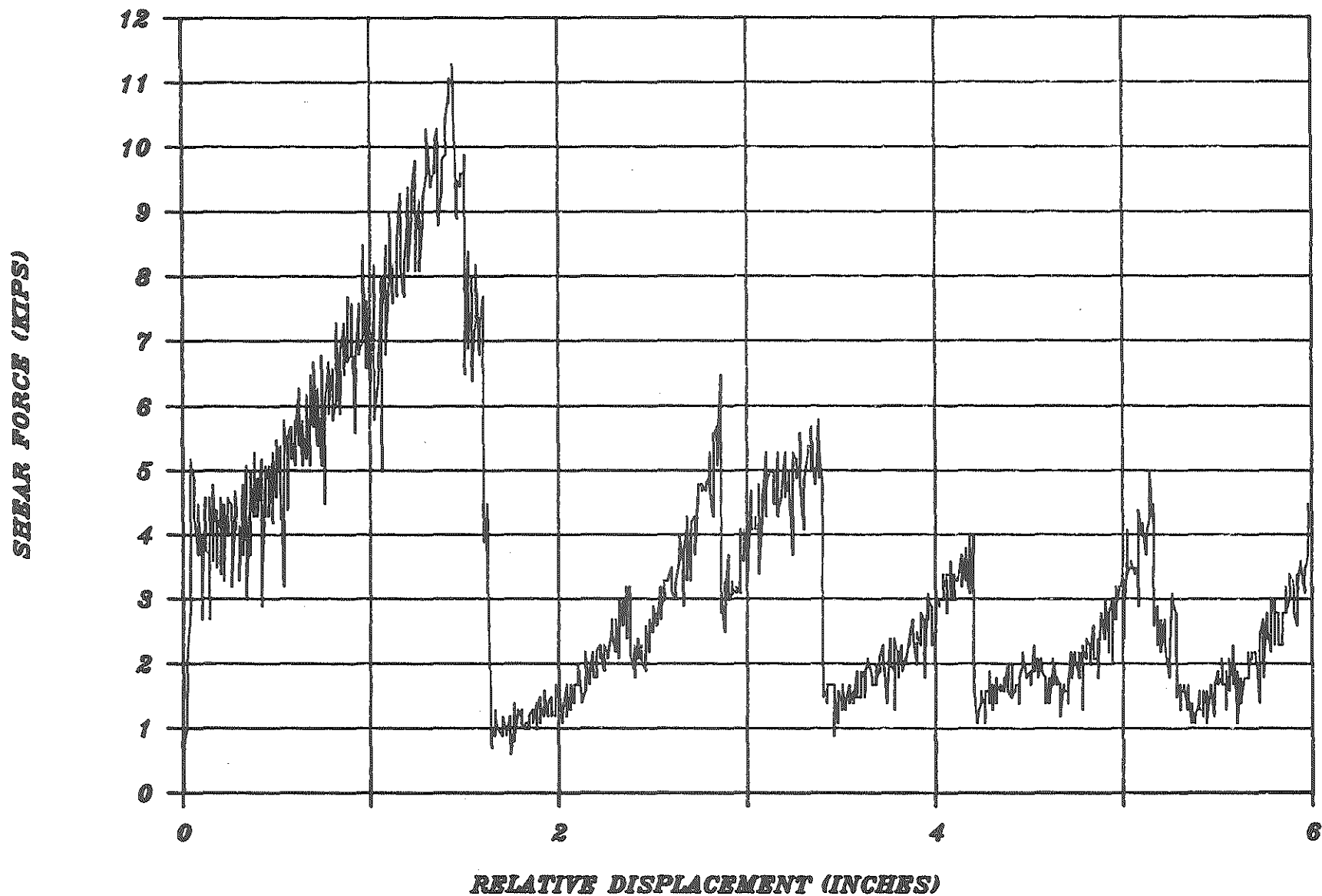


FIG.22: PLOT FOR SPECIMEN 70-2-N

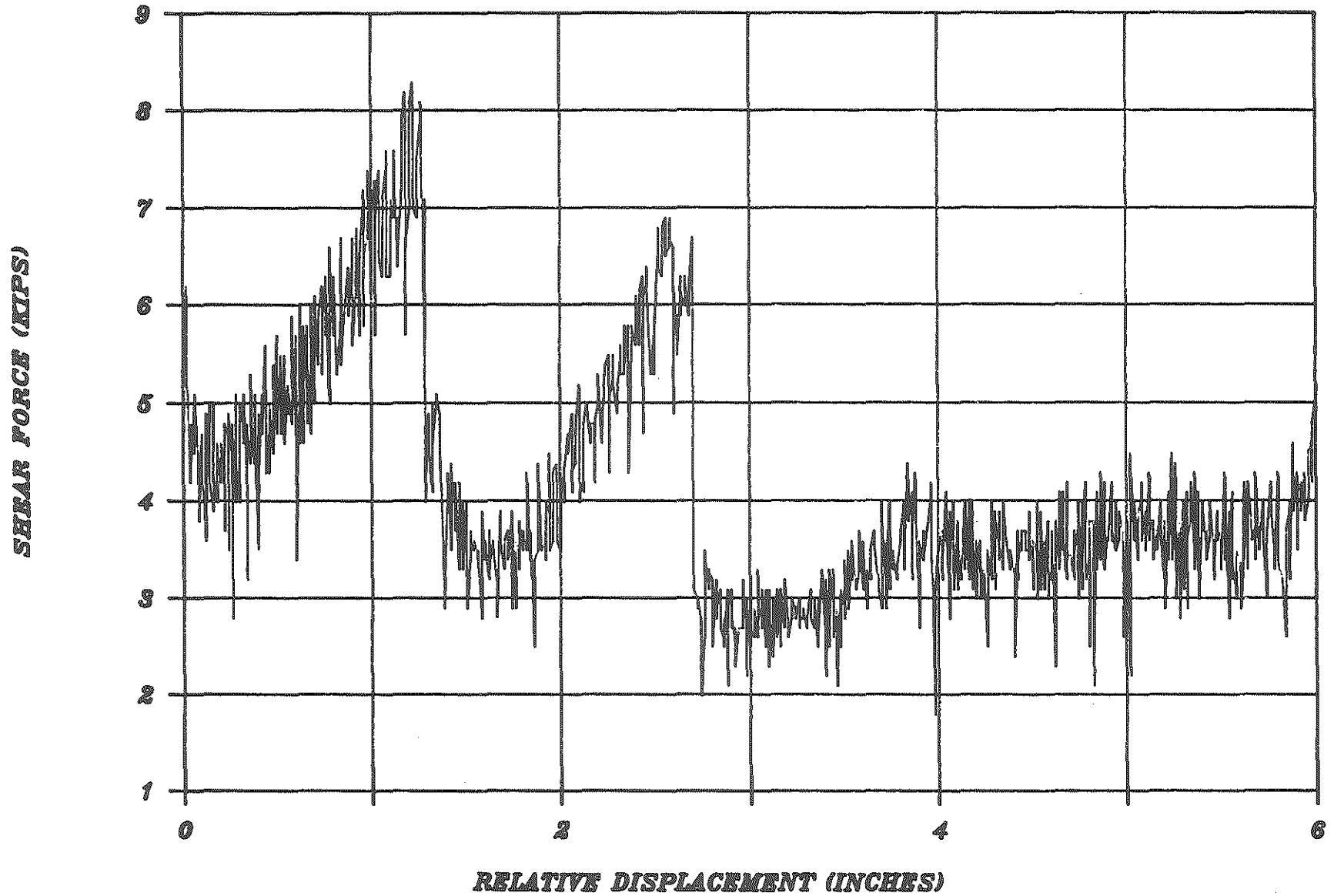


FIG.23: PLOT FOR SPECIMEN 70-2-Y

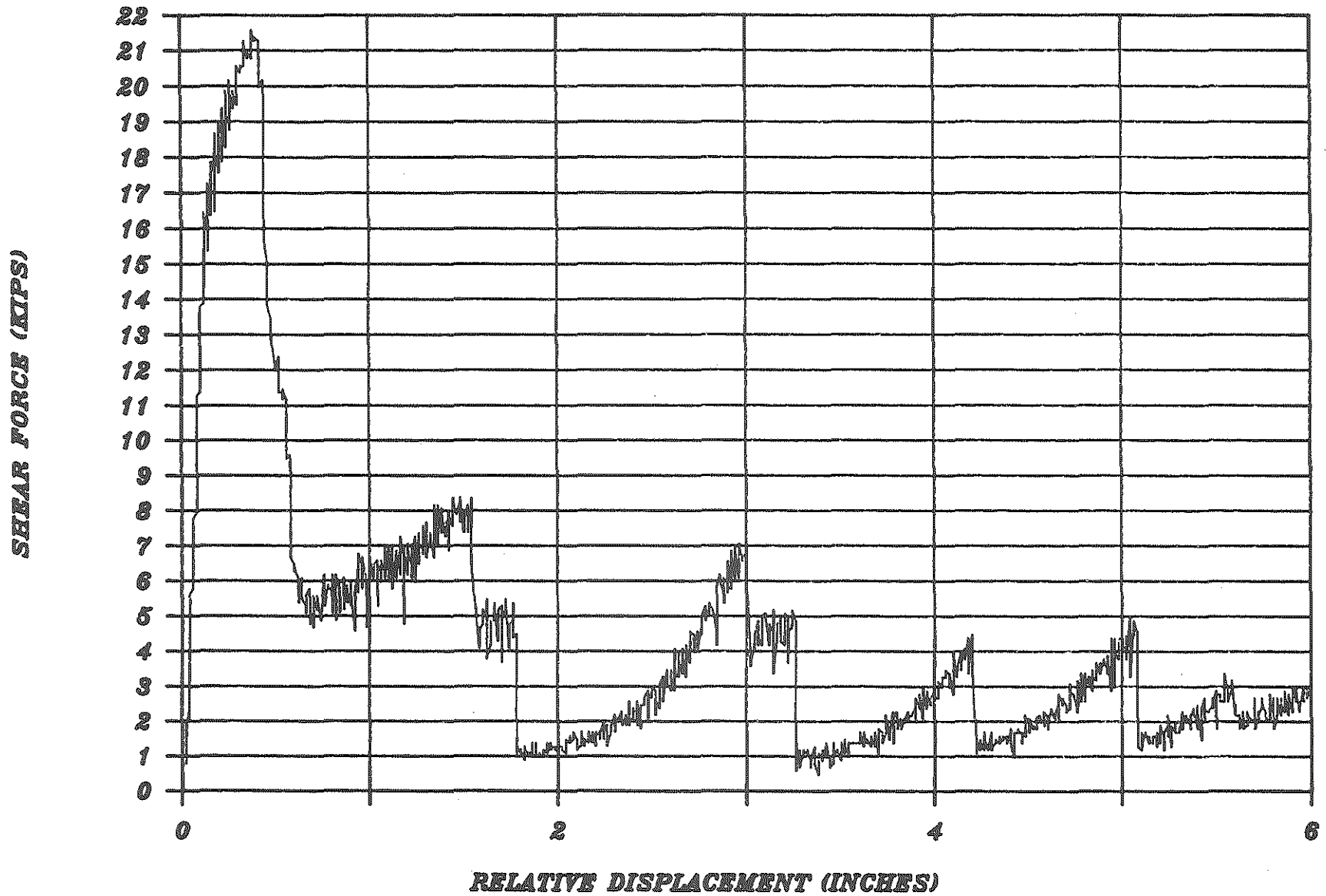


FIG.24: PLOT FOR SPECIMEN 70-3-N

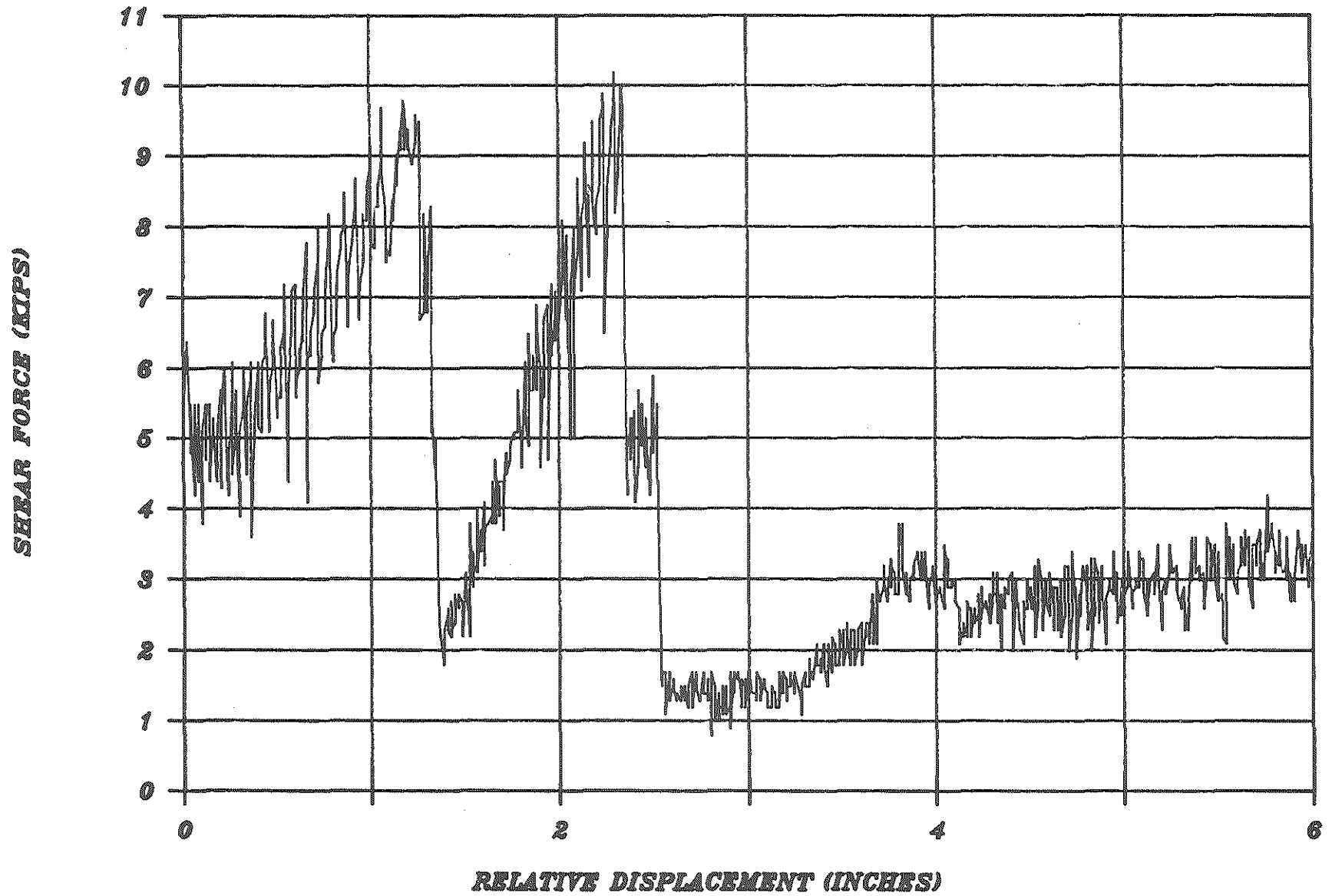
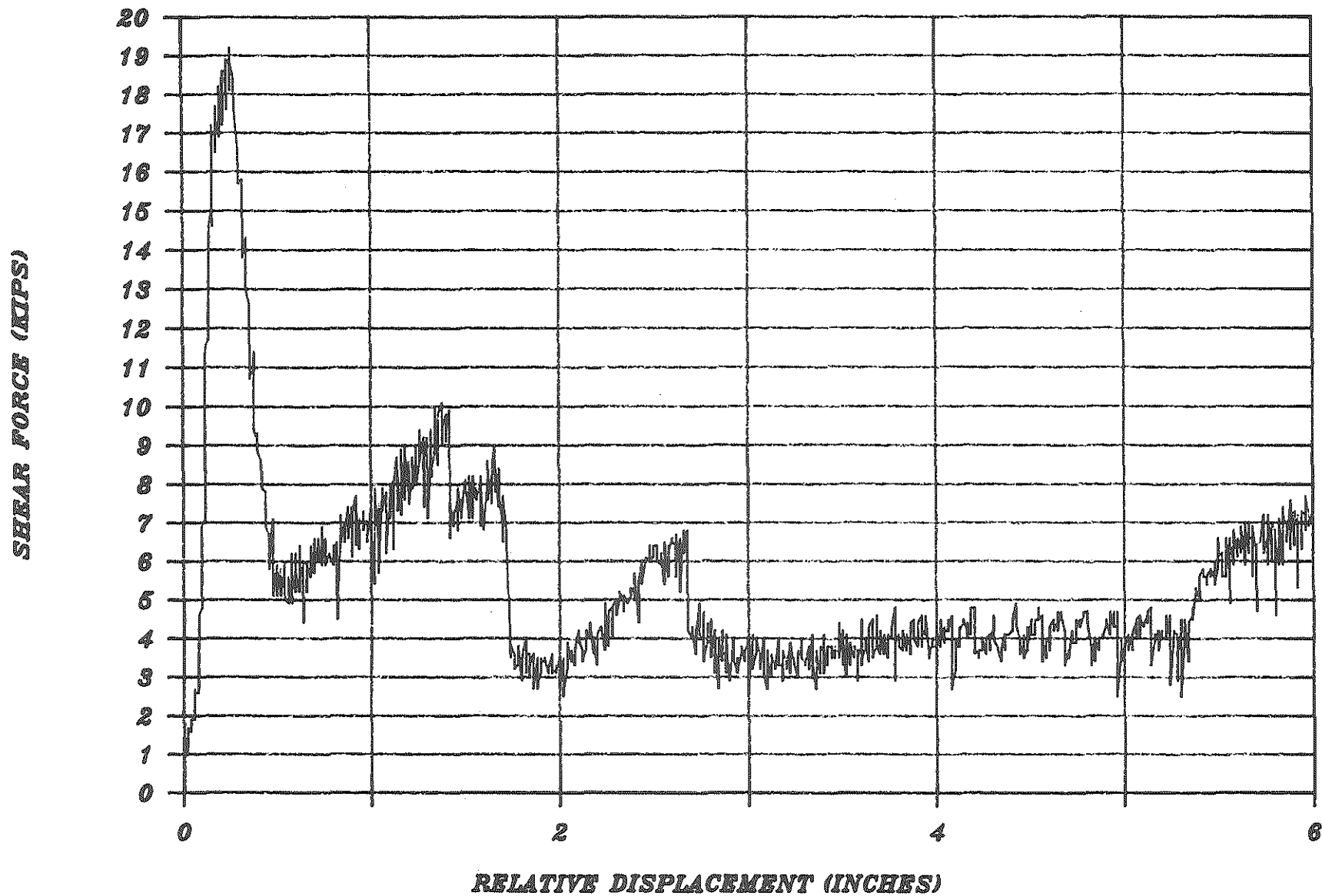


FIG.25: PLOT FOR SPECIMEN 70-3-Y



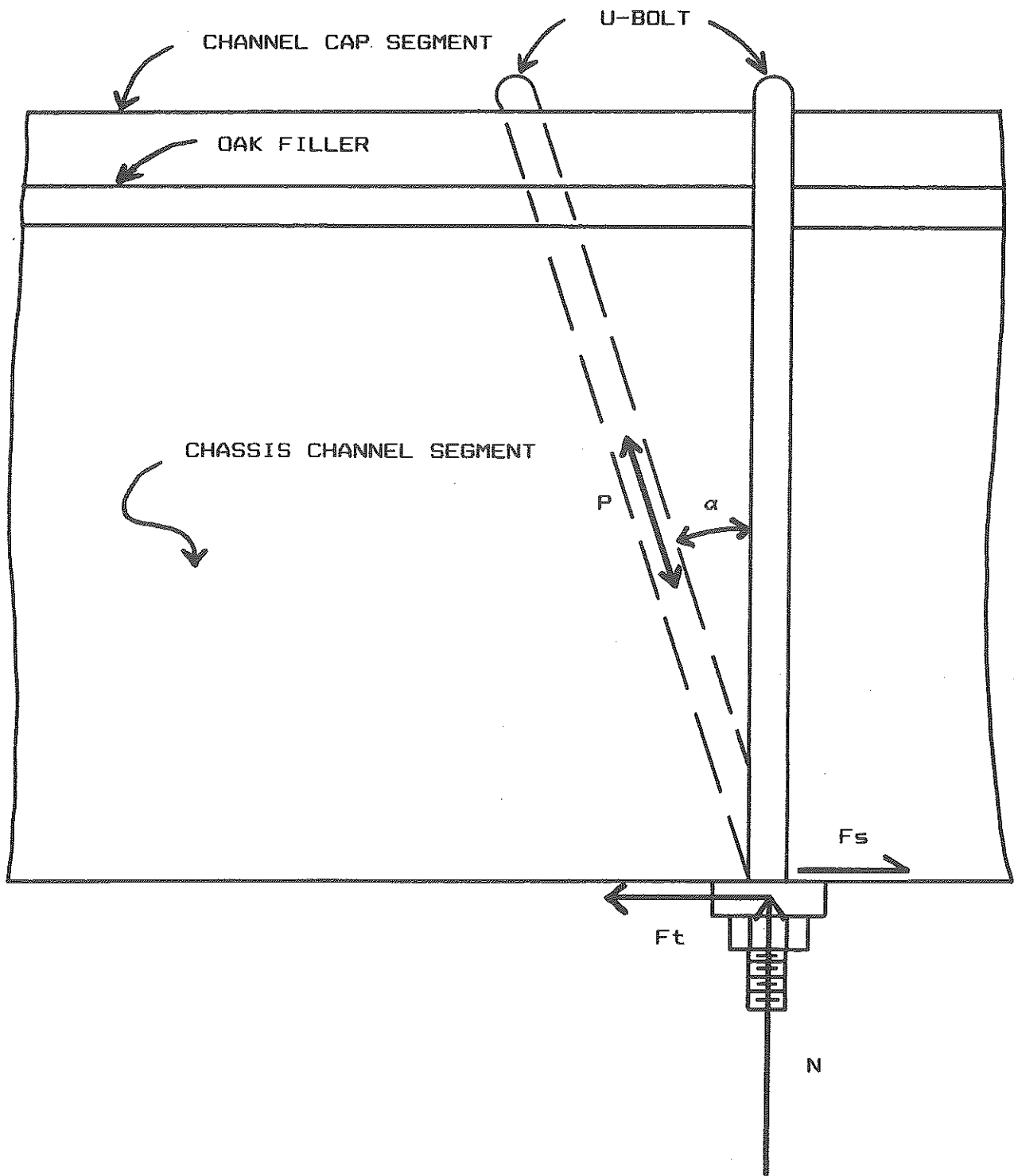


FIG. 26. U-BOLT DEFORMATION DIAGRAM